الشـــــــعبيـة الجـــــــــــــــمهـوريـــة الجـــــــــــزائـريـة الديمـــــــقـراطيـة

DEMOCRATIC AND POPULAR REPUBLIC OF ALGERIA

وزارة التـــــــــــــــــــــــعـليـم العـــــالي و البـــــــــحث العـــلـمـــي

Ministry of Higher Education and Scientific Research

جـــــــــــــامعة أبي بكـــر بـلـقـايد – تـلمســـــــــــــان –

University of Abou Bekr Belkaid – Tlemcen –
Faculty of TECHNOLOGY

THESIS

Presented for the obtaining of a **DOCTORATE** degree **3rd Cycle**

In: Mechanical Engineering

Specialty: Energetics

By: MAHMOUDI Djahida

Topic

Development and thermodynamic characterization of new materials for thermal storage by latent heat

Publicly defended on 23/ 04 /2026, in front of the jury composed of:

M.SAIM Rachid	Professor	Univ. Tlemcen	President
M.KORTI Abdel Illah Nabil	Professor	Univ. Tlemcen	Supervisor
M.GUELLIL Hocine	MCA	Univ. Tlemcen	Co- Supervisor
M.BENZENINE Hamidou	Professeur	Univ. Ain témouchent	Examiner 1
M.SELADJI Chakib	Professeur	Univ. Tlemcen	Examiner 2

Academic year: 2025-2026

ACKNOWLEDGMENTS

First and foremost, I wish to express deep and sincere gratitude to ***Allah*** *the Almighty for having given me steadfastness, patience, and perseverance needed to complete this work.*

I would like to express my profound thanks to my thesis directors, Pr KORTI Abdelillah Nabil and Dr GHELLIL Hocine, for the orientation, encouragement, and support throughout this research. Their expertise and advice helped much in giving an orientation and value to this work.

My sincere thanks also go to the members of my thesis committee,(Pr.SAIM Rachid, Pr.BENZENINE Hamidou and Pr .SELADJI Chakib), for their insight into comments and constructive suggestions, which have greatly enriched this research.

I would also like to express my sincere thanks to the ETAP Laboratory, for providing me with the necessary facilities and stimulating research environment, to my colleagues and friends especially to Houssem for his collaboration, support, and for inspiring discussions.

Allow me to express my deepest gratitude to my beloved family: Dad and Mom, for your endless love, guidance, and sacrifice; and my brothers and sister, for all the encouragement and support throughout my journey. Your faith in me has been a constant source of motivation.

Special thanks go out to my friends, especially to my bestie Rokia, for her continued support, understanding, and being there for me whenever I needed it, sharing the struggle as well as the sweet moments.

Final but most importantly, I want to acknowledge all individuals who helped me complete my internship and to those who were able to assist me during the writing of this thesis.

Djahida

DEDICATIONS

*I dedicate this thesis **first and foremost to my beloved father**, who passed away before witnessing this day. Your love, guidance, and sacrifices continue to inspire me every day. This work is a tribute to you and the values you instilled in me.*

I also dedicate it to my dear mother, whose unwavering support, patience, and encouragement have made this journey possible.

To my brothers (Abdallah et Azeddine) and sister (Fatima) and her family (Alaa,Mohammed et Abdessamie) et Amine , thank you for your constant love, care, and belief in me.

To my closest friend and confidant, my bestie, BOUBLENZA Rokia thank you for being by my side through every challenge and every joy.

I dedicate this work to my friends and colleagues, whose support, collaboration, and encouragement have enriched my journey.

I would like to make a special dedication to the Mahmoudi and Kebir families.

Finally, this thesis is a reflection of all the love, guidance, and support I have received from those who mean the most to me.

Abstract

The need for efficient thermal energy storage materials has escalated with the adoption of sustainable energy systems. Paraffin wax is one of the most widely used phase change materials because of its high latent heat storage capacity, stability, and cost-effectiveness. However, its low thermal conductivity of approximately 0.2 W/m•K and possibility of phase separation hinder its thermal efficiency, despite improvements by nanofilers and carbon additives.

A new approach for enhancement, which can be sustained in an efficient manner using Algerian slack wax, an underutilized petroleum derivative with immense potential, shall be proposed in this research work. PCMs with a combination of 6, 10, 15, and 20 wt% slack wax were studied by using a T-history test. The performance analysis reveals a collective advancement in different properties of PCMs, which is not a common phenomenon in PCM enhancement studies, where trade-off is considered. The combination with 20% slack wax proved to be most effective with a maximum increase of 35.65% in latent heat capacity from 106.93 kJ/kg to 145.06 kJ/kg, 30.48% in specific heat capacity from 3.51 kJ/kg•K to 4.58 kJ/kg•K, and a 33% boost in solid-phase thermal conductivity from 0.18 W/m•K to 0.24 W/m•K. Moreover, solidification time reduced by 25% from 165 s to 120 s and melting time reduced by 20% from 125 s to 100 s, respectively. The observed modifications in PCMs can be attributed to intermolecular interaction among paraffin and slack wax, which leads to an improper crystallization pattern with good transport properties. Use of an industrious waste in this manner can prove beneficial for cost-effective production of a higher-performance PC McA in an economical manner with sound eco-green concepts in the energy department in Algeria.

Keywords: Paraffin wax, Energy storage, Thermal properties, Latent heat of fusion, Melting temperature-history method.

ملخص

يؤدي التحول العالمي نحو أنظمة الطاقة المستدامة إلى زيادة الطلب على المواد عالية الأداء للتخزين الحراري. يظل البارافين أحد أكثر مواد تغيير الطور (PCM) استخدامًا بفضل حرارته الكامنة العالية واستقراره الكيميائي وتكلفته المنخفضة. ومع ذلك، فإن موصليتها الحرارية المنخفضة (0.2 واط/م•ك) وميلها إلى فصل الطور تحد بشكل كبير من أدائها. في حين أن إضافة المواد النانوية أو إضافات الكربون يمكن أن يحسن الموصلية، فإن هذه الأساليب غالبا ما تقلل الحرارة الكامنة، وتزيد التكاليف، وتجعل التنفيذ أكثر تعقيدا.

تقترح هذه الدراسة استراتيجية تحسين مبتكرة ومستدامة من خلال تثمين الشمع الجزائري الراكد، وهو منتج ثانوي صناعي قليل الاستغلال، كمادة مضافة متعددة الوظائف للبارافين. تم تحضير وتوصيف المركبات التي تحتوي على 6، 10، 15 و20% بالكتلة من الشمع الراكد باستخدام طريقة .T-history تظهر النتائج تحسنًا متزامنًا للعديد من الخصائص الحرارية الفيزيائية — وهو تقدم نادر في دراسات تحسين PCM حيث تكون التنازلات متكررة. تُظهر تركيبة الشمع الراكد بنسبة 20% الأداء الأكثر بروزًا، مع زيادة قدرها 65،35% في الحرارة الكامنة (106.93 145.06 كيلوجول/كجم)، وزيادة بنسبة 30.48% في الحرارة النوعية (3.51 4.58 كيلوجول/كجم • ك)، و زيادة بنسبة 33% في التوصيل الحراري للحالة الصلبة (0.18 0.24 واط/م • ك). كما تم تحسين الاستجابة الحرارية، مع انخفاض بنسبة 25% في زمن التصلب (165-120 ثانية) وتسارع الذوبان بنسبة 20% (125-100 ثانية). وتعزى هذه المكاسب إلى التفاعلات الجزيئية بين مكونات البارافين والشمع الراكد، والتي تعطل البنية البلورية وتعزز نقل الطاقة بشكل أفضل

من خلال تحويل النفايات الصناعية إلى مادة مضافة PCM تقدم هذه الدراسة حلاً اقتصاديًا وقابلاً للتطوير وصديقًا للبيئة للتخزين الحراري. يعتبر المركب المطور مناسبًا بشكل خاص لتطبيقات مثل أنظمة الطاقة الشمسية والتنظيم الحراري للمباني واستعادة الحرارة المهدرة، مع دعم نهج الاقتصاد الدائري في قطاع الطاقة الجزائري.

الكلمات المفتاحية: شمع البارافين، تخزين الطاقة، الخواص الحرارية، حرارة الانصهار الكامنة، طريقة تاريخ درجة حرارة الانصهار

Résumé

La transition mondiale vers des systèmes énergétiques durables accroît la demande en matériaux performants pour le stockage thermique. La paraffine demeure l'un des matériaux à changement de phase (PCM) les plus utilisés grâce à sa forte chaleur latente, sa stabilité chimique et son faible coût. Cependant, sa faible conductivité thermique (≈0,2 W/m·K) et sa tendance à la ségrégation de phase limitent considérablement ses performances. Bien que l'ajout de nanomatériaux ou d'additifs carbonés puisse améliorer la conductivité, ces approches réduisent souvent la chaleur latente, augmentent les coûts et rendent la mise en œuvre plus complexe.

Cette étude propose une stratégie d'amélioration innovante et durable en valorisant le slack wax algérien, un sous-produit industriel peu exploité, comme additif multifonctionnel pour la paraffine. Des composites contenant 6, 10, 15 et 20 % en masse de slack wax ont été préparés et caractérisés à l'aide de la méthode T-history. Les résultats montrent une amélioration simultanée de plusieurs propriétés thermophysiques — une avancée rare dans les études d'optimisation de PCM où les compromis sont fréquents. La formulation à 20 % de slack wax présente les performances les plus remarquables, avec une augmentation de 35,65 % de la chaleur latente (106,93 → 145,06 kJ/kg), une hausse de 30,48 % de la chaleur spécifique (3,51 → 4,58 kJ/kg·K), et une augmentation de 33 % de la conductivité thermique à l'état solide (0,18 → 0,24 W/m·K). La réponse thermique est également améliorée, avec une réduction de 25 % du temps de solidification (165 → 120 s) et une fusion accélérée de 20 % (125 → 100 s). Ces gains sont attribués aux interactions moléculaires entre la paraffine et les composants du slack wax, qui perturbent la structure cristalline et favorisent un meilleur transport énergétique.

En transformant un déchet industriel en un additif PCM performant, cette étude propose une solution économique et respectueuse de l'environnement pour le stockage thermique. Le composite développé est particulièrement adapté aux applications telles que les systèmes solaires, la régulation thermique des bâtiments et la valorisation de chaleur perdue, tout en soutenant une approche d'économie circulaire dans le secteur énergétique algérien.

Mots clés : Cire de paraffine, Stockage d'énergie, Propriétés thermiques, Chaleur latente de fusion, Méthode T-history.

Table of contents

List of figures

List of tables

Nomenclature

Latin and Greek Letters

Symbol	Description	Unit
A	Heat transfer surface area	m^2
cp	Specific heat capacity	$J \cdot kg^{-1} \cdot K^{-1}$
h	Convective heat transfer coefficient	$W \cdot m^{-2} \cdot K^{-1}$
Hm	The heat of fusion of the paraffin	$J \cdot kg^{-1}$
k	Thermal conductivity	$W \cdot m^{-1} \cdot K^{-1}$
L	Characteristic length / latent heat	m / $J \cdot kg^{-1}$
m	Mass	kg
R	Radius	m
T	Temperature	K / °C
t	Time	s
u	Flow velocity	$m \cdot s^{-1}$
V	Volume	m^3
α	Thermal diffusivity	$m^2 \cdot s^{-1}$
β	Thermal expansion coefficient	K^{-1}
ΔT	Temperature difference	K
ε	Porosity (EG, foam, etc.)	–
ρ	Density	$kg \cdot m^{-3}$
Ra_L	Rayleigh number	_
Pr	Prandt number	_
Bi	Biot number	_
Nu_L	Nusselt number	_

Subscripts and Superscripts

Symbol	Description
t	Tube
f	final
l	Liquid phase

m	Melting
p	PCM
s	Solid phase
i	Initial condition
∞	Ambient condition
w	water

Abbreviations

Symbol	Description
PCM	Phase Change Material
TES	Thermal Energy Storage
LHTES	Latent Heat Thermal Energy Storage
CPCM	Composite PCM
FSPCM	Form-Stable PCM
EG	Expanded Graphite
CF	Copper Foam
CNT	Carbon Nanotubes
MWCNT	Multi-Walled Carbon Nanotubes
DSC	Differential Scanning Calorimetry
TGA	Thermogravimetric Analysis
SEM	Scanning Electron Microscopy
BTMS	Battery Thermal Management System
CFD	Computational Fluid Dynamics

General introduction

General introduction

The rapid growth of need for energy worldwide, combined with increasing concerns over climate change and environmental degradation, has intensified the need for clean and effective energy solutions. Conventional energy systems, which are largely dependent on fossil fuels, greatly contribute to greenhouse gas emissions and face growing economic and environmental constraints. In this context, incorporating renewable energy sources and increasing energy efficiency have become major priorities for researchers, industries, and policymakers worldwide.

Among emerging energy management strategies, thermal energy storage (TES) has attracted significant interest due to its capacity to balance demand and supply of energy, improve overall system efficiency, and facilitate the integration of intermittent renewable sources like solar and wind power. In particular, latent heat storage with phase change materials (PCMs) is highly promising because of its high energy density, nearly constant operating temperature, and potential for compact, efficient storage solutions. Nevertheless, despite these advantages, many PCMs still encounter limitations, including low thermal conductivity, supercooling, leakage, and concerns over long-term stability, which hinder their widespread deployment.

To overcome these limitations, recent research has explored advanced PCM formulations, composite materials, improved encapsulation techniques, and innovative heat exchanger designs. Understanding the thermophysical behavior of PCMs and developing new composite systems with enhanced performance are essential steps toward achieving reliable and high-efficiency thermal storage technologies. These advancements have important implications across multiple sectors, including building energy efficiency, renewable energy systems, electronics cooling, industrial processes, and transportation.

This thesis aims to contribute to these ongoing efforts by developing, characterizing, and evaluating a phase change material , with the objective of improving thermal performance, stability, and applicability in real systems. The research combines experimental analysis, material characterization, and thermal performance evaluation to address current limitations in PCM technology and propose viable solutions for next-generation TES applications.

The structure of the thesis is organized as follows:

- **Chapter 1** presents a comprehensive literature review on phase change materials, thermal storage mechanisms, and current enhancement strategies.

- **Chapter 2** Addresses the fundamental aspects of thermal energy storage, classification of TES methods, and detailed discussion on phase change materials. It also presents enhancement strategies.
- **Chapter 3** describes the experimental setup and methodology for characterizing PCM properties. The T-history method is detailed for measuring thermophysical properties, and a mathematical model is presented to support analysis. Uncertainty and surface calculations are also covered.
- **Chapter 4** Provides a presentation and analysis of the experimental results. It discusses the measured melting temperature, specific heat, latent heat, and thermal conductivity of the PCM samples. Comparative analysis with existing studies validates the findings and highlights improvements.

Finally, it draws general conclusions and proposes recommendations for future research.

Chapter 1 Bibliography

1.1 Introduction

The urgent requirements of tackling climate change, enhancing energy security, and constructing sustainable and resilient infrastructures in the 21st century are reshaping the global energy landscape. In this scenario, TES has emerged as one of those critical enabling technologies to support the transition toward low-carbon and energy-efficient systems. In this context, TES is so relevant that it is considered the key to balancing energy supply and demand, especially when implementing variable intermittent renewable energies such as solar and wind. This source of energy is intermittent by nature and thus generates variable energy at times when it is not needed. TES makes the integration of such power sources practical by its storage of thermal energy during periods of surplus and its release when it is most needed. This would stabilize the energy system, reduce curtailment, and improve grid reliability. TES can be realized through sensible heat storage, latent heat storage, and thermochemical storage, each suited for a different application based on temperature range, energy density, and duration of storage.

When opposed to traditional sensible heat storage, latent heat thermal energy storage offers several benefits in the realm of TES. Large amounts of energy can be stored and released by LHTES systems through the phase change at almost constant temperatures, using phase change materials or PCMs.

1.2 Previous work

1.2.1 Relevance of Phase Change Materials (PCMs)

Phase change materials (PCMs) lie at the core of latent heat storage systems. During melting and solidification, they either release or absorb significant amounts of heat energy while maintaining a stable phase-change temperature. These unique thermal properties make them attractive for a wide range of engineering applications.

Over the past several decades, Thermal energy storage (TES) technologies have generated a substantial amount of research because of their promise to increase energy system flexibility and efficiency, improve efficiency, and support the integration of renewable energy sources. Thermal Energy Storage involves the temporary storage of thermal energy for later use, allowing excess heat or cold to be conserved and utilized when needed. Latent Heat Thermal Energy Storage (LHTES) has emerged as a critical technology in modern energy systems, offering a high energy density

and the capacity for nearly isothermal energy exchange through the application of phase change materials (PCMs). This approach leverages the substantial quantity of energy emitted or absorbed during the phase transition of substances—typically it is an effective way to store and retrieve thermal energy between solid and liquid phases. In contrast to sensible heat storage, which depends on temperature change, latent heat storage allows for compact system designs and stable temperature maintenance, particularly suitable for solar thermal systems, building energy management, and waste heat recovery [1], another study by Rathod and Banerjee reviews the functional principles, Thermophysical parameters and other material attributes of several PCMs for thermal energy storage systems. The paper discusses long-term stability issues of PCMs and their interactions with storage containers [2].

According to their physical properties, latent heat systems can be categorized into organic, such as paraffins or fatty acids, inorganic, which includes salt hydrates and low-melting metals, and eutectic systems [3]. Paraffin is suitable because they are capable of extending their polymer chains to suit different melting temperatures, are safe and non-reactive, with little or no superfusion [4].Fatty acids are derived from vegetable and animal oils, This makes them more durable, chemically stable, and have a greater latent heat of fusion[5].

Because of their high latent heat, non-toxicity, and biocompatibility, fatty acids have shown great promise as phase transition materials in thermal energy storage. However, limited data on their thermodynamic properties—especially heat capacity over a wide temperature range—restricts their practical use. This study measured the heat capacities of six fatty acids (C8–C18) from 1.9 K to 380 K using relaxation, adiabatic, and DSC methods. Thermodynamic functions, phase transition parameters, thermal stability, and conductivity were also evaluated. The results provide essential data for optimizing fatty acid-based PCMs in thermal energy storage systems [6].

Nazir et al. [7]develop ten eutectic phase change materials (PCMs) using fatty acids such as palmitic, myristic, stearic, lauric acids, and PureTemp68 for low to moderate temperature thermal energy storage. The eutectic compositions are identified using the Schrader equation and phase diagrams, followed by preparation via melt blending and ultrasonication. Differential Scanning Calorimetry reveals melting points ranging from ~27°C to 75°C and latent heats between ~127 210 kJ/kg. FT-IR analysis confirms the presence of carboxylic groups, indicating chemical consistency with fatty acids. These PCMs demonstrate strong potential for thermal storage within this temperature range.

Berroug et al. [8] In an east-west oriented greenhouse, assess the thermal performance of a north-facing wall that incorporates a phase change material (PCM) employed as a heat storage element. The PCM was chosen to be calcium chloride hexahydrate ($CaCl_2$-$6H_2O$). A numerical thermal model, accounting for all major greenhouse components (cover, crop canopy, indoor air, and PCM wall) and based on coupled heat and mass balance equations, was developed to assess the influence of the PCM on internal temperature and humidity. Simulations were carried out for a representative January decade in Marrakesh (31.62°N, 8.03°W). According to the findings, applying 32.4 kg of PCM per square meter of ground area raises plant and air temperatures at night by 6–12 °C while lowering temperature swings. Additionally, nighttime relative humidity decreases by an average of 10–15%.

A comprehensive study [9] was conducted utilizing a full-scale test cell split into two similar compartments to describe the hygrothermal behavior of a building solution using phase change materials (PCMs). One compartment included PCM embedded in the floor mortar, while the other served as a reference. Hygrothermal monitoring focused primarily on indoor air temperature to assess the system's capacity to reduce overheating.
A complementary numerical analysis was performed using EnergyPlus® (v9.0), testing various natural ventilation flow rates to assess the effectiveness of the PCM-based solution. The experimental results showed significant periods of thermal discomfort in both compartments, largely due to overheating. However, the cell equipped with PCM demonstrated a decrease in peak interior air temperature of over 10 °C. Simulation results further indicated that increasing natural ventilation rates decreased overheating hours almost linearly up to one air change per hour, after which the improvement became less pronounced.

Kamil Kaygusuz et al. [10] experimentally assessed Technical-grade paraffin wax's ability to store energy as a phase-change material in a vertical concentric pipe-in-pipe arrangement. The mushy zone of melting and solidification occurred between 38-43°C and 36-42°C, respectively, consistent with DSC analysis. The experiments were carried out by altering HTF's mass flow rate and inlet temperature. Radial and vertical temperature distribution data were measured for rounds of charging and draining. The experiments revealed that natural convection has a larger influence on melting. These experiments also verify that there is a larger influence of heat fraction in charging compared to discharging. This experiment showcases that this configuration has a successful energy storing potential in a passive solar application.

Despite their advantages, the commercialization of PCMs faces several technical difficulties**,** such as: low thermal conductivity, limiting heat transfer rates, leakage during melting,

especially in organic materials, Phase segregation and subcooling in salt hydrates, thermochemical instability over repeated cycles and compatibility issues with storage container materials.

These obstacles highlight the need for new PCM compositions with enhanced thermal performance, enhanced stability, and lower environmental impact.

1.2.2 Improvement of the Melting Behavior of Phase Change Materials (PCMs)

Many studies aimed to improve PCM thermal properties by modifying compositions, adding additives, and optimizing thermal management, Wang et al. [11] developed the paraffin wax (PW) nanocomposites with multi-walled carbon nanotubes (MWNTs) to enhance thermal properties for heat storage. As MWNT content increased, the melting point slightly decreased and latent heat capacity reduced. However, thermal conductivity significantly increased by 40% in the liquid state and 35% in the solid state at 2.0% MWNTs demonstrating the potential of MWNTs to enhance heat transfer in phase change materials.

Another study [12] investigates expanded graphite (EG)/paraffin composite phase change materials (PCMs) with EG mass fractions ranging from 0 to 10 wt.%, SEM images in Figure 1.1 depict the structural evolution from raw expandable graphite (a) to expanded graphite (b–d). As EG content increases compact EG networks are formed, enhancing thermal conductivity significantly—a 10 wt.% EG addition results in over a 10-fold increase compared to pure paraffin. Thermal characterization via differential scanning calorimetry (DSC) revealed that the porous EG structure influences the phase change behavior of paraffin, causing small shifts in melting and freezing temperatures (maximum deviation: 1.2 °C; peak deviation: 5.6 °C). Interestingly, the latent heat initially increased and then decreased with higher EG content. Heat storage and retrieval tests demonstrated substantial performance gains: with 10 wt% EG, the heat storage duration was reduced by 48.9% and heat retrieval by 66.5%, compared to pure paraffin. These findings confirm that EG effectively accelerates thermal response in latent heat thermal energy storage systems.

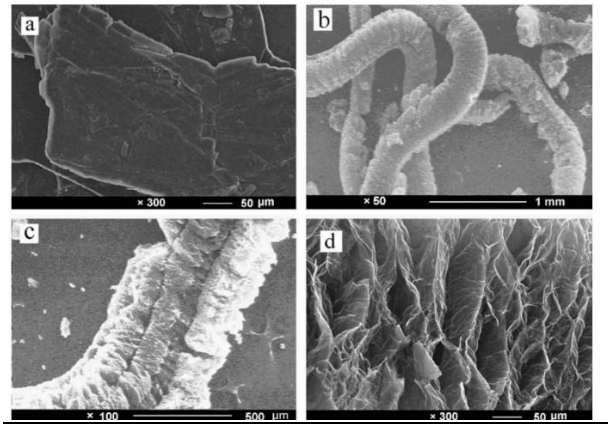

Figure 1.1 SEM images of expandable graphite (EG): (a) Raw EG at ×300 magnification; (b) Large voids among voluble, worm-like EG particles at ×50; (c) Crevice-like surface pores on an EG particle at ×100; (d) Network-like pores on or within the EG particle at ×300[12].

Chen et al. [13] aim to address the common issues of paraffin-based phase change materials (PCMs), specifically leakage and low thermal conductivity, by developing form-stable PCMs (FSPCMs) using a composite of SEBS/paraffin/HDPE impregnated into copper metal foam, as seen in Figure 1.3.The paraffin was absorbed into a SEBS copolymer matrix and encapsulated with HDPE to enhance form stability. Characterization techniques (DSC, SEM, FT-IR, XRD, and Hot Disk) confirmed uniform paraffin dispersion and chemical compatibility. The composite showed a melting temperature of 50.56 °C and latent heat of 151.6 J/g, with minimal leakage (only 2.39 wt% after 50 cycles). Embedding copper foam significantly improved thermal conductivity from 0.272 to 2.142 W/m•K, demonstrating its potential for efficient thermal energy storage.

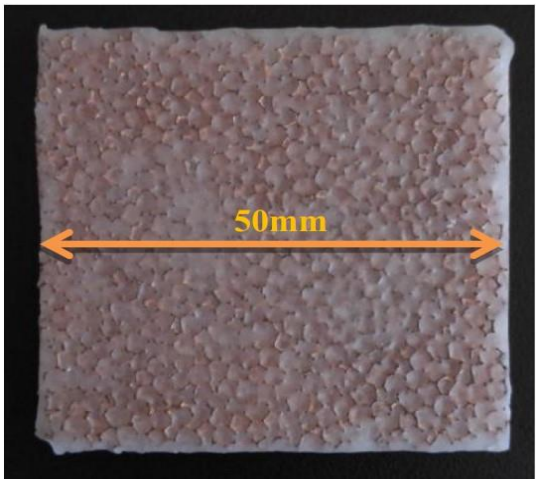

Figure 1.2 Copper foam embedded in FSPCMs[13].

Another method [14] Create form-stable expanded graphite (EG)/stearic acid (SA) composite phase change materials (CPCMs) by compressing liquid SA into EG, Figure 1.4 illustrates how the form-stable EG/SA CPCM can be prepared. The best mixture composition of 25 wt.% of EG with a density of 900 kg/m³ displays superior heat transfer characteristics with a greatly improved thermal conductivity of up to 130 times higher than that of pure SA. Moreover, the prepared CPCMs own low supercooling and anisotropic heat conduction. Another energy storage device with a modular design for efficient energy storage in CPCMs with copper tubes was also introduced

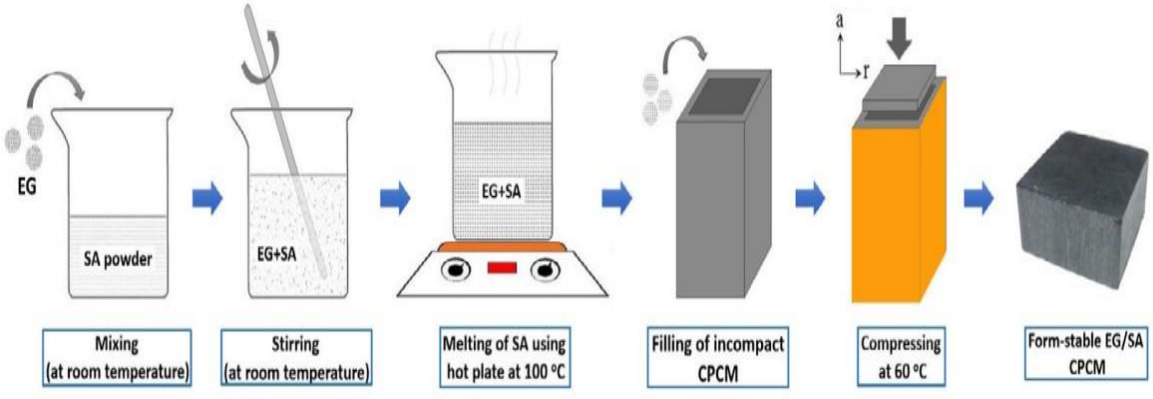

Figure 1.3 Form-stable EG/SA CPCM preparation [14].

Selvam et al. [15] looked into the thermal behavior of nanoparticle-enhanced phase change materials (NEPCM) composed of paraffin and multiwall carbon nanotubes (MWCNTs) without dispersants, Figure 1.6 displays the TEM morphology of MWCNTs and the SEM view of their dispersion . The NEPCMs exhibited significantly improved thermal conductivity in both solid and liquid states due to the high conductivity and network structure of MWCNTs. Compared

to pure paraffin, The NEPCMs exhibited a 29% decrease in melting time and a 42% reduction in solidification time at MWCNT loadings of 0.3% and 0.9%. These enhancements highlight the potential of NEPCMs for developing more efficient thermal energy storage systems across various applications.

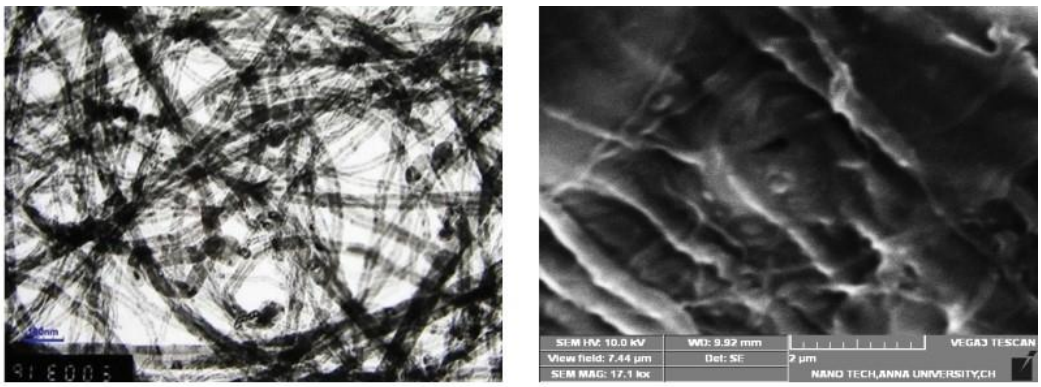

Figure 1.4 The TEM image of the MWCNT (left). The SEM image of the dispersed MWCNT (right) [15].

Amaral et al. [5] highlighted the potential of carbon-based nanostructures (CNs) to enhance hermal conductivity and latent heat performance of nanocomposite PCMs . It emphasizes the importance of balancing both properties for efficient thermal energy storage or dissipation. Most studies focus on thermal characterization using encapsulation methods, though few explain the mechanisms behind the improvements. The paper compiles experimental results, aiming to identify key features responsible for enhanced thermal performance in PCMs/CNs composites.

Another study [16] investigated enhancing the Thermal characteristics of phase change materials (PCMs) based on paraffin by adding nanoparticles to improve latent heat capacity. Paraffin was combined with Fe_3O_4, CuO, TiO_2, and ZnO nanoparticles at 5–15 wt% using a sonification method, Figure 1.7 presents the main steps of the nano-PCM synthesis process. Differential Scanning Calorimetry (DSC) revealed that latent heat increased by 20.67% (Fe_3O_4, 5%), 78.89% (CuO, 10%), 7.5% (TiO_2, 15%), and 20.17% (ZnO, 5%), with CuO at 10 wt% showing the best enhancement. The melting point remained largely unaffected by the introduction of nanoparticles. Table 1.1 summarizes the paraffin-based nano-PCMs' thermal characteristics, including melting temperature, latent heat, thermal conductivity, and specific heat. The outcomes confirm that paraffin-based Nano-enhanced PCMs exhibit excellent performance for energy storage applications.

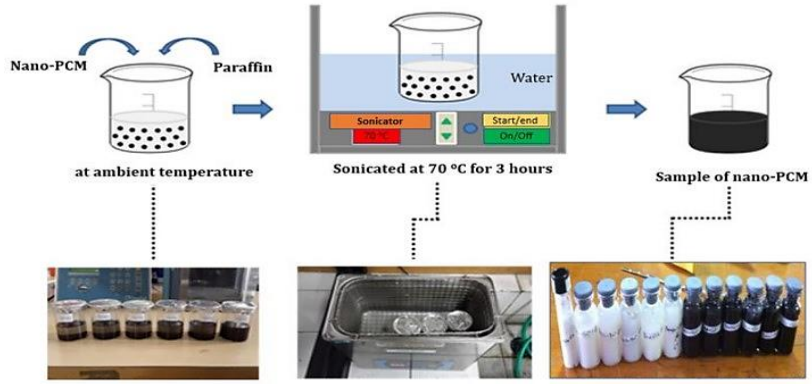

Figure 1.5 Synthesis of nano-PCM[16].

Mekaddem et al. [17] aimed to create a composite for buildings' passive heating and cooling using a paraffin (RT27) and expanded perlite (EP) mixture, which was then mixed with plaster. To make it waterproof, a waterproofing layer was applied to protect it from leakage of paraffin. An optimal amount of 60% paraffin was obtained using direct impregnation. The result of FTIR studies proved that there were no toxicity issues among all components, and DSC values indicated a high level of energy storing capacity of 51.57 kJ/kg for a mixture of RT27, EP, and SL, as well as 49.95 kJ/kg when aluminum powder was also present. Addition of aluminum showed a substantial increase in thermal conduction, increasing by 80% and 68% at 12°C and 40°C, respectively.

Han et al. [18] studied The creation of phase change materials (PCMs) with form stability using aggregated carbon nanotubes (A-CNTs) with interwoven porous structures, As shown in Figure **1.8**, A-CNTs are synthesized using CVD and subsequently compounded with paraffin to prepare nanocomposite PCMs.The capillary action within the A-CNTs enabled effective encapsulation of paraffin, achieving a high loading capacity of up to 88 wt% and a thermal storage capacity of 172.14 J/g exceeding values predicted by the mixing rule. Dispersing CNTs randomly led to reduced performance, confirming the structural advantage of A-CNTs. The composites also showed enhanced heat conductivity and faster thermal response, making them strong candidates for applications of thermal management.

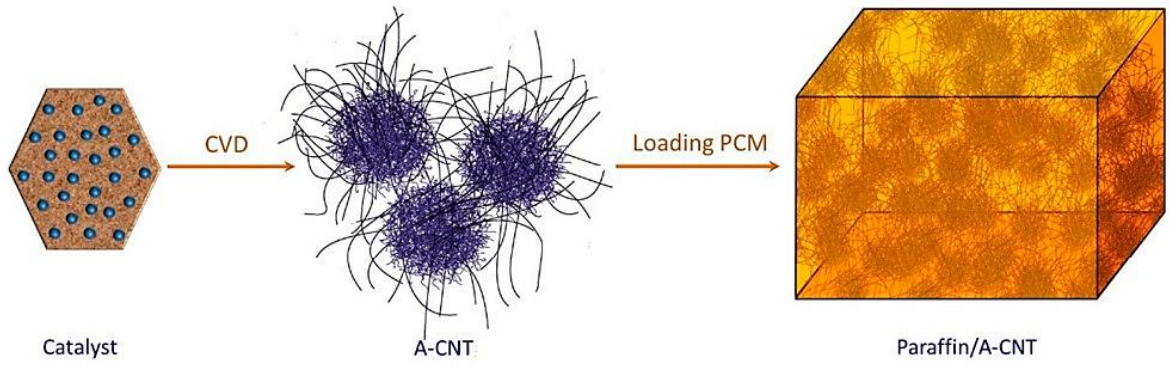

Figure1.6 Schematic of A-CNTs synthesis via CVD and their incorporation with paraffin for nanocomposite PCMs [18].

Shang et al. [19] introduced A thermal storage device that is modular (MTSU) for overcoming disadvantages of traditional solid-liquid phase change materials in continuous thermal energy storing as well as cooling electronic equipment. After completely melting a PCM in a unit, it becomes feasible to replace it with a new unit, which maintains continuous operation of electronic equipment as it provides online charging and offline discharging for it. The proposed "MTSU" structure involves encapsulating paraffin in epoxy resin with copper and nickel foams for enhanced thermal performance. Experiments demonstrated a notable rise in effective thermal conductivity of 376% for copper foam with 95.52% porosity and 205% for nickel foam with 95.61% porosity. It also retains excellent long-term thermal stability for numerous cycles. Contrary to conventional thermal storage units, this MTSU" overcomes delayed re-solidification in continuous long-term thermal energy storage in battery cooling.

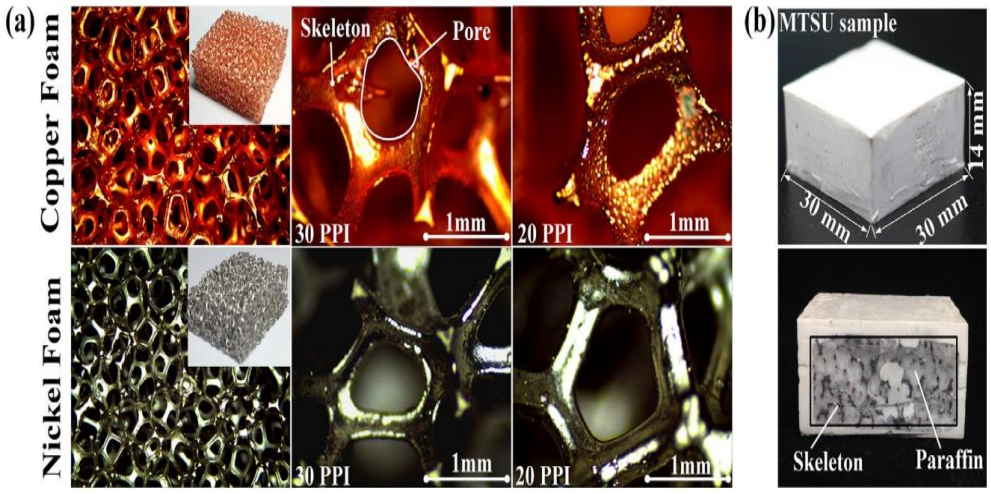

Figure1.7 (a) Skeleton structures of copper foam and nickel foam (b) The prepared MTSU sample. [19]

Al-Jethelah et al. [20] studied melting of a coconut oil nano-PCM increased by CuO inserted in porous aluminum metal foam of 88–96% under constant heat flux. Both nanoparticles and metal foam improve melting, but the foam has the dominant effect: a 1.2% enhancement with nanoparticles alone compared to 41.2% and a 28.81% increase in energy storage rate with the foam. Melting is more uniform at low porosity (88%, conduction-dominated) and becomes non-uniform at high porosity (96%, combined conduction–convection). Figure 1.9 shows the temperature evolution at an internal point. These results draw attention to the possibilities of such structures for thermal energy storage, BTMS, and electronics cooling.

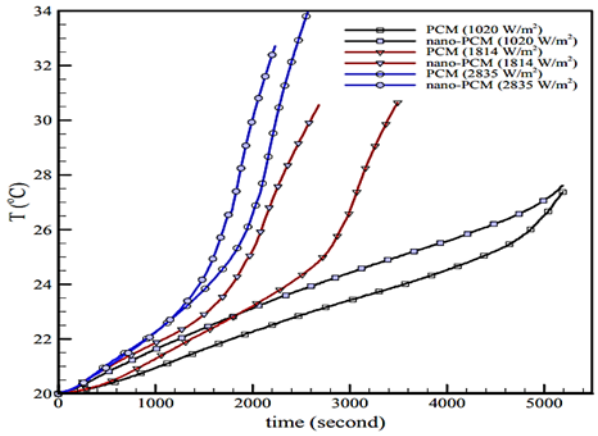

Figure 1.8 Temperature–time curves of PCM and nano-PCM for various heat fluxes[23]

The impact of low SiO_2 nanoparticles concentrations on the thermal properties of paraffin wax for solar thermal energy storage was studied by Manoj Kumar et al. [21]. Four nano-paraffin composites were ready with 0.0, 0.5, 1.0, and 2.0 mass% SiO_2, respectively (Figure 1.9). Experimental characterizations demonstrated that the nanoparticles dispersed well and the thermal conductivity was enhanced by 12.78%, 22.78%, and 33.34% at those respective concentrations. Similarly, the addition of SiO_2 improved thermal stability, slightly altered the melting/solidification temperatures, and did not change the chemical structure. Conversely, latent heat dropped as a function of increasing nanoparticle content, especially after 1.0%. Conclusions are that low-mass SiO_2 additions enhance the thermal performance of paraffin for uses in energy storage.

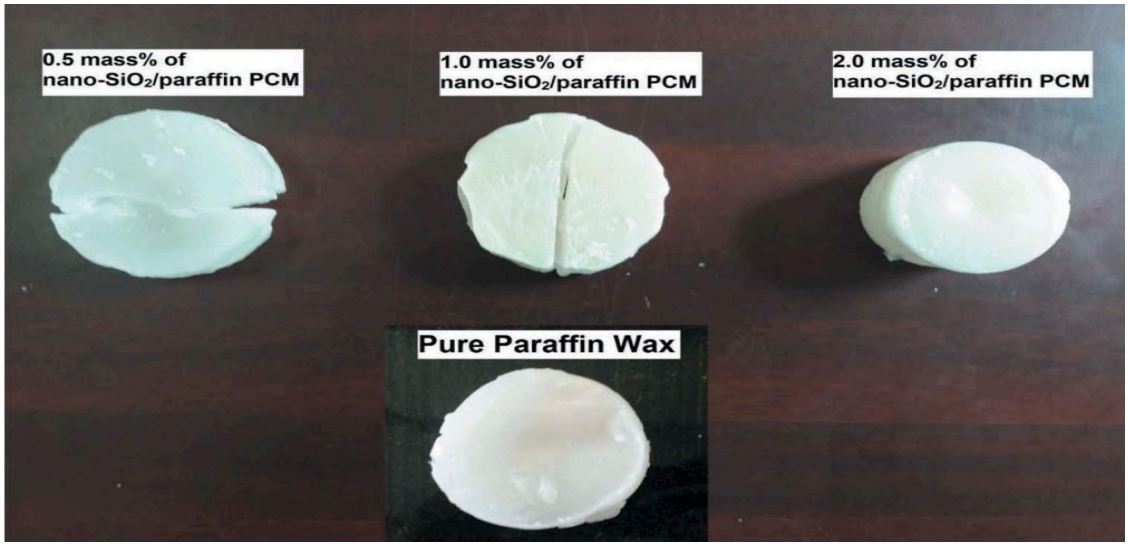

Figure 1.9 Photograph of nano-SiO_2/paraffin composite phase change material samples [21].

George et al. [22] investigated enhancing paraffin wax for solar energy storage by adding polyaniline (PANI) and cupric oxide (CuO) nanoparticles. Characterization via FTIR, TGA, DSC, UV–VIS, and thermal conductivity testing revealed improved properties. Paraffin/PANI and paraffin/CuO composites showed latent heat increases of 8.20% and 7.81%, respectively. Thermal conductivity improved by 46.8% for 1 wt% PANI and 63.6% for 1 wt% CuO. After 200 thermal cycles, the paraffin/PANI composite demonstrated superior thermal reliability and performance, turning it into a promising candidate for solar thermal energy storage applications.

Chen et al. [23] developed a composite phase change material (PCM) (Figure1.10) using paraffin wax (PW) and a hybrid graphene aerogel (HGA) made of carbon nanotubes and graphene oxide. The HGA serves as a thermally conductive skeleton, sealing the PW and enhancing heat transfer. With just 2.2 wt% HGA, the composite PCM attained a thermal conductivity of 0.46 W/m·K—1.77 times that of pure PW—and high solar absorptance, 1.4 times higher than PW. Despite the added materials, the PCM maintained comparable heat storage capacity. Numerical simulations confirmed its effectiveness in solar thermal storage systems, showing rapid charging and discharging speeds and high energy storage.

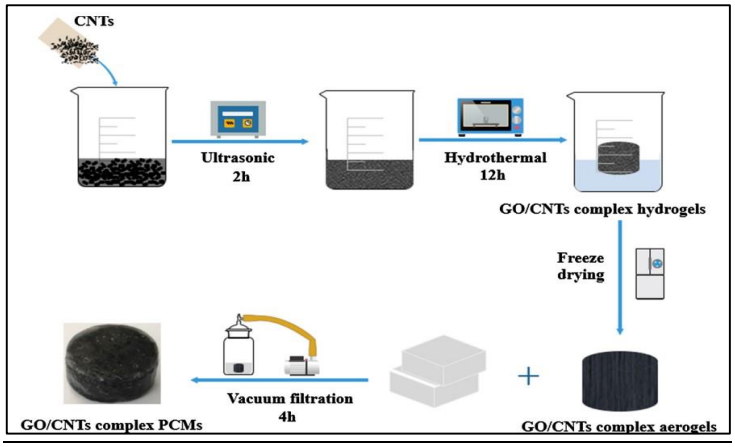

Figure 1.10 Schematic representation of the preparation process of composite phase change materials [23].

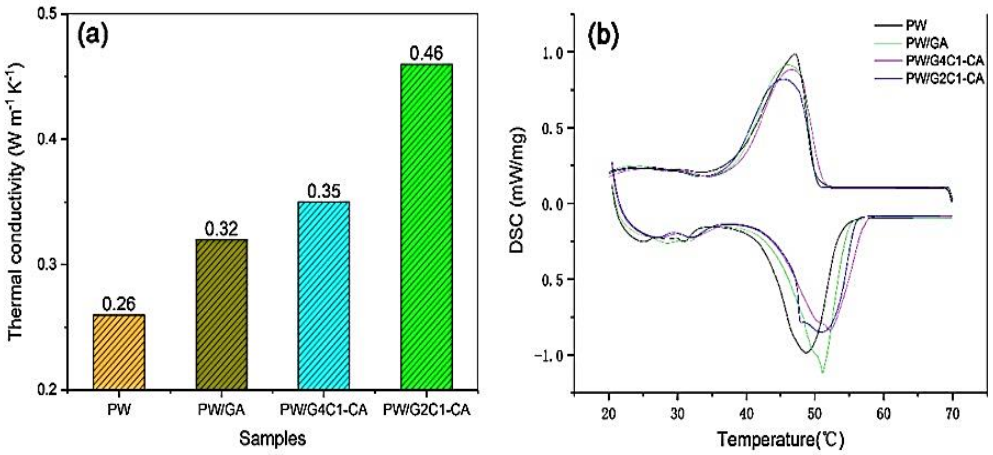

Figure 1.11(a) Thermal conductivity of pure paraffin (PW) and composite PCMs,(b) Differential scanning calorimetry (DSC) curves of PW and composite PCMs.

[23].

Zhang et al. [24] presented a paraffin/diatomite composite for thermal energy storage, enhanced by modifying diatomite with an oleophobic agent (1H,1H,2H,2H-perfluorodecyltriethoxysilane) to prevent leakage during phase transitions. The composite achieves a high percentage of encapsulation 84.5% and maintains thermal stability over 50 melting/freezing cycles. Simulations show that using this composite in building windows can reduce indoor temperatures by 5.3 °C, highlighting its potential for smart, energy-efficient building applications.

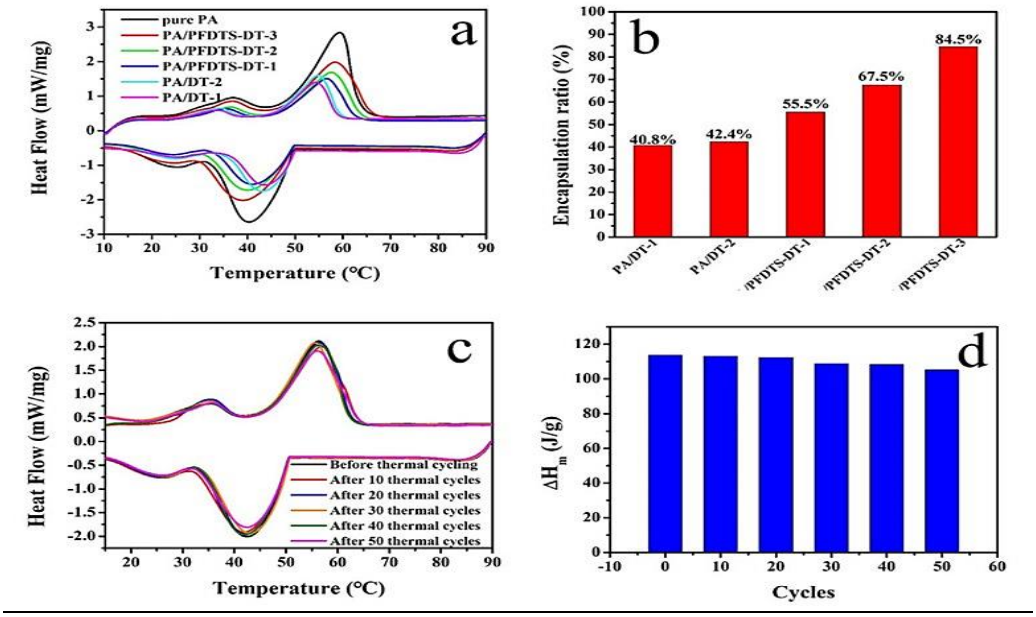

Figure 1.12 (a) DSC curves and (b) corresponding encapsulation ratios, calculated from melting enthalpy, for PA, PA/DT, and PA/PFDTS-DT composite PCMs with varying PA contents.(c) DSC curve of PA/PFDTS-DT-3 composite PCM and (d) corresponding melting enthalpy before and after multiple thermal cycles[24] .

Gogoi et al. [25] introduced waste carbon exhaust particles into paraffin wax, achieving a 155% increase in thermal conductivity while maintaining 92% of the original latent heat after 60 cycles.

A study was carried out by Gunjo et al. [26] regarding the performance analysis of a latent heat storage device using a paraffin-based nanofluid with aluminum oxide nanoparticles. A 3D numerical model was employed utilizing the COMSOL Multiphysics program. The results reveal that when 10% of Al_2O_3 nanoparticles are being used in paraffin, it enhances the rate of melting by 2.25 and solidification by 1.8 times. Although this has decreased the specific heat and latent heat values, it has slightly impacted energy storage. This technology has potential in being coupled with solar-based water heaters for use in biogas productions

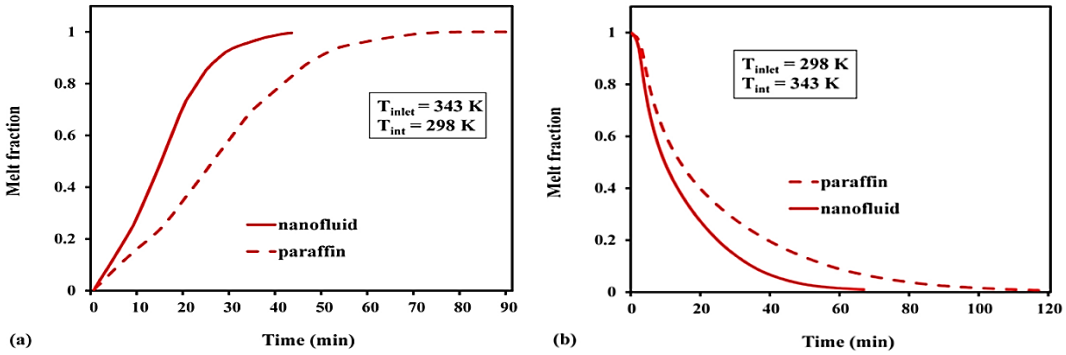

Figure 1.13 fraction (average): (**a**) during charge; (**b**) during discharge [30].

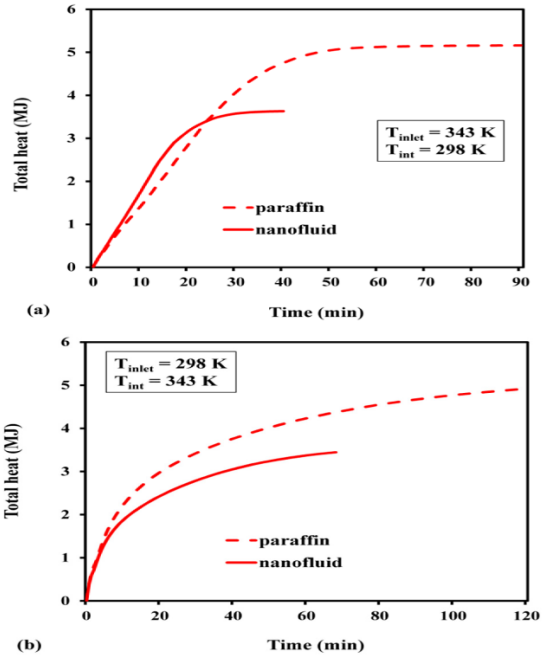

Figure 1.14 Total heat: (a) during the charging process; (b) during the discharging process [26].

Also, a study has been done to leverage a hierarchical macro-nanoporous metallic structure for a shape-stabilized PCM without leakage and with high thermal conductivity. Grosu et al. [27] show that immobilizing PCMs in a hierarchical trimodal macro-nanoporous metallic structure like copper can provide a marked improvement in thermal conductivity with no leakage. This study reveals that it has a thermal conductivity of at least three times more than paraffin-based.

Suraparaj et al. [28] introduced a method of composite thermal energy storage (CTESS) using a 1:1 blend using paraffin wax (PW) and used cooking oil (UCO) to improve solar still (SSUCO) performance for seawater desalination. In contrast to a traditional solar still (CSS), the SSUCO achieved 56.83% and 53.14% higher freshwater yields on days 1 and 2,

respectively, and thermal efficiencies of 45.52% and 41.67% (vs. 29.03% and 27.21% for CSS). Economic analysis showed a 40.54% reduction in cost per liter and a shorter payback period. Environmentally, SSUCO gained 64.2% more carbon credits than CSS, highlighting CTESS as an effective, sustainable desalination method.

Tetukoet al. [29] investigated the use of phase change materials (PCMs) paraffin-magnetite composite, paraffin, and polyethylene glycol (PEG) encapsulated in copper tubes within concrete for thermal energy storage. Copper tubes arranged in different patterns were embedded in concrete blocks and filled with PCMs. Analysis included morphology, melting point, latent heat, and thermal conductivity. PEG showed the highest melting point (61.65 °C) and latent heat (161.53 J/g). Adding magnetite to paraffin improved thermal conductivity (0.53 W/m·°C) compared to pure paraffin (0.32) and PEG (0.28). The PCM's thermal performance in concrete depended on its thermal properties, with copper tubes providing minimal thermal resistance.

Younis et al. [30] was icorporating anisotropic metal foam layers into LHTES systems was found to enhance thermal performance. Strategically placing the metal foam to direct heat towards specific areas reduced the phase transition time by up to 13.12%. Adjusting the anisotropy parameter (Kn) from 0.1 to 0.2 and optimizing the orientation angle (ω) to 45° further improved melting efficiency. These findings highlight the importance of metal foam orientation and properties in optimizing LHTES systems.

Samara et al. [31] improved paraffin wax (Bio-PCM) by adding 1% and 3% alumina (Al_2O_3) nanoparticles, achieving a nonlinear thermal conductivity increase but reducing latent heat. The optimal composition (1% VF) had 0.307 W/m•K thermal conductivity and 207.43 J/g latent heat. Stability tests confirmed reliability under thermal cycling.

Another study [32] experimentally examined how graphite powder affects the thermal behavior of a paraffin–ceresin (PC) composite PCM that uses water as the fluid for heat transfer. Tests were performed to evaluate the heating response of PC with different graphite contents. As shown in Fig. 1.17, graphite was added in various amounts to assess its influence on heating rate and melting time. Results showed that graphite significantly accelerated heating Combining water and PC because of its high heat conductivity. The melting time of PC decreased by up to 17.2% when 40 g of graphite were added to 500 g of PC, beyond which the improvement stabilized, indicating 40 g as the optimal dosage. These outcomes provide useful guidance for optimizingPCM-based thermal storage systems With uses like greenhouse heating and heat pump drying, and solar thermal storage.

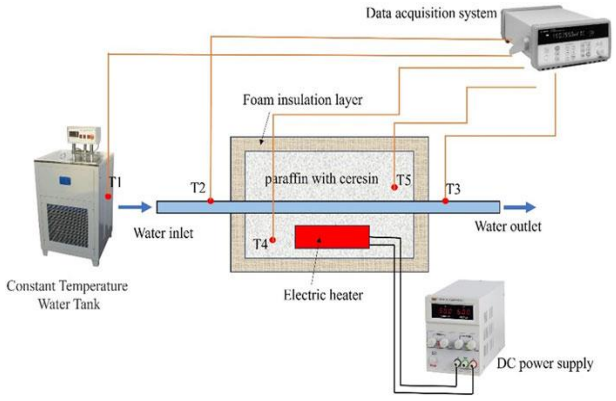

Figure 1.15 Experimental apparatus for assessing phase transition materials' thermal performance [32].

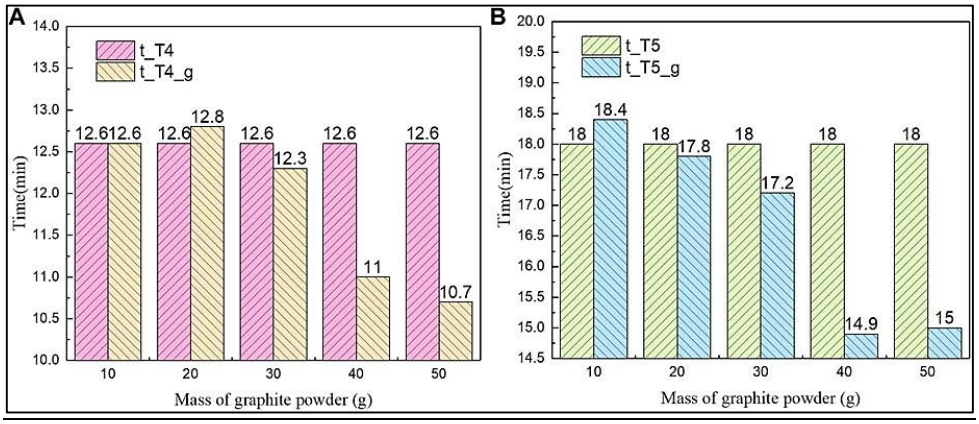

Figure 1.16 Time required to reach the melting temperature of PCM samples with and without graphite powder: (A) T4; (B) T5 [32]

Figure 1.16 displays the time required to get the PCM to its melting point material at positions T4 and T5 decreases slightly with graphite powder additions up to 30 g, but drops significantly at 40 g and stabilizes beyond that.

Meanwhile, erythritol-based PCMs have been explored for solar thermal fuels, demonstrating latent heat releases of up to 224.9 J/g and temperature elevations of 91°C upon mechanical stimulation. These innovations highlight a shift toward multifunctional, sustainable PCMs capable of addressing diverse energy storage challenges [33].

Yadav et al. [34] addressed the low latent heat and conductivity of organic PCMs by creating a composite with wheat husk microparticles in paraffin wax, achieving a 4.57% and 66.66%

enhancement in conductivity and latent heat, respectively, with consistent performance across 500 thermal cycles.

Similarly, Emeema et al. [35] used carbon quantum dots, enhancing latent heat storage by up to 65.1% and improving the material's thermal stability.

Castell et al. [36] demonstrated that the addition of external vertical fins improves PCM's performance during the solidification process, this effect can be observed by the full time necessary for the solidification of the PCM from 60ºC to 45ºC, when using 20 mm fins and 40 mm fins, the needed time reduced (a reduction of 23.53% and 58.82% respectively), while the increase of the heat transfer area enhanced the performance of the PCM.

Gasia et al. [37] examines two methods for improving heat transmission in a latent heat thermal energy storage (TES) system: metal wool and fins. Although fins are effective, their implementation increases system cost, motivating the evaluation of low-cost, commercially available metal wool as an alternative. Four shell-and-tube TES units (Figure1.17) using n-octadecane were built: one reference system, one with seventeen rectangular fins, and two with metal wool (randomly distributed or compacted into a fin-like shape) (Charging and discharging tests were performed under constant temperature and flow rate of the heat-transfer fluid. Findings indicate that randomly distributed metal wool improves charging performance by more than 10%, while the compacted wool configuration offers almost no benefit. During discharging, both metal wool arrangements provide only minor improvements. These findings highlight metal wool as a simple and inexpensive enhancement option for retrofitting existing heat exchangers.

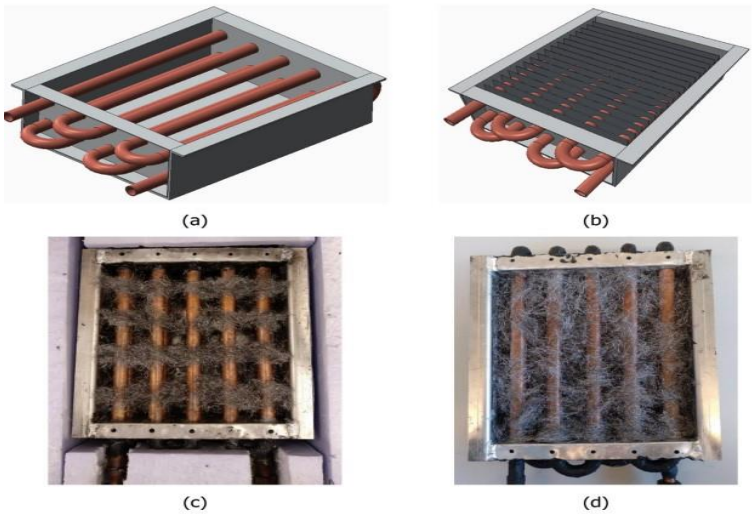

Figure 1.17 Schematic overview and photographs of the latent heat exchangers tested in this study:(a) HEX_NF: Reference configuration;(b) HEX_17F: With seventeen fins; (c) HEX_MW1: Metallic wool arranged in a finned pattern around the HTF tube bundle; (d) HEX_MW2: Metallic wool randomly distributed around the HTF tube bundle. [37]

Another study [38] examines the liquefaction of phase-change materials both computationally and experimentally in an LHTES tank using a dynamic melting approach based on Recirculation of liquid-PCM. Experiments evaluate melting time and mean power under different flow configurations and inlet velocities, while CFD simulations analyze liquid fraction, vorticity and temperature fields to clarify heat-transfer mechanisms. Images of the ice–water interface and temperature measurements validate the numerical model. Results identify an optimized top-down recirculation layout with an inlet velocity of 0.22 m/s, reducing total melting time by 48.1% and increasing mean power by 132.6%.

J. Wang et al. [39] investigate applying (PCMs) as effective stores of thermal energy to improve the working solar heating and cooling systems' adaptability and stability. With their latent heat property, PCMs are able to counteract the intermittence of solar energy input. This study aims to look into the HT of a PCM-based triplex-tube heat exchanger with a structure of lobed surfaces and Y-type fins, using RT58 as PCM. The innovations of this research are focused on assessing HT of sensible, latent, and total energy as well as instant and averaged HT release rates in HT processing.

A CFD-based numerical study [40] analyzed LiCl as PCM in a triplex-tube heat exchanger for nuclear thermal energy storage, comparing finned and unfinned configurations (Fig 1.18) with fin lengths from 5 to 35 mm. The analysis focused on melting evolution, temperature fields,

enhancement ratio, and heat flux. According to Fig. 1.19, fins markedly accelerated LiCl melting by increasing the heat-transfer area and improving interaction with the FLiBe coolant; 35 mm fins cut melting time by about 50% due to stronger convection and more uniform temperatures. However, increasing fin length from 5 to 35 mm reduced the average heat flow at the surface. The results provide useful guidance for designing more efficient heat exchangers in nuclear TES systems.

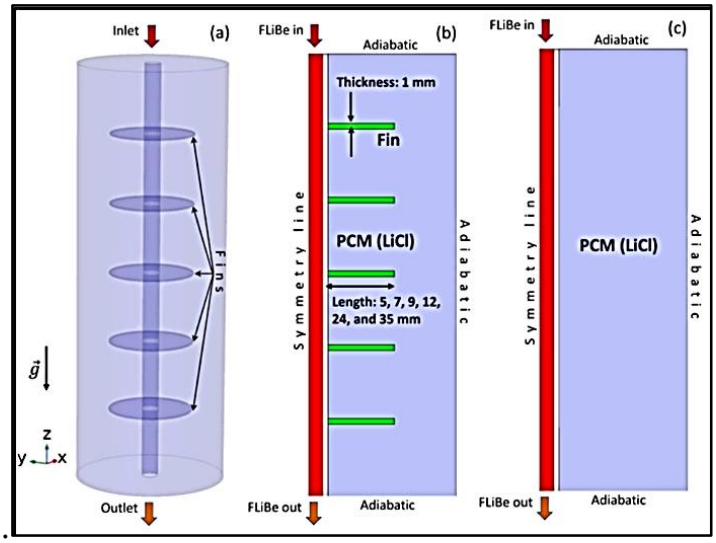

Figure 1.18(a) 3D schematic of the charging mode with fins;(b) 2D axisymmetric computational domain with fins;(c) 2D axisymmetric computational domain without fins, as used in the numerical simulations. [40].

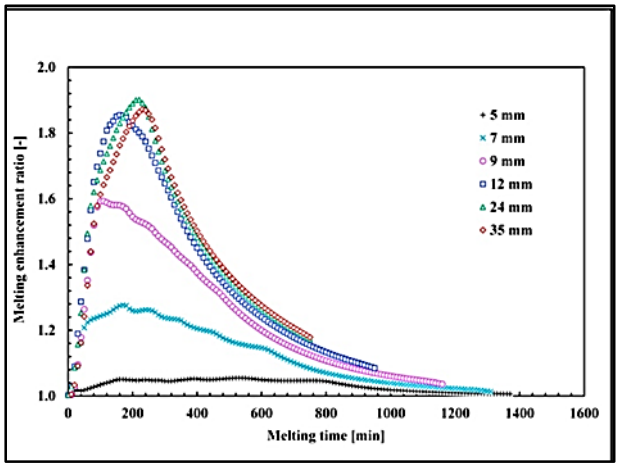

Figure 1.19 Comparison of melting enhancement ratios for the base case and configurations with different fin lengths [40].

Latent heat TES systems can smooth fluctuations between solar heat supply and heating demand, However, the limited heat conductivity of PCMs limits their performance. Crnjac et

al. [41] evaluated A four-pass storage module with a rectangular shape enhanced with steel wool, aluminum wool (Fig. 1.20), and an aluminum honeycomb (Fig. 1.21), comparing them to an unenhanced unit. Steel wool showed the weakest effect, lengthening charging time by 60% and improving discharging only modestly (factor 1.28). Aluminum wool performed better, reducing charging and discharging times by factors of 1.62 and 2.33. The aluminum honeycomb offered the strongest enhancement, with improvement factors of 3.11 (charging) and 3.88 (discharging), owing to deeper heat penetration and maintained natural convection within its narrow vertical channels. These results provide useful guidance for designing high-performance solar thermal storage modules.

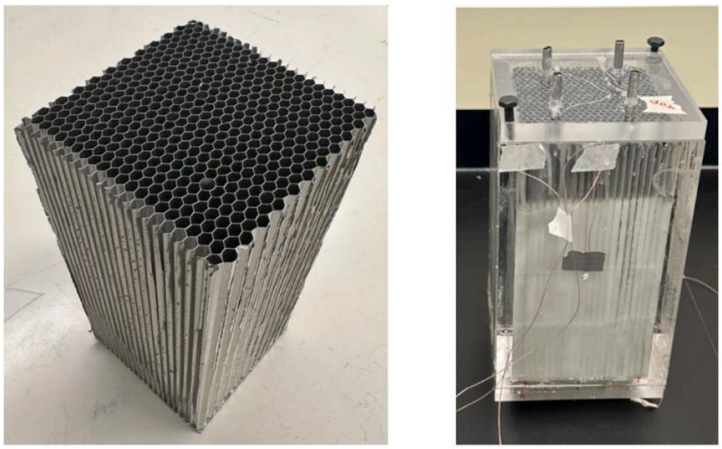

Figure 1.20 Photo of the raw aluminum honeycomb core (left) and the honeycomb core integrated into the PCM module with inserted tubes (right).[41]

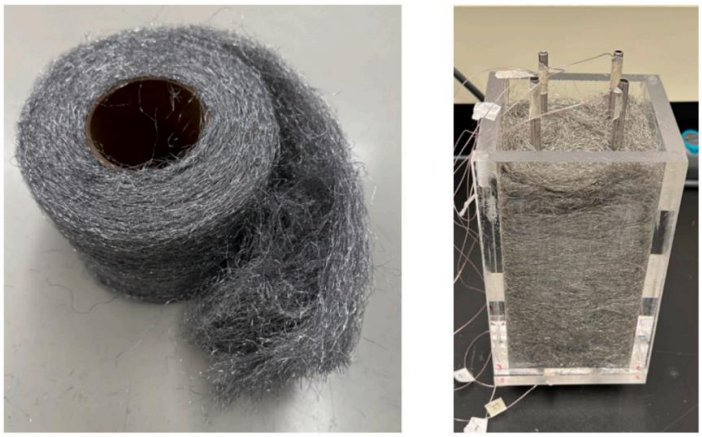

Figure 1.21 Image of metal wool (left) and the thermal storage module containing metal wool and PCM (right)[41].

Marzouk et al [42] investigates PCM melting in a heat exchanger using a helical coil and a simple tube, longitudinal fins, and constructed fins (Fig.1.22). Water is used as the heat transfer

fluid and paraffin wax as the PCM. Numerical simulations performed in Ansys Fluent evaluate the temporal evolution of liquid fraction, temperature, and overall melting effectiveness. Results show that longitudinal fins and constructed fins increase the liquid fraction by 52% and 65%, respectively, while reducing melting time by 29% and 50%. The melting effectiveness decreases over time as the outlet water temperature drops. Constructed fins provide superior enhancement by enlarging the heat-transfer surface and strengthening conduction–convection interactions. Melting initiates radially from the tube wall, and the presence of fins accelerates heat transfer, increases the liquid fraction, and significantly improves PCM melting performance.

Figure 1.22 Configurations of the HCHX: (a) plain tube; (b) longitudinal fins; (c) constructed fins[42].

Ahmed et al. [43] whereby it numerically analyses a combination of heat flux incidence and system orientation as a mechanism of influencing finned LHTES unit charging. A numerical simulation of n-docosane mushy layer melt-down in a rectangular enclosure with four different heat flux incidents and four different orientations of 0°, 10°, 20°, and 90° illustrates that for a vertical position of 90°, a melt rate can increase by over 30% compared with a 0° position for a similar value of heat flux. Higher orientations result in lower peak temperatures of the absorber plate.

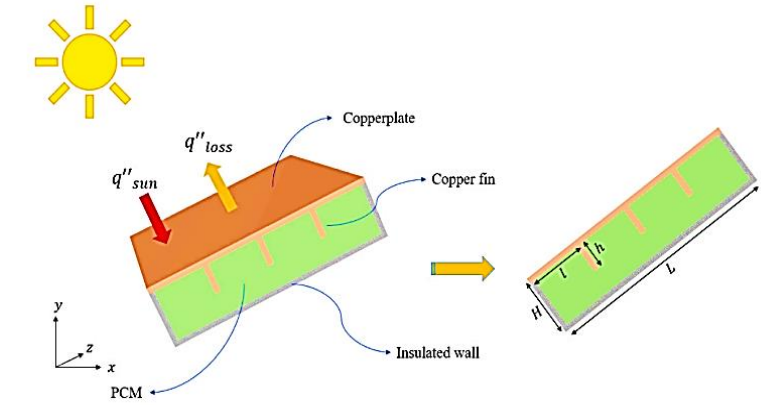

Figure 1.23 Schematic of the rectangular thermal storage unit, showing the geometry and applied boundary conditions. [43].

Another study [44] experimentally examined the impacts of fins and enclosure inclination on the melting of lauric acid in side-heated rectangular cavities. Using acrylic enclosures with an aluminum heating plate, melting behavior was evaluated for 0 and 3 fins at 90°, 45°, and 0° inclination angles. According to Fig. 1.23, temperature fields revealed that lowering the inclination angle strengthens natural convection and markedly speeds up melting. A horizontal (0°) finless enclosure enhanced heat transfer by 115% compared to the vertical (90°) case, exceeding even the 56% improvement of the 3-fin vertical setup, while the 3-fin horizontal configuration melted fastest. The results show that inclination can influence melting more effectively than fins and provide useful data for future numerical simulations.

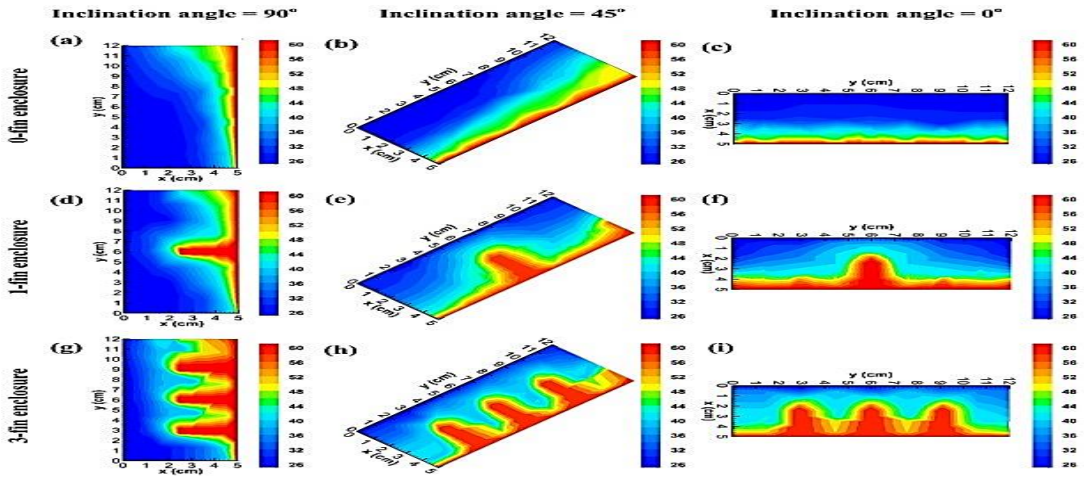

Figure 1.24 Temperature distributions in finned and unfinned enclosures at t = 45 min for different inclination angles [44].

Another research [45] focused on the thermal and flow characteristics of a low-temperature phase change material (PCM) composed of paraffin wax encapsulated in melamine-formaldehyde and mixed with water, with a phase change range of 4–6 °C and a heat storage capacity of 72 kJ/kg. Experimental tests were conducted using cylindrical modules of varying diameters in a wind tunnel under Reynolds numbers from 15,250 to 52,750 to simulate real operating conditions. An enthalpy-porosity method-based numerical model was created and verified, showing a relative error under 20% during phase transitions. SEM analysis confirmed the PCM maintained a stable and homogeneous structure throughout phase changes, demonstrating suitability for industrial thermal energy storage applications.

1.2.3 Determination of the thermophysical proprieties of PCM

Lately, assessing the thermal properties of Phase Change Materials using modern techniques has been very important for identifying their potential in storing thermal energy. Differential Scanning Calorimetry (DSC) has proved to be a popular tool for analyzing various parameters of PCM, including their phase change temperatures, enthalpy of fusion, and specific heat. The principle of Differential Scanning Calorimetry involves analyzing the heat flow, which depends on a certain range of temperatures. Another popular analysis technique that has been used, comparable to Differential Scanning Calorimetry, has been Differential Thermal Analysis. This involves analyzing the differences in temperatures of a sample, which requires a counterpart that has similar conditions, hence analyzing the variations in phase. Another technique that has been applied to analyzing Phase Change Materials has been the T-History analysis, which has been suggested by Zhang et al. [46] in his study as a method for analyzing "melting point, enthalpy of fusion, specific heat, and thermal conductivity of PCMs."

In contrast to conventional techniques like calorimetry, DTA, and DSC, this method offers key advantages: it uses a straightforward experimental setup, allows simultaneous testing of multiple samples, and enables direct observation of the phase change process. It was used to measure the thermal properties of various PCMs, including salt hydrates, paraffin, and newly developed materials.

Many researchers are using this methods such as Ana Lazaro et al. [47], who validated a T-history setup using three reference materials (gallium, water, hexadecane) and two PCMs (RT27 and a sodium acetate trihydrate–graphite composite, SAT+G). For gallium, the

measured enthalpy was 79.5 $J \cdot g^{-1}$, in excellent agreement with the literature value of 79.88 $J \cdot g^{-1}$. The phase change temperature of water also closely matched published data, and the enthalpy curve of hexadecane obtained by T-history was consistent with DSC results. For the non-pure materials RT27 and SAT+G, the method also performed well. The authors emphasized careful sensor calibration, accurate temperature measurement, and correct enthalpy evaluation. Overall, the research verified that the T-history approach is suitable for characterizing latent heat storage materials for practical applications.

Chiu and Martin [48], they employed the T-history approach to describe the phase transition range, specific heat, and total heat capacity of the salt hydrate and paraffin, Figure 1.25 shows (a) The experimental setup's schematics, (b) the probe positioning, and (c) the insulation. From the results obtained by this study the T-history is demonstrated to be a consistent and appropriate technique for proprieties characterization, allowing for the implementation of specific heat values obtained from the PCM into numerical models for TES system design and performance studies.

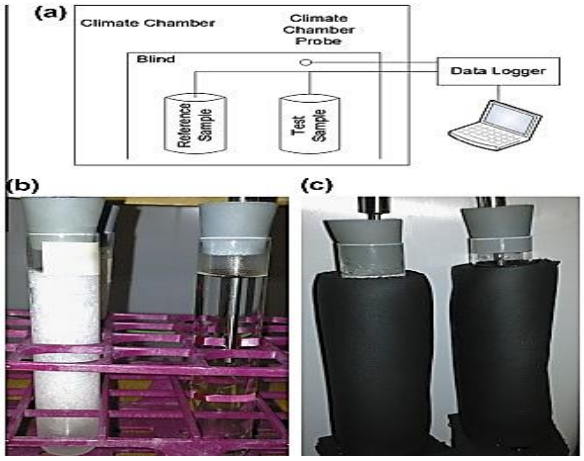

Figure 1.25 (a) Schematic of the experimental setup ;(b) Probe positioning;(c) Insulation arrangement. [48].

Rady [49] has published a study using the T-history method for granular phase changing composites, and amendments were also introduced for those materials that are in a phase of change over a range of temperatures, whereupon they noted that it has been found that “the accuracy of the T-history test is, in principle, limited by model simplifications in assuming a constant specific heat with respect to temperature, as well as uncertainties in defining boundaries between solid and liquid phases,”

The enthalpy-temperature and apparent heat capacity plotted for granular encapsulated phase change material are similar to those produced by using Differential Scanning Calorimetry.

Lovelyn Theresa and Velraj R. R. [50] evaluated the thermophysical properties of phase change materials using both DSC analysis and T-History experimental setup, in this paper, three organic PCMs are used, namely, RT27, RT28 HC, and OM21, and inorganic hydration salt PCMs, namely, HS24 and HS29, it was found that the characterization technique of T-History is efficient when compared to that of DSC analysis.

The presentation given by I. M. Sutjahja et al. [51] in this conference examined how different concentrations of dopants in nanoparticles of graphite, CuO, and ZnO affect the values of the thermal conductivity of a coconut oil-based phase change material PCM using a "T-history" method, with a concentration of 2% and 1%, as shown in Figure 1.26. The scanning electron microscopy images of (a) graphite, (b) CuO, and (c) ZnO used as dopants for PCM co-oil are shown. The result of this experiment showed that a dopant of 1% gave a peak value in solid thermal conductivity. This experiment proved that it was a proper methodology for measuring the value of PCM coconut oil's thermal conductivities, as well as analyzing effects from different dopants.

Lovelyn Theresa and Velraj R [50] examined the thermophysical characteristics of phase change materials (PCMs) using both DSC analysis and T-History experimental setup. This study examined two inorganic or hydrated salt PCMs (HS24 and HS29) and three organic PCMs (RT27, RT28 HC, and OM21). The findings indicated that the T-History method of characterization is superior to DSC analysis.

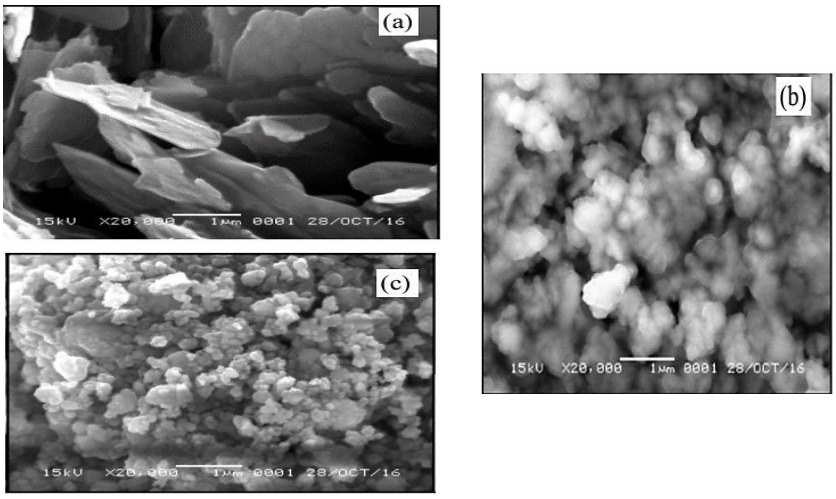

Figure 1.26 Scanning electron microscope (SEM) images of dopant materials for PCM co-oil: (a) graphite, (b) CuO, and (c) ZnO [62].

This technique has also been utilized to determine the thermophysical characteristics of the nano-enhanced phase change materials (NEPCMs) [52], like their specific heat, enthalpy of solidification, and thermal conductivities, NEPCMs are prepared with three different dispersions of GNP aggregates and alumina and silica nanoparticles in a binary combination of stearic acid and paraffin wax (Figure 1.27), then the results of the values obtained from this method were compared using other methods of measurement, which are Transient planar source with DSC. The findings gave a deviation of 10% for enthalpy of solidification and 7% for thermal conductivities of NEPCMs, The thermophysical characteristics' values for the PCM were discovered to be consistent with values published in literature.

Figure 1.27 Photographs of the basic PCM was distributed via 1.0 wt.% nano-additives: (a) after 1 h in the molten state, and (b) after maintaining for 18 h [52].

Table 1.1 Comparison of the phase change onset temperature, enthalpy of fusion, and thermal conductivity obtained using various measurement techniques [52].

Samples	*Solidification temperature (°C)*		H_m *(solidification) (J/g)*	H_m *(J/g)*		*k (W/m·K)*	
	DSC	T-history	DSC	T-history (t–T curve)	T-history (T–H curve)	TPS	T-history
Base PCM	53.7	54.1	171	168	170	0.294	0.267
Base/Al_2O_3_0.1	52.6	53.8	162	157	151	0.315	0.295
Base/Al_2O_3_1.0	52.7	54.2	137	124	138	0.345	0.338
Base/SiO_2_0.1	52.6	53.8	163	156	148	0.280	0.288
Base/SiO_2_1.0	52.4	53.9	156	149	136	0.319	0.317
Base/GNP_0.1	53.6	54.2	160	156	161	0.324	0.299
Base/GNP_1.0	52.4	54.4	143	134	137	0.376	0.348

Chapter 2 Thermal Energy Storage Concepts and PCM Technologies

2.1 Introduction

The increasing reliance on renewable and technology for sustainable energy underscores the critical role of energy storage systems. Since renewable sources such as solar and wind are inherently intermittent, efficient storage solutions are necessary to ensure a reliable balance between energy supply and demand. In this context, thermal energy storage (TES) is particularly important, as it enables the retention of excess heat or cold for subsequent use. Among the various TES approaches, latent heat storage with phase change materials (PCMs) is especially promising, owing to its high energy density and nearly isothermal operation within a narrow temperature range.

2.2 Thermal energy storage concepts

TES offers a high-capacity and economically viable pathway for both heat management and electricity generation. However, the inherent intermittency and uneven availability of solar radiation reduce system reliability. To overcome these challenges, advanced TES technologies are being developed to enhance dispatch ability, enable load shifting, and maximize the utilization of stored energy, even under conditions of low or fluctuating solar input [53] .

2.2.1 Classification of TES Methods

TES technologies are generally classified according to the mechanism of storing energy. Depending on the chosen storage medium, Latent heat and sensible heat are two ways that energy may be stored, or through thermochemical processes [54].

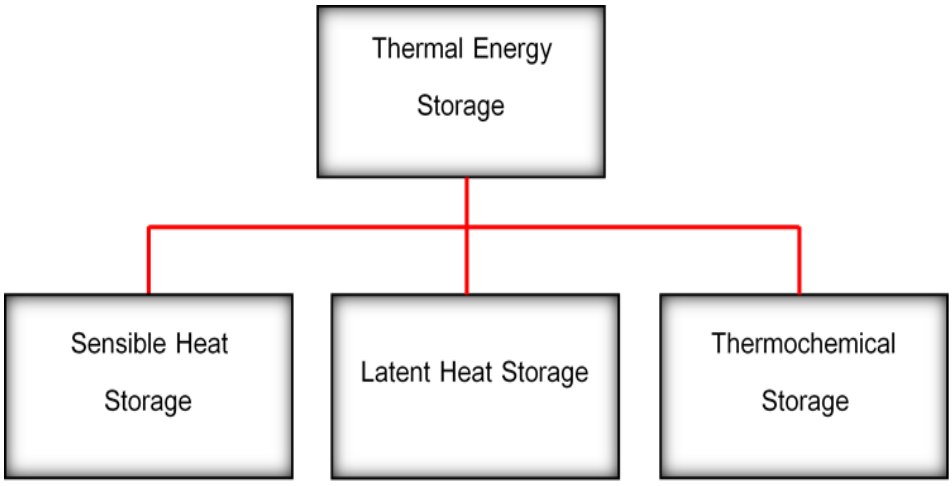

Figure 2.1 Classification of TES Methods

2.2.2 Sensible Heat Storage

The most basic method is SHS, which stores thermal energy by heating or cooling a solid or liquid medium like rocks, water, sand, or molten salts. Among these, water is the most cost-effective and widely used material, having a wide range of uses in the home and commercial domains. For large-scale systems, underground sensible heat storage is also employed using either liquid or solid media. The main advantages of SHS lie in its low cost and its operation without the risks typically associated with other storage technologies[55].

The mass of the material, its specific heat capacity, and the temperature differential between the starting and final states all affect how much energy is stored [56].

$$Q_s = \int_{T_i}^{T_f} m\ cp\ dt = mcp(T_f - T_i)$$

Q_s: Amount of heat (kJ)

m: Mass of storage material (kg)

cp: Specific heat capacity (kJ/ kg°C)

T_i: Initial temperatures of SHS (°C)

T_f: Final temperatures of SHS (°C)

2.2.3 Latent Heat Storage or Phase-Change Storage

Latent heat storage (LHS) has been developed with a principle based on the absorption of heat energy due to a transition of a material from a liquid to a solid, and vice versa, mostly in a solid to a liquid transition. LHS, unlike sensible heat storage, takes place near a constant temperature. The most used substances that take advantage of this technology are molten salts, paraffin wax, and water and ice [57]. Latent heat storage can be done using four major kinds of transition processes of a material, including solid to solid, solid to liquids, liquids to gases, and solid to gases [58]. With solid to solid, a substance undergoes a transition without going through a melt. This provides many advantages such as small volume expansion, no leaking, and no disformation. The only disadvantage with this technology involves a low value of stored latent heat. The other major transition that has been most taken advantage of in TES systems involves a change from a solid to a liquid. This takes place in substances like paraffin, fatty acids, salts, and eutectics due to their relatively high values of latent heat, but with disadvantages that

involve leakage of liquids, super cooling, and other conditions. Liquid–gas transitions, as in water or refrigerants, deliver very high latent heat values, but their practical use is restricted due to the need for pressurized containers to manage the significant volume change, which increases system cost and complexity. Finally, solid–gas transitions, such as the sublimation of CO_2 or naphthalene, also provide very high energy densities but are rarely applied in TES because of the difficulties in containment, safety concerns, and large volume variations. Among these options, solid–liquid PCMs remain the most practical and extensively studied for thermal energy storage applications.

The storage capacity of a latent heat storage system may be found using the following formulas

$$Q_L = \int_{T_1}^{T_m} m.cp_s\,.dT + m\,.\Delta H_m + \int_{T_m}^{T_2} m.cp_l\,.dT$$

T_m: The phase change temperature. [°C]

ΔH_m: The phase change enthalpy. [KJ/kg]

cp_s : The heat capacity of the solid phase PCM. [KJ/ kg°C]

cp_l : The heat capacity of the liquid phase PCM. [KJ/ kg°C]

2.2.4 Thermochemical Storage

Thermochemical energy storage (TCES) is distinguished by its high energy density, superior exergy efficiency, and elevated operating temperatures [59]. During thermochemical processes, thermal energy is stored and released through reversible chemical reactions. In the charging stage, heat input drives an endothermic reaction, breaking chemical bonds and separating the reactants into high-energy products. These products can then be stored separately, often at ambient conditions, without significant energy losses over time. In the storage phase, the energy remains preserved in the form of chemical potential, independent of temperature, allowing long-term and even seasonal storage. Finally, in the discharging stage, the reactants recombine through an exothermic reaction, releasing the stored heat-based energy that can be transformed into useful thermal or electrical energy depending on the application. This unique mechanism provides high energy density and virtually loss-free storage, distinguishing thermochemical storage from sensible and latent heat storage systems.

The following equation can represent the described procedures:

$$C + heat \leftrightarrows A + B$$

where A and B are the reactants and C is the thermochemical substance.

2.2.5 Relative Advantages and Limitations of TES Methods

Thermal energy storage (TES) methods include sensible heat storage (SHS), latent heat storage (LHS), and thermochemical storage (TCS). SHS is simple and low-cost but offers low storage density and suffers from heat losses. LHS, using phase change materials, provides higher density and nearly isothermal operation, though limited by low conductivity and supercooling. TCS, based on reversible chemical reactions, achieves the highest storage density and enables long-term or seasonal storage with minimal losses, but remains at research stage due to cost and technical challenges. In general, SHS is suited for short-term use, LHS for medium-term stable temperature applications, and TCS for future large-scale, long-duration storage.

Table 2.1 Comparative evaluation of several methods for thermal energy storage (TES) [60]

Performance Parameter	Sensible TES	Latent TES	Thermochemical TES (TCES)
Temperature range	Up to 110 °C (water tanks); 50 °C (aquifers and ground storage); 400 °C (concrete)	20–40 °C (paraffin); 30–80 °C (salt hydrates)	20–200 °C
Storage density	Low (for high temperature interval): ~0.2 GJ/m³ (typical water tanks)	Moderate (for low temperature interval): 0.3–0.5 GJ/m³	Generally high: 0.5–3 GJ/m³
Lifetime	Long	Often limited due to repeated cycling of storage material	Dependent on reactant degradation and side reactions
Technology status	Commercially available	Commercially available for certain materials and temperature ranges	Mostly in research and pilot projects; not widely commercialized
Advantages	Low cost; reliable; simple implementation with available materials	Moderate storage density; compact volumes; feasible short-distance transport	High storage density; low heat losses (can store at ambient temperatures); long storage duration; long-distance transport possible; highly compact energy storage
Disadvantages	Significant heat loss over time (depending on insulation); requires large volumes	Low thermal conductivity; material corrosivity; potential heat losses	High capital costs; technically complex

2.2.6 Applications of Thermal Energy Storage Technology

TES systems are becoming more deployed across multiple sectors to enhance energy efficiency, stabilize thermal loads, and enable higher integration of renewable energy sources. Their applications span from industrial processes to building energy management, in addition to emerging fields like electric mobility and smart grids.

2.2.7 Renewable Energy Integration

Including renewable energy systems, particularly solar and wind, faces major challenges related to intermittency, temporal discrepancy between energy production and consumption, and stability of power supply. Thermal Energy Storage (TES) offers a practical way to improve dispatchability, efficiency, and reliability of renewable-based systems by storing extra heat energy and releasing it as needed. Depending on the operating temperature and application, TES enables both short-term (hourly) and seasonal storage for a long time in renewable energy infrastructures.

R. N et al. introduced a black date drying design involving three different solar drying techniques. These include solar chimney dryers with phase change material (PCM) integration, open sun drying, and solar chimney dryers. Models for machine learning were used for prediction and optimization of performance. Results show that PCM addition significantly enhances efficiency, with values for both thermal and drying reaching 49% and 59%, performing better than open sun drying with 20% efficiency and 41% for the standard solar chimney. PCM energy storage also extends drying performance late into the evening, sustaining efficiency of 25% until 16:00h, compared with 11% efficiency of open sun drying. On different Machine Learning models used—MLP, RF, and SVR—the Multi-Layer Perceptron model showed enhanced accuracy in experiments. This involved RMSE of 0.85 and R^2 of 0.92 for training, with RMSE of 1.10 and R^2 of 0.90 for testing. Irradiance and air flow rate were found to be most important considerations. A perfect integration of PCM for thermal improvement using AI for prediction provides a viable and efficient opportunity for overcoming post-harvest losses as well as promoting sustainable food processing techniques [61].

2.2.8 Building Heating, Ventilation, and Air Conditioning (HVAC)

The energy consumed by the construction industry makes a contribution greatly to overall energy consumption, particularly in relation to space heating and cooling. Thermal Energy Storage, as a means of enhancing HVAC efficiency, peak energy savings, and increasing thermal comfort, has demonstrated efficacy. This technology involves storing energy when it is in low demand and when electricity costs are low, with a view to offering a means of efficient operation for buildings without relying on mechanical heating and cooling.

Vedrtnam et al. [62] offer a hybrid optimization approach for increasing HVAC energy efficiency in commercial buildings by means of passive thermal energy storage with Phase

Change Materials. This model emphasizes the huge energy demand and low efficiency of air conditioning systems, which are key sources of carbon emissions from buildings. A shopping center, where different types of temperature zones exist, in Coimbra, Portugal, has been employed as a test example. A finite element model developed in Python with a transient enthalpy model describes PCM characteristics. The zone-wise optimal application of PCM is obtained by a hybrid of Response Surface Methodology and Genetic Algorithms, which aims to minimize peak loads and subsequently lower energy consumed by air conditioners. The results reveal potential peak reductions of up to 30% with annual energy savings of 18–22%. Furthermore, it has been established that with actual data from air conditioners, a ME of below 5% would be obtained. An economic analysis of selective retrofitting has led to a payoff period of 2.5 years. This energy-efficient development model provides a scalable and low-cost approach for PCM incorporation in commercial buildings and aids in developing next-generation energy-efficient infrastructure.

Most new buildings are constructed to energy-passive standards, which impose limits on heating demand, primary airtightness and the usage of non-renewable resources, and allowable summer temperature exceedances. These exceedances depend on a space's thermal stability, itself linked to the heat-storage capacity of surrounding structures. In lightweight buildings, Thermal Energy Storage (TES) can substantially enhance this capacity. A study [63] examines the development and evaluation of a cutting-edge dynamic ventilation and cooling ceiling system, integrating PCM-based TES to improve thermal stability and lessen the need for mechanical cooling. A new methodology for evaluating the energy performance of modular cooling ceiling systems is introduced and applied. Performance was assessed for a reference building with lightweight, medium, and heavy construction types. Depending on the structure, the range of possible energy savings is 13% to 32% while maintaining required thermal comfort.

2.2.9 Electric Vehicles and Battery Thermal Management

The increasing need for sustainable public transport has accelerated the deployment of battery electric rail vehicles, but cabin heating still relies heavily on the battery, reducing range in cold conditions. Thermal storage systems offer a promising solution to lower battery-based heating demand. A study by Wieser et al. define the requirements (Figure 2.3) for such systems by developing a Python-based thermal car body model and simulating HVAC energy needs under realistic operating conditions. Environmental, track, vehicle, and HVAC parameters follow

current rail standards. For a representative scenario in climate zone III (DIN EN 14750), thermal power demand reaches 48 kW in summer and 92 kW in winter. The corresponding thermal storage capacity required ranges from 52 to 255 kWh. Integrating these systems can increase the vehicle's operational range by up to 5.6 %, enhancing flexibility and resilience during daily service [64].

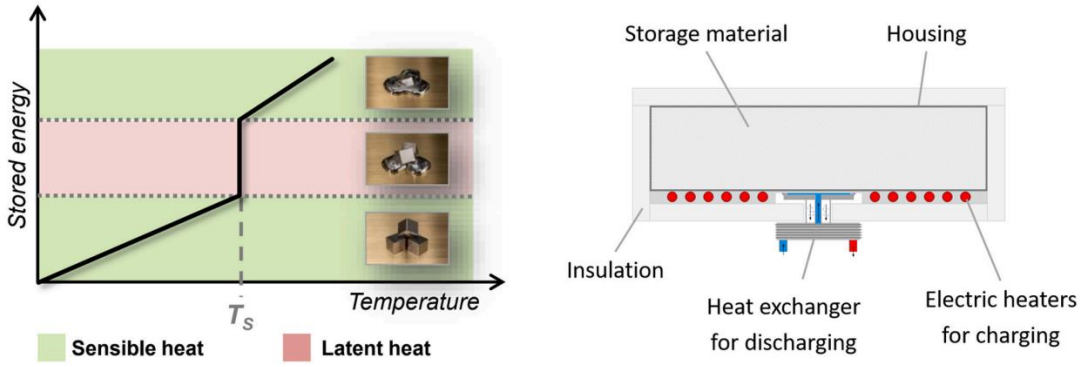

Figure 2.2 Thermal storage using metallic phase change material: phase change process (left) and experimental setup (right) [77].

Another study [65] investigates a Hybrid Battery Thermal Management System (HBTMS) for electric car lithium-ion battery packs, combining phase change material (PCM), metal foam, liquid cooling, and porous layers, Figure 2.5 shows the diagram of the proposed HBTMS. The goal is to improve thermal control under high discharge rates and reduce thermal runaway risks. A 3D CFD model evaluates how different PCM and porous-layer configurations affect maximum temperature, temperature uniformity, PCM melting behavior, and heat transfer efficiency. The dual-porosity architecture of the system—porous inserts in coolant channels and metal foam embedded in the PCM region—offers greater convective cooling and increased latent heat utilization within a single integrated structure. Findings show that the fully coupled HBTMS maintains the battery at about 301 K under a 5C rate, outperforming conventional PCM-based systems. Metal foam and liquid cooling delay PCM saturation, enabling sustained heat absorption, while greater PCM thickness reduces temperature gradients. The porous layer further boosts convective heat transfer and lowers dependency on PCM alone, with optimal performance achieved at a 3 mm thickness. Nusselt number and PEC analyses confirm efficient thermal dissipation and manageable pressure drop. Overall, the proposed HBTMS delivers superior temperature stability and safety, demonstrating strong potential for applications requiring high-performance battery cooling.

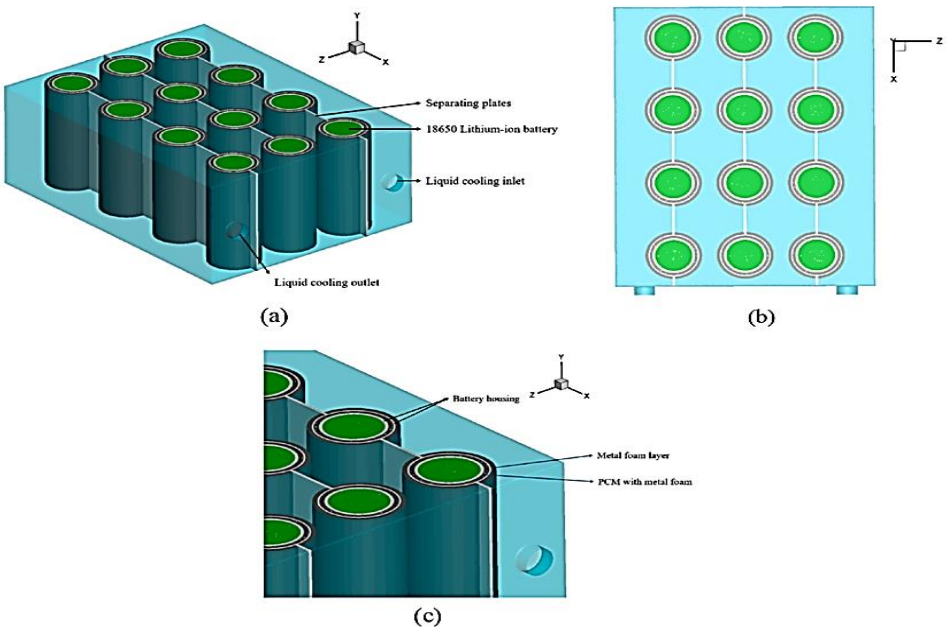

Figure 2.3 Schematic representation of the proposed HBTMS [78].

2.2.10 Agricultural and Greenhouse Applications

TES technologies have a vital role in modern agriculture, where temperature regulation directly influences crop productivity, water usage, and energy consumption. Greenhouses, in particular, require continuous climate control due to large diurnal temperature variations and the combined effects of solar radiation, humidity, and ventilation. Integrating TES systems helps stabilize internal conditions, lessen the need for traditional heating and cooling systems, and enhance overall sustainability.

Greenhouses play a key role in sustainable agriculture but require advanced climate control due to complex heat and mass transfer phenomena. In order to control heating, cooling, and ventilation in a controlled greenhouse, a research creates a novel simulation model for a solar-assisted chiller and heat pump system connected with a thermal energy storage unit. Using an in-house MATLAB code, the thermal effects of two passive strategies—ventilation control and shade cloth—are analyzed. Implementing these measures reduces the energy used by the system from 160,447.9 to 80,540.3 kWh and cuts carbon emissions by 49.8 %, from 86,882.5 to 43,612.6 kg-CO_2. The results demonstrate the significant potential of integrating passive control techniques with solar-assisted HVAC systems for more energy-efficient greenhouse operation [66].

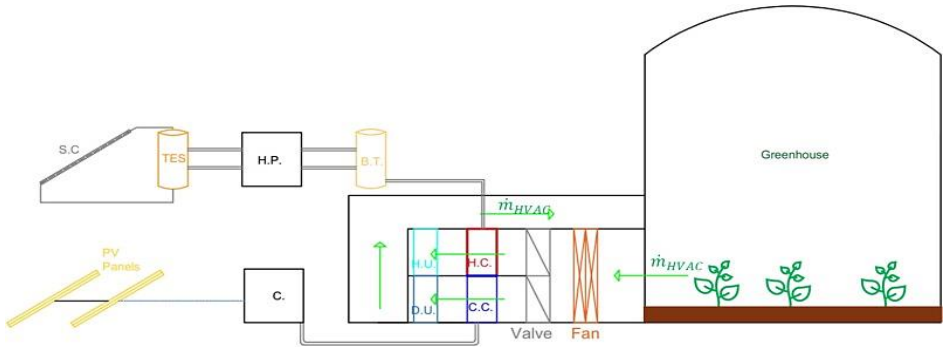

Figure 2.4 Schematic representation of the greenhouse integrated with a solar-aided heating and cooling system [66].

2.3 Classification of phase change materials (PCMs)

PCMs are materials that have the capacity to store and release significant quantities of latent heat during a phase transition, usually between the solid and liquid phases. Unlike sensible heat storage, PCMs operate almost isothermally, making them highly efficient for applications requiring stable temperature regulation. The perfect PCM should have an appropriate transition temperature, high latent heat, good thermal conductivity, minimal supercooling, and long-term stability across multiple cycles. Due to these properties, PCMs find applications in building thermal regulation, solar energy storage, refrigeration, electronics cooling, and industrial waste heat recovery, although difficulties like phase segregation and leakage still restrict large-scale implementation. A wide variety of phase change materials (organic, inorganic, and eutectic) is available , covering almost any desired temperature range [3] , a PCM categorization is provided in Figure2.

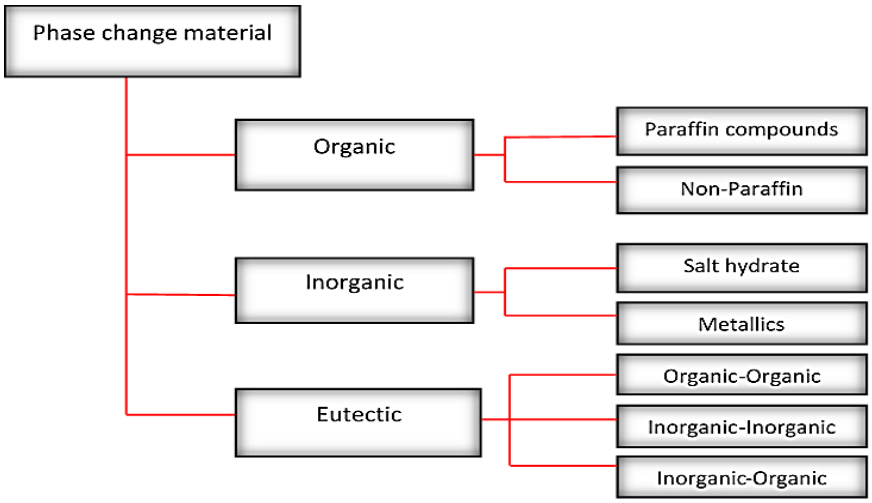

Figure 2.5 Classification of phase change materials (PCMs)

2.3.1 Organic phase change materials

Organic materials are commonly categorized into paraffins and non-paraffins. They exhibit several favorable properties, including congruent melting, which allows them to undergo repeated melting and solidification without phase segregation or a reduction in latent heat storage capacity. They also possess self-nucleating ability, meaning they crystallize with little or no supercooling, and are generally non-corrosive, making them compatible with common container materials [3].

2.3.1.1 Paraffin

Paraffin wax is primarily composed of straight-chain n-alkanes ($CH_3–(CH_2)_n–CH_3$). During crystallization, the alkyl chains discharge a significant amount of latent heat. Both the melting point and the latent heat of fusion increase with the length of the carbon chain. because to their large melting temperature range and reliable thermal performance, paraffins are well-suited as latent heat storage materials [3]. They don't react chemically and remain stable at temperatures below 500 °C, exhibit minimal volume change upon melting, and possess low vapor pressure in the liquid state. Paraffin's latent heat of fusion varies from around 170 kJ/kg to 270 kJ/kg within the temperature interval of 5 °C to 80 °C, making them very appropriate for applications in buildings and solar energy systems. Despite their advantages, paraffins have certain drawbacks that limit their practical applications, including low thermal conductivity (approximately 0.2–0.4 W/m·K) and significant volume expansion during phase transition[67].

2.3.1.2 Non Paraffin

Non-paraffin organic phase change materials include compounds like fatty acids, esters, alcohols, and glycols. Fatty acids, in particular, are attractive due to their strong thermal reliability, congruent melting, and renewable origin. However, non-paraffin PCMs are typically more expensive than paraffins and may present issues such as odor or chemical reactivity, which can limit their large-scale application. These materials typically possess a high latent heat of fusion but suffer from low thermal conductivity, flammability, toxicity, and limited stability at elevated temperatures. While fatty acids perform comparatively superior than other organics without paraffin , their higher cost compared to paraffins remains a significant drawback [68].

2.3.2 Inorganic materials

Inorganic solid-state PCMs (SS-PCMs) able to emit and retain thermal energy in the solid phase through one or more mechanisms, comprising magnetic transformations, crystallographic

structure changes, order–disorder transitions, and transformations between amorphous and crystalline structures. Among these, the first two mechanisms are particularly effective, as they involve large volumes of latent heat are stored[69].They are further categorized into salt hydrates and metallic materials.

2.3.2.1 Salt hydrates

Inorganic salts with water of crystallization are known as salt hydrates. Among PCMs, they are some of the most extensively studied for thermal energy storage (TES) and are also among the least expensive. In these systems, thermal energy is stored by drying the salt hydrate, while the anhydrous Water and salt are stored apart. The reversible hydration–dehydration reaction of salt hydrates forms the basis of their energy storage capability, as represented by the following reaction:

$$\text{Salt} + H_2O \leftrightarrow Salt.nH_2O + heat$$

Salt hydrates are particularly appealing because of their high latent heat of fusion per unit volume, relatively high thermal conductivity, and minimal volume change upon melting. While some exhibit congruent melting behavior, many others melt incongruently. The main limitation is that most salt hydrates suitable for thermal storage tend to undergo incongruent melting, which reduces their long-term stability and performance [70].

2.3.2.2 Metallics

This category encompasses low-melting metals and metal eutectics. Despite their weight restrictions, metallics have not been extensively used in PCM technology, they are promising candidates in applications where volume is a critical factor, as they offer very elevated latent heat of fusion relative to volume. Their inherently high thermal conductivity eliminates the need for additional conductive fillers, but their use also introduces unique engineering challenges. A key distinction between metallic PCMs and other types lies in their exceptionally high thermal conductivity [3].

2.3.3 Eutectics

Eutectic phase change materials are formed by combining two or more components, and they can be classified into different categories depending on their composition. Typical systems include organic–organic mixtures (e.g., capric–lauric, lauric–palmitic, or myristic–stearic acids), inorganic–inorganic mixtures (e.g., LiOH–KOH, $MgCl_2$–KCl, or $BaCl_2$–KCl–NaCl),

and inorganic–organic mixtures (e.g., naphthalene–benzoic acid or urea–NH_4Br [71] .In eutectic materials, during the crystallization process, every component melts and solidifies congruently, creating a combination of the individual component crystals [72] . Compared to pure inorganic PCMs, eutectic mixtures generally exhibit superior resistance to phase segregation[68].

Since phase change temperature (T_{pc}) and enthalpy of phase change ($\Delta_{pc}h$) are the main criteria for selecting a PCM, early classification naturally combined material families with these properties. Initial PCM groups included inorganic materials such as salts (nitrates, hydroxides, chlorides, carbonates, fluorides), salt hydrates, clathrates, water, and eutectic water–salt mixtures. Organic PCMs followed, mainly paraffins, fatty acids, sugar alcohols, and polymers such as polyethylene and polyethylene glycols. These materials may also be categorized based on their operational range as low-, medium-, or high-temperature PCMs [73].

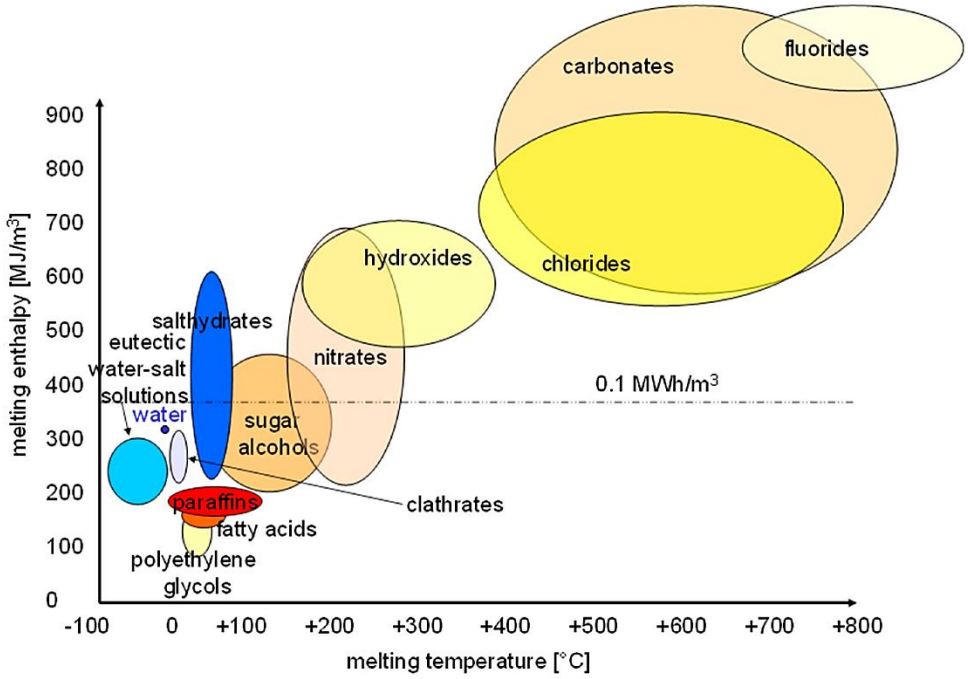

Figure 2.6 Types of phase change materials (PCMs) with typical ranges of melting temperature and latent heat [73].

2.4 PCM selection for TES

The choice of a suitable phase change material (PCM) ultimately depends on finding the right balance between performance and practicality. Key criteria include thermophysical characteristics like melting temperature, latent heat, and thermal conductivity, as well as chemical stability and compatibility with encapsulation and heat transfer materials. In addition,

factors like long-term cycling reliability, resistance to subcooling or segregation, cost, availability, and environmental impact are equally decisive in determining the most suitable PCM for a specific application. Table 2.2 provides a thorough categorization of phase change materials (PCMs) based on their chemical nature, highlighting the main categories such as

Table 2.2 PCM Categorization and Thermophysical Characteristics by Chemical Nature [87].

Phase Change Materials (PCM)	**Organic**	**Inorganic**	**Eutectics**
Composition / Examples	Long-chain hydrocarbons, e.g., paraffin (CnH2n)	Salt hydrates, metals	Mixtures of organic and/or inorganic compounds
Supercooling	None	May occur	Depends on composition
Temperature Range	Wide range of operating temperatures	Moderate to high	Variable, depends on constituents
Chemical & Physical Stability	High	Moderate	Limited data available
Heat of Fusion	High	High	Moderate to high
Melting Behavior	Congruent melting	Often incongruent	Sharp melting point
Flammability	Flammable	Non-flammable	Usually non-flammable
Thermal Conductivity	Low	High	Moderate
Volume Change	Low	Low	Moderate to high
Volumetric Energy Density	Low	High	High
Corrosion / Material Issues	Minimal	Possible corrosion	Depends on components
Availability / Cost	Widely available	Widely available	High cost; limited property data

Another study [69] investigated the connection between solid-solid PCMs' internal molecular structures and their thermal characteristics, such as enthalpy and phase transition temperature,

emphasizing the potential for application based on four different structural types reported in the literature. Table 2.3 gives an overview of the relative benefits and drawbacks connected to each type of SS-PCM.

Table 2.3 Assessment of the performance, advantages and restrictions of various solid–solid PCMs [82]. Ratings are indicated as follows: + Poor, ++ Fair, +++ Good, ++++ Excellent

Property	**Polymeric**	**Organic**	**Organometallic**	**Inorganic**
Transition temp. (°C)	11–65	25–190	32–160	680–988
Enthalpy (J/g)	10–205	15–270	62–154	34–56
Thermal conductivity	+	+	+++	++++
Phase change kinetics	+	+	+++	+++
Phase separation	++++	++	+++	++++
Chemical & thermal stability	+++	+++	+++	++++
Volume change	++	++	++++	++++
Non-toxicity	+++	+	++++	++++
Fire resistance	+	+	++	++++
Ease of production	+++	+++	+	++++

2.5 Limitations and Challenges of Phase Change Materials (PCMs)

PCM exhibits several advantageous Properties making it is ideal for applications involving thermal energy storage. The key desired attributes include wide availability at a discount, relatively high latent heat capacity, on-toxicity, on-corrosiveness, environmental friendliness, minimal volumetric variation during phase transition, and long-term chemical stability without segregation[3] [74] Despite their wide applicability in thermal energy storage, phase change materials (PCMs) present several limitations that restrict their large-scale deployment. These challenges include low thermal conductivity, subcooling effects, and in some cases high material cost. Addressing these drawbacks through composite formulations, encapsulation techniques, and the incorporation of thermal conductivity enhancers remains a key focus of current research aimed at improving PCM performance and reliability.

2.6 Enhancement Methods for Addressing the Thermal proprieties of PCM

Low thermal conductivity is a common characteristic of PCMs, which leads to extended melting and solidification times and consequently limits their overall thermal performance. To overcome this drawback, numerous improvement techniques have been investigated, including the incorporation of conductive nanoparticles, the use of metallic foams, and encapsulation techniques with extended surfaces, Figure 2.8 illustrates the different methods employed to enhance the poor thermal conductivity of PPCMs.

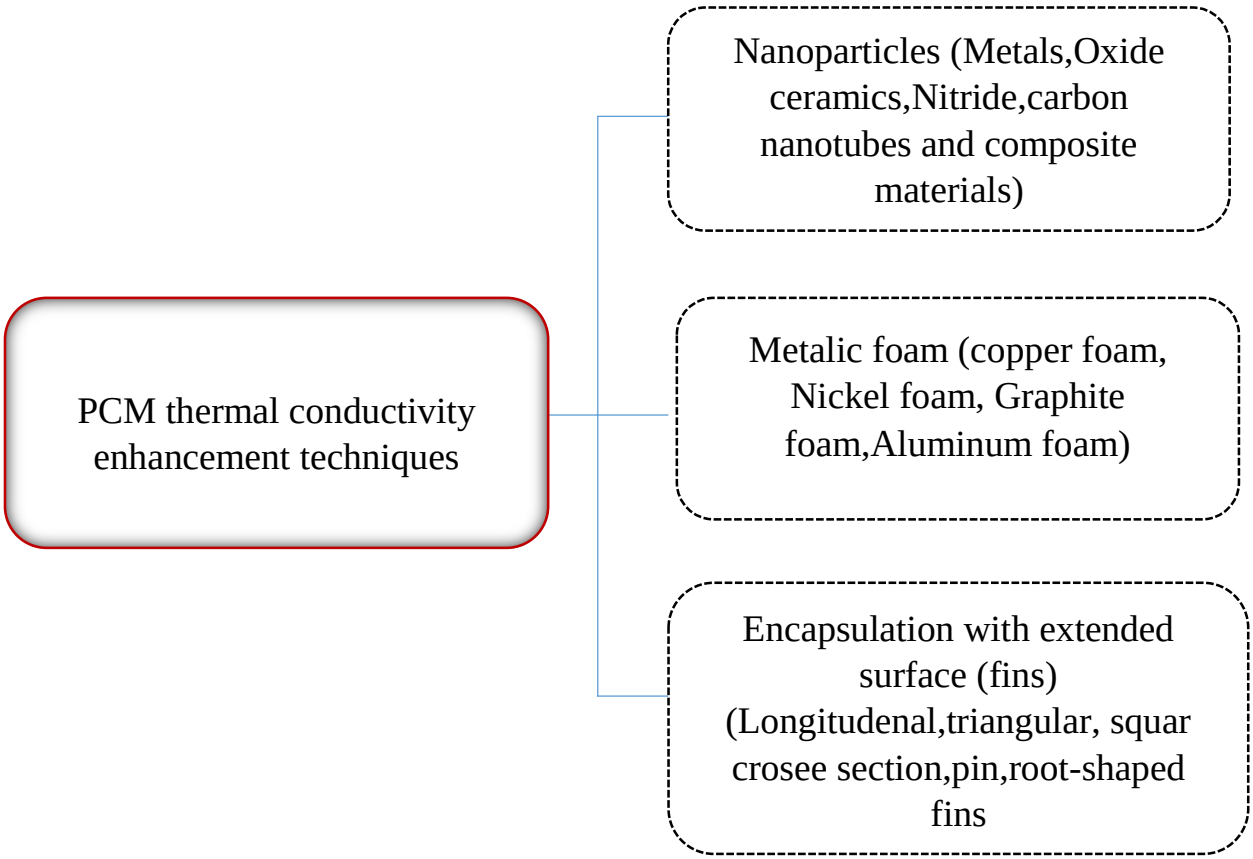

Figure 2.7 Techniques to enhance PPCM poor thermal conductivity.

2.6.1 Classification of Nanoparticle Additives for PCMs

PCMs are attractive for managing and storing heat primarily because of their high latent heat capacity. However, attempts to increase their thermal conductivity often compromise this property [75]. The extent of this trade-off depends strongly on the additive loading ratio. Nanoparticles provide a promising solution, offering a high ratio of surface area to volume that enhances heat transfer with minimal loading. Moreover, Nanoparticles (NPs) can significantly enhance the paraffin's thermal conductivity and heat storage capacity, without notably affecting its melting temperature [16]. Nanoparticle additives used to enhance phase change materials (PCMs) may be roughly divided into three main categories: metal-based nanoparticles, carbon-

based additives, and structural/conductive frameworks. Each class contributes differently to improving thermal conductivity, stability, and melting/solidification behavior while maintaining acceptable latent heat capacity.

2.6.1.1 Metal-Based and Metal-Oxide Nanoparticles

This category includes classical conductive nanoparticles (e.g., Al_2O_3) as well as high-performance ceramics such as cubic boron nitride (cBN). Metal-based NPs exhibit high intrinsic thermal conductivity and strong interfacial heat-transfer capability, enabling significant improvements in melting rate and thermal response with very low loading. For example, dispersing 0.5–2 wt% cBN nanoparticles into RT54HC paraffin increased thermal conductivity by 59% (solid) and 27% (liquid) while causing only a modest latent heat reduction (207 → 190 J/g). Supercooling dropped from 2.68 to 1.33 °C, and thermal stability improved due to a higher decomposition onset (186.77 °C). Such nanocomposites maintain nearly unchanged melting temperature and are suitable for solar thermal applications and electronics cooling. This demonstrates the effectiveness of metal-based NPs in enhancing PCM pe studied the melting behavior of a vertical cylindrical thermal energy storage unit using a phase change material (PCM) enhanced with Al_2O_3 nanoparticles and horizontal radial copper fins. Increasing the number of fins improved heat transfer, reducing melting time by up to 25.7%. Using 5% nano-PCM alone reduced melting time by only 5.5%. The best performance was achieved by combining 5% Al_2O_3 nano-PCM with three fins, which shortened melting time by 28.3%.

Jowzi and Jamaati [76] introduces combined experimental, numerical, and analytical approaches to enhance PCM thermal performance using metal fibers. The effects of fiber material, diameter, length, and volume fraction on the composite's effective thermal conductivity were investigated. Results showed that incorporating 2 % metal fibers into paraffin increased its thermal conductivity by over four times, and numerical simulations predicted further improvement at 5 % fiber content. Additionally, 2 % copper fibers reduced the PCM discharge time by nearly 50 %, indicating faster heat transfer. An innovative analytical–empirical approach was proposed to estimate the effective thermal conductivity, taking into account both the material microstructure and the characteristics of its components. Microstructural analysis revealed anisotropic behavior, suggesting that optimized fiber alignment could yield materials that conduct heat efficiently in one direction while providing insulation in other.

2.6.1.2 Carbon Additives

Graphite, expanded graphite (EG), graphite foam (GF), carbon fibers, carbon nanotubes, SWCNTs, MWCNTs, and graphene nanoplatelets (GNPs) are among the most effective additives for improving the thermal conductivity of paraffin and other organic PCMs. Their diverse morphologies—platelet, tubular, or porous—enable tailored heat-transfer pathways. Each morphology provides distinct heat conduction mechanisms and interfacial effects that influence the overall heat transfer behavior of PCM composites. Wu et al. [77] Developed a form-stable PCM composite of paraffin and hydrophobic expanded perlite to improve thermal transfer efficiency in cementitious materials. They incorporated carbon-based additives—graphite (G), carbon nanotubes (CNT), and graphene nanoplatelets (GNP). An ultrasonic bath was used to disseminate the carbon ingredient in acetone, yielding a homogeneous suspension, as shown in Figure 2.10 and compared their effects. Every addition demonstrated high latent heat, strong chemical compatibility, and a notable improvement in thermal conductivity by 45%, 30%, and 49%, respectively. Despite similar conductivity improvements, GNP showed the highest heat transfer performance, while graphite showed the lowest. The study concluded that overall performance relies on the development of a continuous conductive network within the porous matrix. High specific surface area additives with reduced particle size proved most effective, with prototype tests showing heat gain increases of 78%, 122%, and 200% for G, CNT, and GNP, respectively.

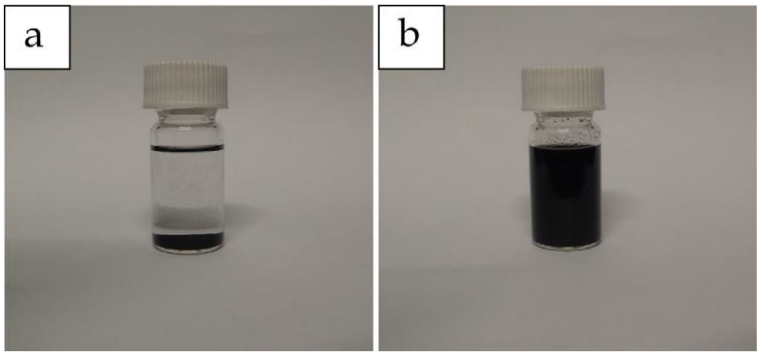

Figure 2.8 Dispersion of carbon nanotubes (CNTs) in acetone using an ultrasonic bath: (a) before dispersion, (b) after dispersion [93].

Zhou et al. [78] prepared expanded graphite (EG)/adipic acid (AA) composite PCMs and analyzed their structure and properties using FTIR, DSC, and FE-SEM. Figure 2.10 shows SEM photographs of the fractured surfaces of (a) pure EG, (b) pure AA, and (c–g) AA composites containing 2, 4, 6, 8, and 10 mass% EG, respectively. The findings revealed that AA was effectively adsorbed within the porous structure of EG, showing good chemical compatibility. Increasing EG content reduced both latent heat and thermal conductivity, yet at 10 wt% EG,

the composite reached a conductivity of 4.35 $W \cdot m^{-1} \cdot K^{-1}$, much greater than that of pure AA. After 1000 thermal cycles, melting and freezing enthalpies decreased by only 16.1% and 13.7%, indicating excellent thermal stability and durability.

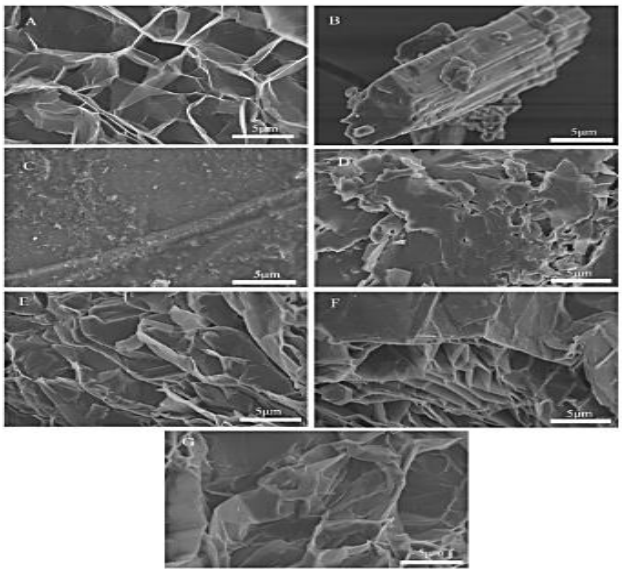

Figure 2.9 SEM images of the fractured surfaces of: (a) pure EG, (b) pure AA, (c) AA with 2 wt.% EG, (d) AA with 4 wt.% EG, (e) AA with 6 wt.% EG, (f) AA with 8 wt.% EG, and (g) AA with 10 wt.% EG [94].

Rising temperatures reduce photovoltaic (PV) panel performance, necessitating efficient thermal management. A study improved PCM conductivity by adding randomly oriented short carbon fibers and modeled the system using a homogenization-based finite element approach. Optimized fiber content increased thermal conductivity by 47 % (solid) and 75 % (liquid) while preserving latent heat. The enhanced PCM lowered the PV panel's peak temperature from 72.5 °C to 57 °C, boosting efficiency by 0.61 % and daily power output by 4.6 W. Carbon fiber–reinforced PCMs effectively reduce hotspots and improve energy performance, offering a scalable passive cooling solution for solar panels [79].

Song et al.[80] Prepared high-density graphite foams (GFs) from mesophase pitch, with or without mesocarbon microbeads, under various carbonization and graphitization after foaming pressures and temperatures. In some cases, repeated pitch infiltration increased foam density. Paraffin was then impregnated to form GF/paraffin composites. The foams' microstructure and thermophysical characteristics were strongly affected by pitch content and foaming conditions, which in turn governed the thermal performance of the composites. The thermal diffusivity of the GF/paraffin composites was enhanced 768–1,588 times compared with pure paraffin, while

the latent heat showed an almost linear relationship with the paraffin fraction. These materials show promise for passively cooling electrical equipment.

2.6.2 Metallic and Highly Conductive Foams

The combination of metallic foams and PCMs is an successful strategy to overcome the low thermal conductivity problem of PCMs utilized in LHTES systems, highly conductive metallic foams (aluminum, copper, or nickel foams) are introduced as porous matrices within the PCM, The solidification of distilled water in metallic foams with graded topologies in open cells (Figure 2.12) was examined. Foams with various porosities, pore densities (PPI), and base materials were stacked to create a layered gradient structure. Evaluations of the solidification front and total freezing duration, supported by numerical simulations on uniform foams, showed that morphological gradients significantly accelerate solidification. Properly designed graded foams reduced the overall freezing time more effectively than single-layer foams due to improved heat transfer [81].

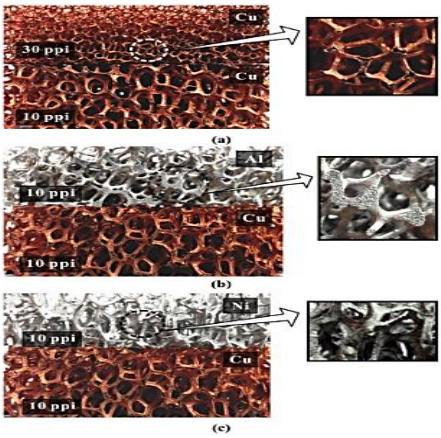

Figure 2.10 Photographs of open-cell metallic foams with gradient pore structures: (a) copper foam pack with 10 and 30 ppi; (b) 10 ppi copper foam combined with aluminum foam; (c) 10 ppi copper foam combined with nickel foam [100].

Dinesh et al. numerically [82] examined energy absorption in PCM-based thermal energy storage systems enhanced with metallic foam. A generalized geometric model generated random foam structures using overlapping spheres with constant or variable radii, allowing analysis of pore radius, overlap, and porosity effects. Unlike volume-averaged models, this approach resolved individual pores, improving accuracy in PCM–metal heat transfer. In conjunction with a phase transition model based on enthalpy, results showed that smaller pores consistently enhance heat transfer, while optimal overlap and porosity depend on the amount

of time of heat transfer. These findings highlight the need to optimize foam geometry according to transient system behavior to maximize thermal efficiency.

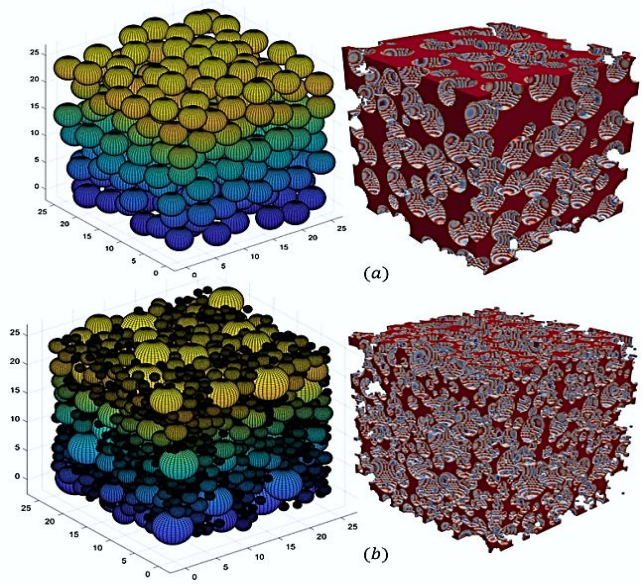

Figure 2.11 (a) Geometry generated using Method 1 with uniform sphere size; (b) Geometry generated using Method 2 with specified porosity and variable sphere sizes. [82].

Liu et al. [83] investigated numerically how to improve melting rates and storage efficiency by using various PCMs with varying melting points in conjunction with metal foams with porosity gradients. The findings showed that multi-PCM configurations accelerated heat transfer, reducing total melting time by 9.18% compared to single-PCM systems. Introducing one- and two-dimensional porosity gradients in metal foams further improved performance: While a negative gradient lengthened the melting time but improved temperature uniformity, a positive gradient along the heat flow direction reduced thermal resistance and decreased melting time by 6.18%. The optimized two-dimensional gradient multi-PCM design achieved the best balance, compared to homogeneous structures, reducing the overall melting time by 17.96% and boosting energy storage efficiency by 20.16%. Finally, dimensionless correlations relating liquid fraction to modified Fourier, Stefan, and Rayleigh numbers were developed, providing predictive tools for optimizing (LHTES) systems.

Dhabarde et al. [84] assesses a passive TMS for an 18650 Li-ion battery's thermal performance using three organic PCMs combined with porous copper foam inside a honeycomb enclosure. The melting behavior is simulated using an LTNE model with non-Darcy flow to capture detailed pore-scale heat transfer. At a 2C discharge rate, the effects of enclosure thickness (1–4 mm) and foam porosity (92–98%) are analyzed for each PCM. Results show that n-eicosane

provides the lowest surface temperature (309.6 K) and highest heat flux, RT44HC ensures the most uniform temperature distribution, and n-octadecane melts the fastest. Copper foam is shown to markedly improve heat transfer, while optimized geometry further enhances passive cooling. Overall, the work offers useful guidance for designing high-performance passive BTMS.

2.6.3 Encapsulation (Micro- and Macro-Encapsulation)

The technique of encasing a PCM core in a shell material that keeps the PCM's form throughout melting and solidification is known as encapsulation. The shell also provides mechanical protection, chemical stability, and thermal conductivity improvement. The thermal performance of finned PCM systems (PPCM) is significantly affected by the fin type, dimensions, spacing, and number of fins[85] .

khan et al. [86] carried out a 3D numerical analysis of the LHS system integrating multiple thermal enhancement techniques to improve charging rate, enthalpy, and temperature distribution. Paraffin was used as the PCM, graphene nanoplatelets (GNPs) as nano-additives, and three fin types—longitudinal, circular, and wire-wound— (Figure 2.12) were examined in a vertical shell-and-tube design. The findings indicated that fins provided greater thermal enhancement than nano-additives. The wire-wound fin configuration achieved the best performance, increasing heat flux from 2.25 kW/m² (pure PCM) to 88.13 kW/m² and reducing charging time for 11.09 MJ from 23.5 h to 1.02 h. The charging rate was 89.9% higher than nano-PCM without fins. Increasing GNP concentration beyond 1% reduced overall performance, making the 1% GNP wire-wound fin configuration the optimal design for efficient LHS systems.

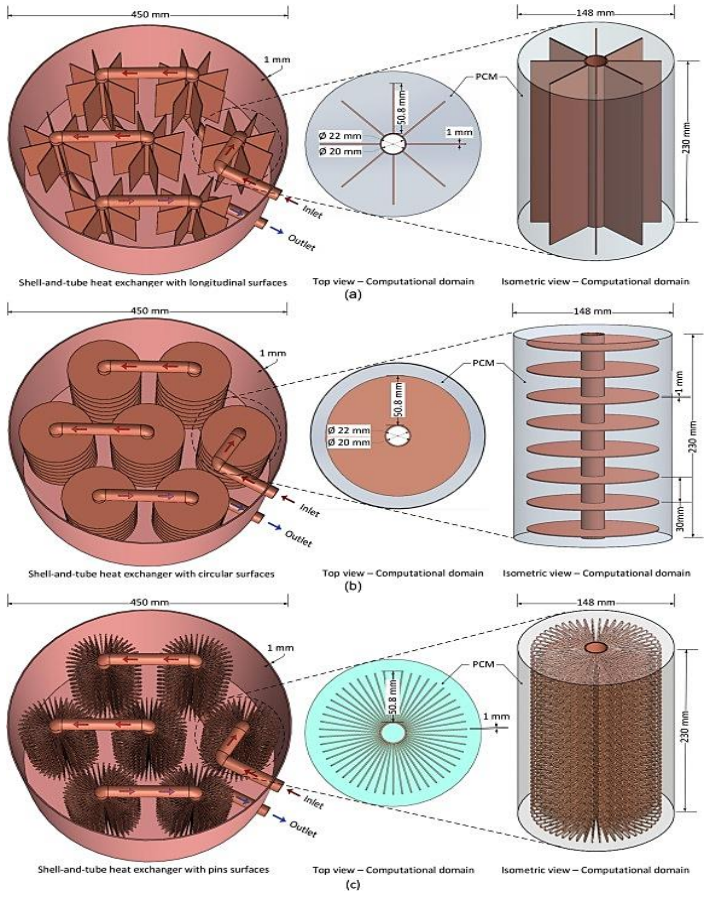

Figure 2.12 Shell-and-tube heat exchanger with multiple tube passes and different extended surface orientations: (a) longitudinal fins, (b) circular fins, and (c) wire-wound fins [86].

2.6.4 Finned Structures (Internal/External Fins)

Fin-based enhancement is a common strategy to enhance the thermal response of PCMs by adding extended metal surfaces to make up for their low thermal conductivity. To address the limitations of PCM heat sinks under high heat fluxes, a research presents a hybrid structure that allows for both vertical and multidirectional heat transmission by combining copper foam with high-conductivity plate heat-pipe fins. Using a visualization-based setup, three heat-sink designs—Al alloy fins, heat-pipe fins, and heat-pipe fins combined with copper foam (Figure 2.14)—were tested under heat fluxes of 4.2–7.0 kW/m². When compared to Al fins, the hybrid design extended the duration to achieve the set-point temperature by 1.25 during pre-sensible heating and 2.2 during melting, while reducing the maximum internal temperature difference by 25%. These results show that integrating heat-pipe fins with copper foam significantly enhances thermal conductivity and promotes a more uniform phase transition, making it a promising solution for aerospace electronics, data centers, and EV battery systems.[87].

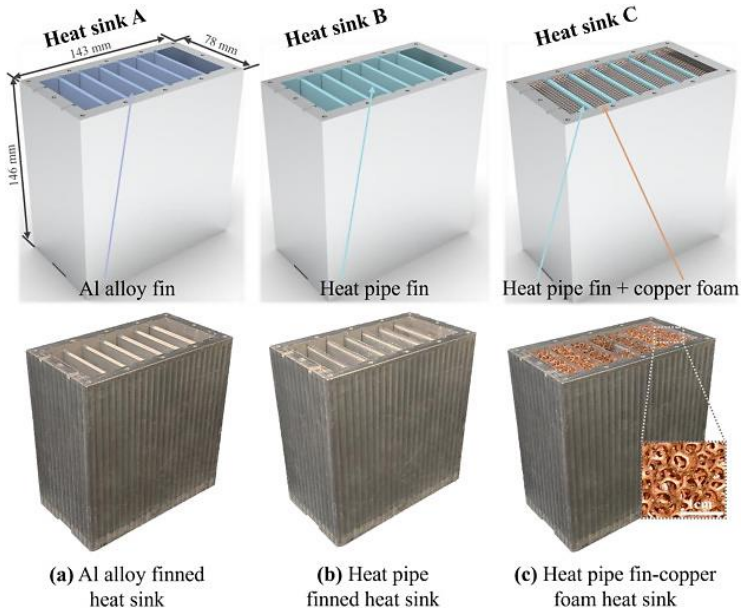

Figure 2.13 Images of different heat sink configurations [87].

Fins act as macroscale heat-transfer accelerators, enabling the PCM to melt and solidify more rapidly by spreading heat deeper into the material. Efficient heat transfer and operational safety are key challenges for energy piles. Xia et al. [88] introduced an innovative energy pipe pile (EPP) incorporating phase change material (PCM), metal fins, and spiral heat exchange pipes to enhance thermal performance. Laboratory investigations and numerical simulations were carried out to assess the effects of different pipe configurations—5U series (5US), 5U parallel (5UP), and spiral—on heat transfer efficiency, temperature distribution, Regarding the use of PCM in both continuous and sporadic circumstances. Results show that the PCM–fin integration improved heat exchange capacity by 7.84%, thereby lessening the pile's thermal stress and temperature variations. PCM utilization efficiencies reached 49.06% (5US), 22.2% (5UP), and 56.33% (spiral). The spiral configuration provided the best temperature uniformity and overall heat transfer, with only 26.6% temperature deviation compared to 86% for 5US.Overall, the proposed spiral PCM–metal fin EPP design demonstrates a promising solution for improving the thermal efficiency, reliability, and durability of next-generation geothermal energy piles.

Another study presents a PCM-based BTMS that uses combined internal and external fins to form PCM silos and improve heat transfer. Using a lumped-capacitance battery model and an enthalpy–porosity PCM model, the system was evaluated under various discharge rates. Figure 2.15 shows the diagram of the proposed BTMS, including (a) the isometric view, (b) its dimensions, and (c) the top view, the BTMS with four fins showed the best balance of cooling

performance and energy density, reducing surface temperature by up to 17.45 K compared with a finless PCM system and maintaining temperatures below 318.15 K even at high ambient conditions. It also provided more uniform cooling, identified distinct melting regimes, and produced correlations for PCM liquid fraction and Nusselt number prediction, offering practical guidance for PCM-based BTMS design [89].

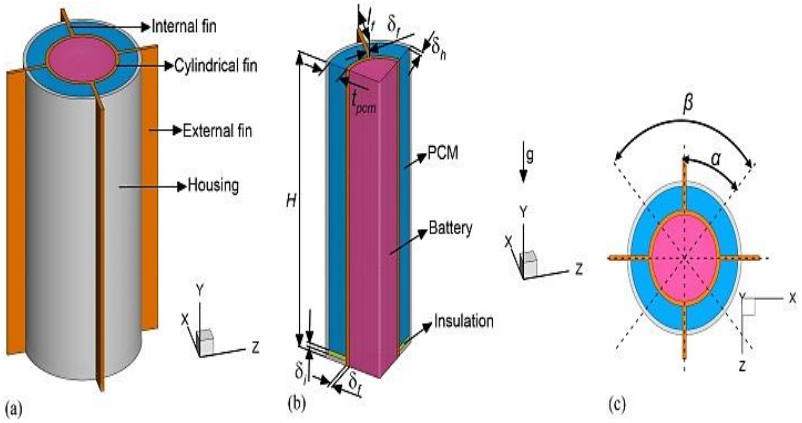

Figure 2.14 Schematic of the proposed BTMS showing (a) isometric view, (b) dimensions, and (c) top view [89].

2.7 Subcooling and phase segregation

A phenomenon known as "supercooling" occurs when a PCM stays liquid even after being chilled below its normal freezing point, due to the absence of spontaneous nucleation that would trigger solidification. This delayed phase transition can negatively affect thermal energy storage systems' dependability and effectiveness by making the solidification process unpredictable. Therefore, reducing supercooling is essential for achieving stable and consistent PCM performance.

A common strategy documented in the literature is the incorporation of nucleating agents to suppress supercooling. One of the most used additions is borax; when added at 4 wt.%, it has been shown to lower the supercooling degree of SSD from 14 °C to 4 °C [90]. Ayyagari et al. presents melting and solidification enthalpy–temperature curves, measured using the T-history method, for two Glauber's salt–NaCl composites with a melting point of 21 °C. Both formulations contain sodium polyacrylate as a thickening to increase cycle stability, borax to lessen supercooling, and NaCl to lower the melting point. The latent heat of fusion of the composite containing 12 weight percent NaCl was 139 $kJ \cdot kg^{-1}$, while the composite with 9 wt.% NaCl reached 171 $kJ \cdot kg^{-1}$. In both cases, the volumetric energy density is significantly higher than that of organic PCMs with similar melting temperatures [91].

Another study [92] proposes a new preparation route for a calcium-chloride-based salt-hydrate PCM formulated from mixtures of calcium chloride dihydrate ($CaCl_2·2H_2O$) and anhydrous calcium chloride ($CaCl_2$) to overcome the severe supercooling of $CaCl_2·6H_2O$. Six compositions were ready to evaluate the impact of the $CaCl_2·2H_2O/CaCl_2$ ratio on thermal behavior, and Table 2.4 presents the resulting formulations. Increasing the $CaCl_2·2H_2O$ content significantly decreased supercooling, with the composition containing 66.21 wt% $CaCl_2·2H_2O$ achieving a 96.8% reduction, as shown in Figure 2.18. All samples delivered high latent heat values (>155.29 J/g), confirming their suitability for building energy-storage applications.The influence of Nano-SiO_2 additions (0.1, 0.3, and 0.5 wt%) was also examined. For Samples 6 and 5, supercooling was decreased to 0.2 °C and 0.4 °C, respectively. Moreover, two cooling strategies—frozen storage at −20 °C and cold storage at 5 °C—further suppressed supercooling. The combination of optimized $CaCl_2·2H_2O$ content and Nano-SiO_2 additives substantially enhanced PCM performance, making these newly developed composite PCMs strong candidates for thermal energy-storage systems.

Table 2.4 PCMs based on salt hydrates, formulated with different ratios of $CaCl_2·2H_2O$ and $CaCl_2$ [92].

Parameters and Items	Sample No.					
	1	2	3	4	5	6
x (g)	50.00	39.58	29.17	18.75	8.33	0.00
y (g)	0.00	20.42	40.83	61.25	81.67	98.00
z (g)	50.00	50.00	50.00	50.00	50.00	50.00
x + *y* (g)	50.00	60.00	70.00	80.00	90.00	98.00
y/(*x* + *y*) (%)	0	34.03	58.32	76.56	90.74	100
x/(*x* + *y* + *z*) (%)	50.00	35.98	24.31	14.42	5.95	0
y/(*x* + *y* + *z*) (%)	0	18.56	34.03	47.12	58.34	66.21

Notes: *x*: mass of $CaCl_2$; *y*: mass of $CaCl_2·2H_2O$; *z*: mass of H_2O.

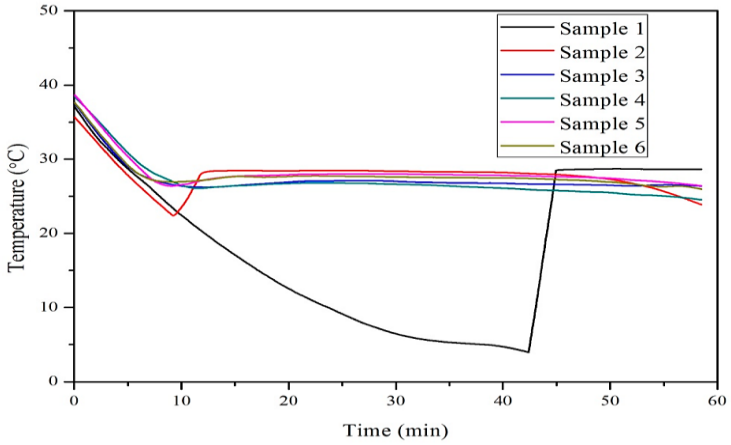

Figure 2.15 Temperature–time cooling curves of the six $CaCl_2 \cdot 2H_2O$–$CaCl_2$–H_2O samples.

Therefore, the subcooling degree is strongly influenced by the final CPCM's composition and characteristics. Although a reduction in subcooling is generally expected when preparing a composite PCM, this improvement is not always guaranteed. For instance,a blend made with OM-11 (initial subcooling of about 24 °C) and charcoal/silica gel as supporting materials achieved only a modest reduction of around 7 °C—far less effective than the OM-11/activated charcoal composite, which lowered the subcooling degree to approximately 3 °C.) [93]. Recently, myristic acid (MA) and expanded graphite (EG) were combined to produce shaped CPCMs at different ratios using a melt-blending and press-forming technique. This approach led to a noticeable reduction in the supercooling degree (Figure 2.19 b and c). According to the authors, the improved heat transfer provided by EG, along with the promotion of heterogeneous nucleation, facilitated the solidification of MA, thereby narrowing the gap between its melting and freezing temperatures[94].

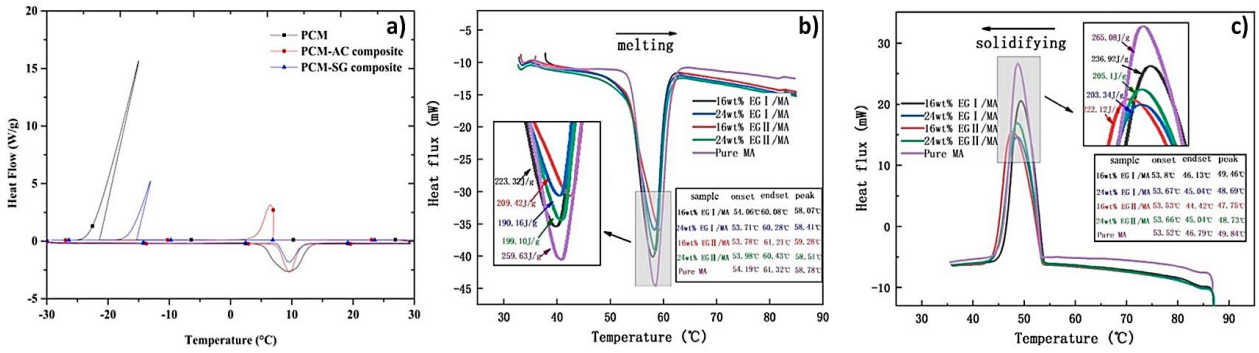

Figure 2.16 Subcooling degree representations determined by DSC:

(a) Pure PCM OM-11 and composites with activated charcoal (PCM-AC) and silica gel

(PCM-SG) [93], (b) Pure myristic acid (MA); (c) Shape-stable MA–expanded graphite (EG) composite PCMs [94].

Similarly, solid waste steel slag has been combined with polyethylene glycol (PEG) for low-temperature applications, successfully reducing the subcooling degree to below 5 °C, compared to the original ~25 °C subcooling of pure PEG. 56 [95].

2.8 Enhancement of Leakage Resistance in PCMs

Among the principal limitations of solid–liquid PCMs is their tendency to leak during melting, which causes material loss, reduced thermal performance, and instability during repeated cycling. To overcome this, researchers have developed several leakage-prevention enhancement strategies that enhance the shape stability of PCMs during phase transition. Porous supporting materials such as silica, diatomite, perlite, vermiculite, and expanded graphite can physically confine the liquid PCM through capillary forces, effectively producing form-stable composites.

As a promising battery thermal management strategy, PCM cooling still faces major issues such as leakage, volume change, and structural inhomogeneity during repeated melting–solidification. To address this, a nanosilica-enhanced composite PCM CPCM-NS (Figure 2.19) was developed, offering strong anti-leakage and anti-volume-change performance. The nanosilica, with pores of 30–100 nm, effectively adsorbs liquid paraffin, improving stability and uniformity of the PCM module. As a result, CPCM-NS provides superior cooling and durability: with 5.5 wt% NS, maximum temperatures are reduced by 1.6–5.9 °C over the first several cycles compared to CPCM without NS, and a stable temperature drop of 6.22 ± 0.05 °C is maintained in later cycles. [96]

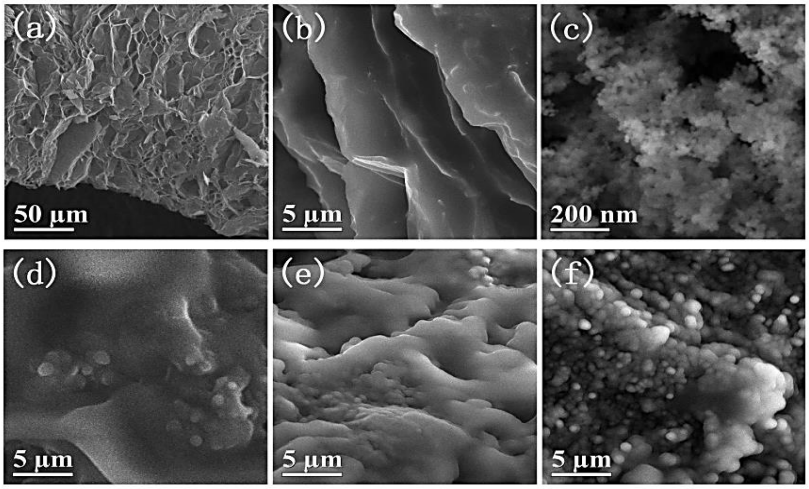

Figure 2.17 Scanning electron microscope (SEM) images of EG, NS, and CPCM samples with varying NS content: (a) EG, (b) CPCM-NS0, (c) NS, (d) CPCM-NS3, (e) CPCM-NS5.5, and (f) CPCM-NS7.[96].

Şenocak et al. [88] develop a physicochemical crosslinking transformation strategy to produce flexible, leakage-proof PCMs by incorporating paraffin wax (PW) into a strong polymer network. The resulting composites demonstrated outstanding leakage- and water-resistance, along with high phase change enthalpy (>150 J g^{-1}) and excellent ductility (>60 %), effectively balancing shape stability, flexibility, and energy storage capacity. Moreover, these flexible PCMs exhibited superior cooling performance for electronic devices, highlighting their potential in thermal management of wearable electronics and outdoor systems.

Another study [98] presents a novel approach to developing highly conductive, leakage-proof PCM composites via ultrasonic and vacuum impregnation, using lauric acid as the base PCM and hexagonal boron nitride (h-BN) along with expanded graphite (EG) as thermally conductive additives. Compositional and structural analyses (FTIR) confirmed the chemical stability of the composites and complete encapsulation of the PCM within the EG framework. The resulting form-stable PCMs exhibited a 450 % increase in thermal conductivity and a 77 % reduction in photo-transmittance relative to the base PCM. Although the latent heat decreased slightly by 11.5 %, the composites maintained thermal stability up to 220 °C and excellent cyclic reliability after 500 melting/freezing cycles. When integrated into heat sinks, the composites effectively lowered the peak operating temperature by 16 °C, demonstrating superior heat dissipation and reliability for advanced electronic thermal management systems. Electronic thermal management systems increasingly rely on organic solid–liquid phase change materials (PCMs) for their high latent heat storage capacity; however, their practical deployment remains limited because these materials suffer from leakage during phase transition.

Yu et Feng [99] introduce a scalable and efficient strategy to develop form-stable, high-conductivity PCMs by Developing thermal conduction networks of separated boron nitride (BN) in a poly(styrene-b-ethylene-butylene-b-styrene) (SEBS)/paraffin wax (PW)composite to enhance thermal transport. Using a solvent-exchange-driven solution-spray coagulation method inspired by wet spinning, SEBS/PW (SP) microparticles were prepared and dynamically co-suspended with BN platelets before gel-state hot pressing to form a continuous segregated BN network. The optimized composite, with a SEBS/PW ratio of 20/80 and a BN loading of 30 wt% (16.3 vol%), achieved outstanding stability of form, a latent heat of 129.8 J/g, and an in-plane thermal conductivity of 1.51 $W \cdot m^{-1} \cdot K^{-1}$, corresponding to 50% and 293% improvements over BN systems that are randomly distributed and empty, respectively. In electronic cooling tests, the composite decreased the chip operating temperature from 95 °C to 80 °C, surpassing the performance of conventional silicone-based thermal interface materials. Combining low-cost raw materials, scalable fabrication, and superior heat storage and dissipation, this SEBS/PW–BN composite represents a promising candidate for next-generation electronic thermal management applications.

Sun et al. [100] developed a hierarchical porous scaffold using diatom frustules (DFs) and cellulose nanofibers (CNFs) via freeze-drying and carbonization. DFs tuned the pore structure of carbonized CNFs (CCNF) from microporous to mesoporous, balancing leakage prevention and crystallization. Mesopores enhanced beeswax (BW) crystallization, while micropores confined molten BW to prevent leakage. COMSOL simulations showed micropores could convert macropores into leakage-resistant regions, improving adsorption. The CCNF/DF scaffold achieved 93.7 wt% BW loading and 129.8 J/g melting enthalpy. This scalable approach offers insights for designing high-performance, shape-stabilized PCMs with improved stability and energy storage.

Another study [101] developed a simple, safe method to fabricate shape-stable PCMs (SSPCMs) via in-situ polymerization, encapsulating PEG in a PMMA matrix and adding expanded graphite (EG) as a performance enhancer. The SSPCMs showed <1 % leakage. Increasing EG from 0 to 2.5 wt% improved thermal conductivity (0.23 → 1.73 $W \cdot m^{-1} \cdot K^{-1}$) and latent heat (85.11 → 116.10 $kJ \cdot kg^{-1}$), while enhancing structural and thermal stability. Building simulations indicated that 2 wt% EG in wall middle layers achieved optimal energy savings, reducing cooling demand by 8.64 %. Sensitivity, uncertainty, and economic analyses confirmed the robustness and cost-effectiveness of this approach.

Chapter 3 Experimental Procedure and Mathematical Modeling

3.1 Introduction

Paraffin wax is among the most widely PCMs in latent heat thermal energy storage systems due to its favorable melting point range, chemical stability, and high latent heat of fusion. However, to ensure efficient system design, accurate modeling, and reliable performance, it is essential To establish its thermophysical characteristics precisely. This chapter's goal is to estimate these properties by experimentation, this chapter outlines the experimental procedure and the measuring instruments employed in the study. All experiments were conducted at the Energy and Applied Thermal Laboratory (ETAP) of the University of Tlemcen.

3.2 Determination of the thermophysical proprieties of the paraffin wax/ slack wax using the T-history method

3.2.1 Presentation of the experimental setup

The experimental setup regarding the T-history approach used to characterize paraffin consists of a controlled thermal environment, in which identical test tubes containing the paraffin sample and a reference material (such as water with known thermal properties) are placed. Each tube is equipped with thermocouples precisely inserted at the samples' upper and lower surfaces to monitor the temperature change over time.

Figure 3.1 An image of the experimental setup for T-history measurements.

3.2.2 Materials

Phase change material (paraffin wax)

The paraffin wax incorporated in this work was provided by Sigma-Aldrich (Merck KGaA, Germany). It is a high-grade material containing less than 1% residual mineral oil, which gives it very good thermal stability, a narrow melting interval, and reproducible solidification properties. Conversely, the slack wax used originates from the Arzew refinery in Algeria and contains a much larger proportion of petroleum oil (approximately 20–30%). Although this composition makes it less pure, it also imparts higher viscosity and greater deformability. These intrinsic differences were intentionally exploited in order to regulate both the mechanical response and the thermal performance of the developed composite PCM.

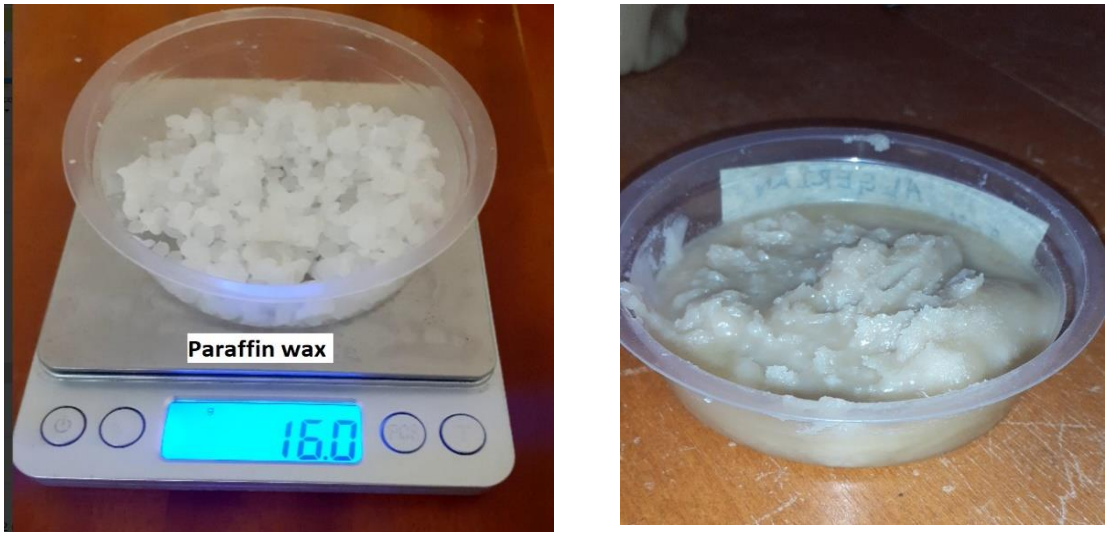

Figure 3.2 Photographs of the raw PCM materials.

U-shaped aluminum heat exchanger filled with paraffin and reference material (water); it consists of several parallel aluminum tubes bent into U-shaped channels and mounted vertically. It has an internal capacity of 0.0218 L.

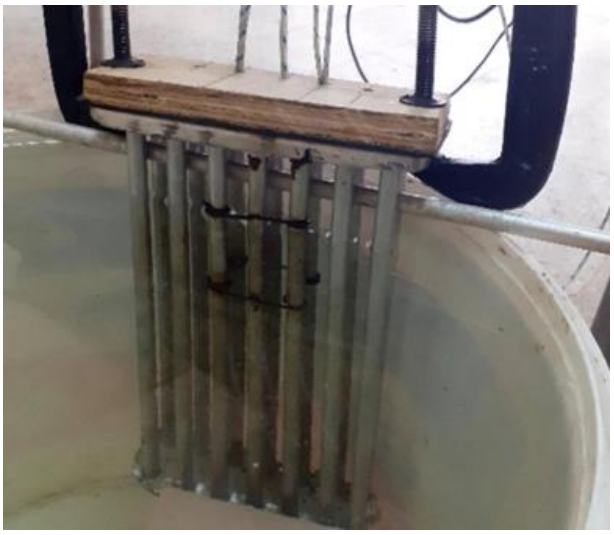

Figure 3.3 Tubes used in U-shape

Thermostatically controlled heating element, operating within a temperature range of 10 to 80 °C, was installed inside the water bath to regulate and maintain the desired water temperature throughout the experiment.

Figure 3.4 Thermal resistance

Data acquisition (DAQ) system from National Instruments, used to record temperature measurements during the experiment. Several thermocouples are connected to the DAQ module

through a thermocouple terminal block, allowing multi-channel temperature monitoring. The module is interfaced with a laptop via USB for real-time data logging and processing.

Figure 3.5 National Instruments cDAQ-9174 system

3.2.3 Preparation of the samples

The synthesized material consists of a binary combination of two PCMs. Particular attention was given to establishing a controlled and reproducible preparation procedure to ensure good compatibility, uniform distribution, and long-term stability. First, the paraffin wax was melted by heating it to 65–70 °C, providing complete liquefaction and a homogeneous temperature field. Afterwards, the slack wax was introduced progressively while applying continuous magnetic stirring in order to minimize thermal gradients and phase separation. The mixture was kept under agitation for a minimum of 20 minutes to guarantee sufficient dispersion and mixing at a molecular scale.

Figure 3.6 Photographic images of PCM (After mixing)

The mixtures of paraffin–slack wax were prepared with different weight proportions of 0%, 6%, 10%, 15%, and 20%, respectively, as seen in Fig. 1. During the preparation, temperature was kept as controlled as possible to keep both components well above their melting points, so that the risk of viscosity-driven segregation, premature crystallization, or component incompatibility was minimized. Preventive steps have been taken to address the potential dangers of phase separation, agglomeration, or sedimentation. First, to ensure total miscibility, heating and stirring conditions have been tuned. Second, ocular examinations upon mixing revealed combinations that were completely clear, homogenous, and free of any obvious signs of phase instability, such as wax clustering or oil leakage. These findings suggest that paraffin and slack wax have strong thermodynamic compatibility. Under carefully regulated laboratory circumstances, many heating-cooling cycles were undertaken to assess the mixes' physical and chemical stability over time and under thermal stress. After repeated cycling, the samples' appearance, color, texture, and behavior showed no discernible or quantifiable changes. Specifically, no phase separation, oil exudation, or degradation effects were seen, indicating combinations with exceptional long-term stability and no requirement for additional stabilizers or surfactants.

To examine the thermal properties of the PCM mixtures, a technique called the T-history test method, which has been demonstrated to be particularly efficient for large-scale PCM analysis, was used. This test involved packing a sample of a PCM mixture in an aluminum tube with a known thermophysical property substance, distilled water.

Temperature measurement

Two calibrated type-K thermocouples were positioned symmetrically at the top and bottom of the PCM sample and the reference tube.(Fig. 2.7) in order to monitor vertical temperature variations and accurately identify phase-change events. Temperature data were recorded using a National Instruments cDAQ-9174 acquisition unit combined with a LabVIEW-based monitoring interface, with measurements taken every 2 s to provide high temporal precision.

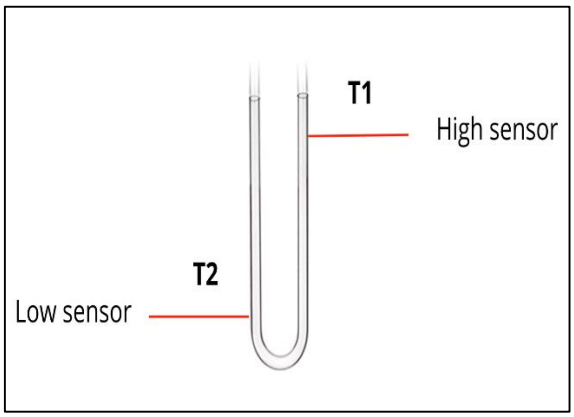

Figure 3.7 Temperature Sensor Placement in the U-Shaped Heat Exchanger

3.2.4 The principle of measurement

In the T-history approach, the PCM and the reference (distilled water) are first heated to a temperature exceeding the melting point of the wax and subsequently allowed to cool to room conditions without external intervention. To account for thermal expansion and avoid air gaps, each cylindrical tube was packed with approximately 80% of its internal volume, ensuring stable thermal contact throughout the test. All tubes used in the experiments possessed identical dimensions (length 26.5 cm, internal diameter 1 cm, wall thickness 1 mm), which maintained consistent geometry and improved the reproducibility of the measurements.

The latent heat of fusion and the specific heat of the PCM were founded by heating both the sample and the reference above the melting point $T_0 > T_m$, after which they were suddenly subjected to the ambient temperature T_∞. Throughout the cooling phase, water and paraffin temperatures are recorded as a function of time until the complete solidification of paraffin and the sample temperature reach T_∞, The tubes whose (L/D) > 10 achieve the condition Bi < 0.1 and verify the lumped capacity method.

To calculate the effective thermal conductivity of liquid state, the tube containing melted samples with temperature T_0 (is a little higher than T_m), is placed into a cool water bath. To establish the effective thermal conductivity for the paraffin in the solid state, the tubes filled with the solid paraffin are subjected into a hot water bath.

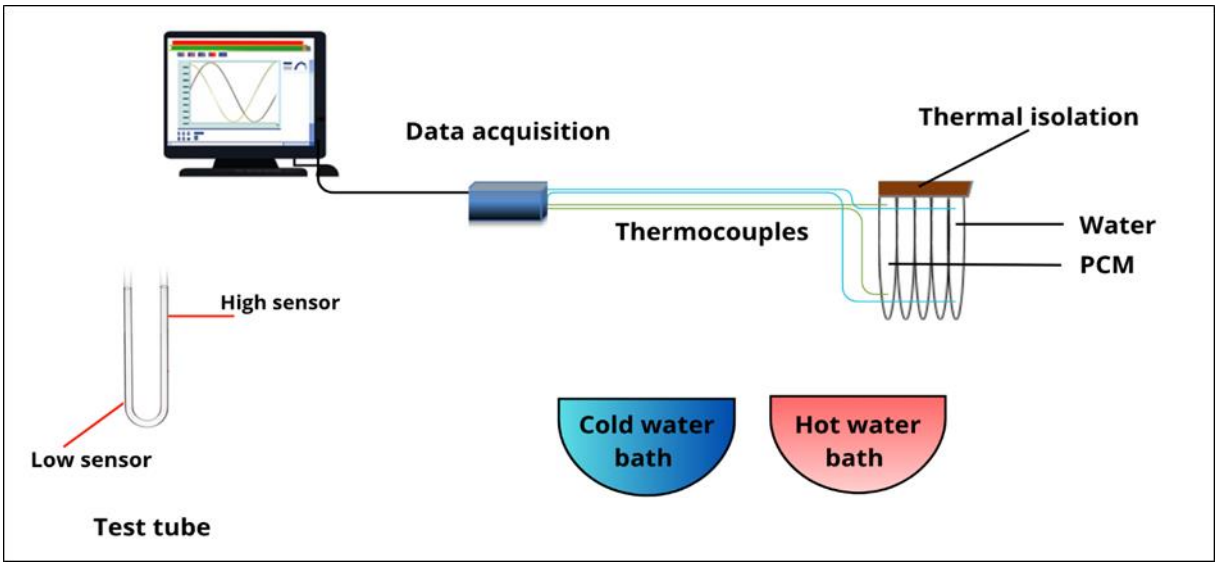

Figure 3.8 A representation showing the experimental configuration for using the T-history approach in the cooling phase.

All thermophysical measurements were conducted in triplicate under identical conditions, and results were reported as mean values with standard deviations to ensure statistical robustness. Additionally, solid and liquid phase densities were determined through precise mass and volume measurements, offering further insight into the thermal behavior of the blends.

Table 3.1 The most crucial information about slack and paraffin wax

	color	Oil content	Appearance (form)	Density [kg/l]	Melting point [°C]
Paraffin wax	white	< 1%	Pastilles	0.770-0.880	43-61
Slack wax	beige	20% to 30%	Soft and greasy blocks	0.830-0.850 [45]	40- 65 [45]

In summary, the careful mixing protocol, stability-enhancing precautions, repeated thermal cycling, and comprehensive thermophysical characterization demonstrate that the paraffin–slack wax blends are chemically and physically stable, homogeneous, and fully compatible. These composites can be employed as PCMs with no detectable phase separation,

agglomeration, or degradation, confirming their suitability for practical thermal energy storage applications.

3.2.4.1 Labview interface

LabVIEW (an acronym for Laboratory Virtual Instrument Engineering Workbench) is a visual programming environment developed by National Instruments. Firstly, it was used for data acquisition, instrument control, and automation. Unlike other programming languages, it has a visual programming language known as "G" or "G-code." This programming language lets a programmer create a program, known as a "Virtual Instrument" or "VI," by connecting "G-code" blocks.

Presentation of the interface (Labview)

To perform the digital acquisition of the measured temperatures, a graphical program was developed using LabVIEW. The program features two interfaces: a back-end interface for graphical programming and a front-end interface for data management:

Block Diagram – Programming Logic

The Block Diagram in LabVIEW represents the core programming logic of the application. It is where the user creates the functional flow of the program by connecting graphical blocks, which represent operations, functions, and data structures. Using the Block Diagram, you can implement loops, conditionals, mathematical operations, and hardware communication (such as reading temperature data from sensors via a DAQ system). Data flows through wires that connect these blocks, defining the execution sequence. For example, in a temperature measurement setup, the Block Diagram includes a While Loop that continuously acquires data, processes it (e.g., scaling or filtering), and sends the results to indicators or graphs on the Front Panel. This visual programming environment makes it easy to develop and debug complex measurement and control systems without writing traditional code.

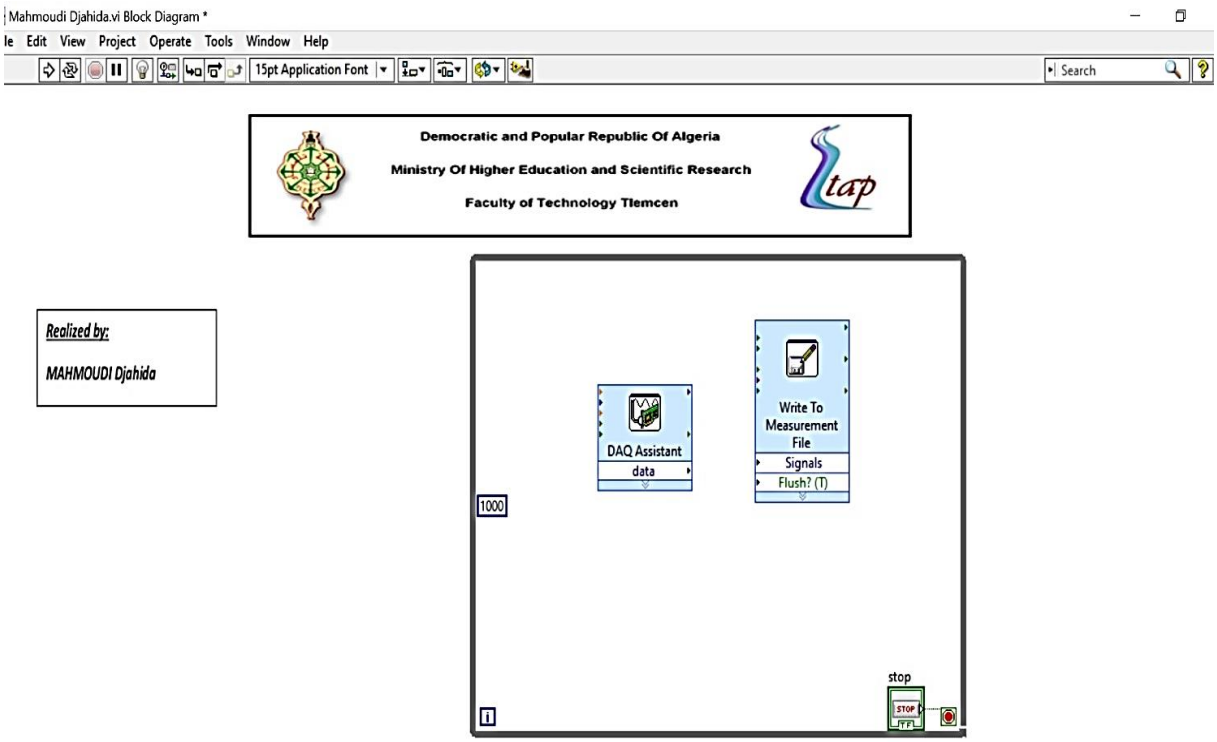

Figure 3.9 Block diagram in LabVIEW illustrating the data acquisition and logging system.

Front Panel – User Interface

The Front Panel in LabVIEW serves as the user interface of the application, enabling users to communicate with the system in a visual and intuitive way. It contains graphical elements such as controls (inputs) and indicators (outputs) that resemble real-world instruments like buttons, switches, numeric displays, and charts. For example, in a temperature acquisition system, the Front Panel may include a numeric indicator to display the measured temperature, a waveform chart to visualize temperature over time, and a stop button to control data acquisition. Users can enter values, start or stop the measurement process, and monitor results in real time. The Front Panel is directly linked to the Block Diagram, and any changes made to the interface elements are reflected in the program's logic, making LabVIEW especially suitable for experimental setups and real-time monitoring applications.

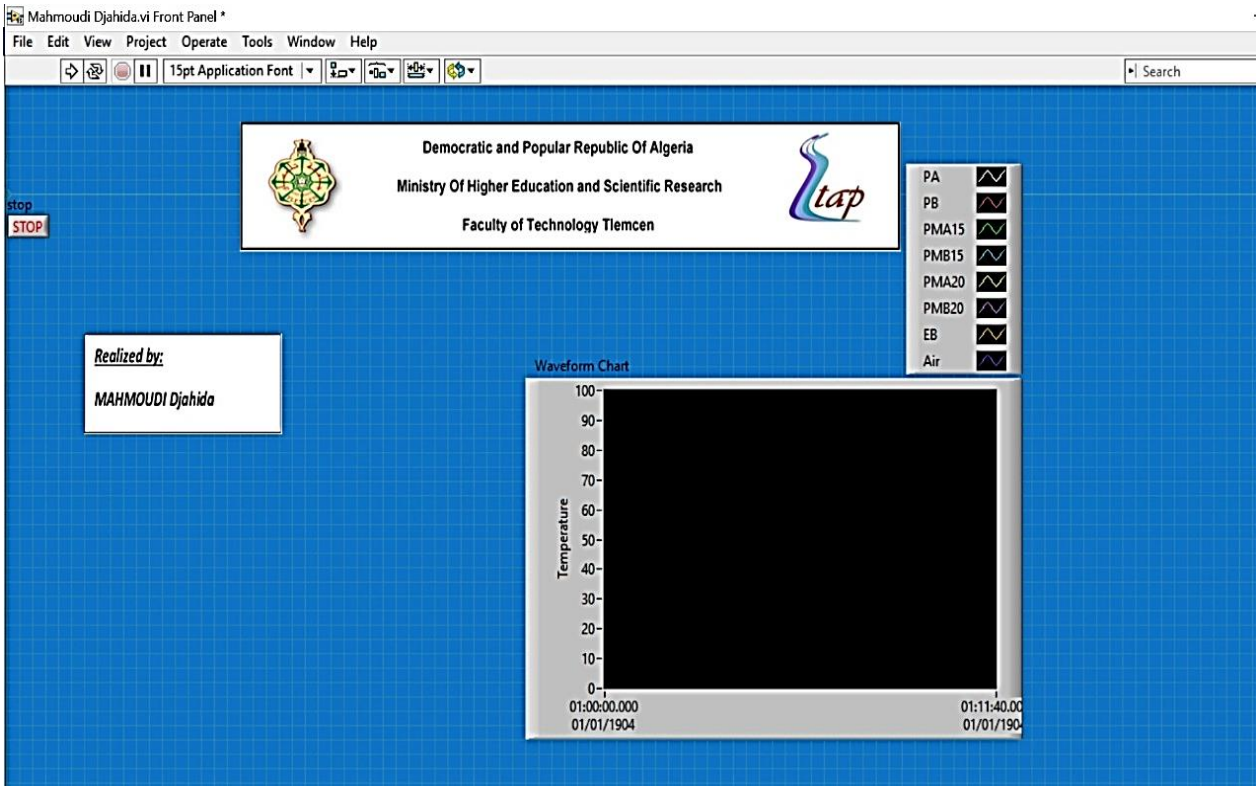

Figure 3.10 Front panel in LabVIEW for monitoring temperature in real time

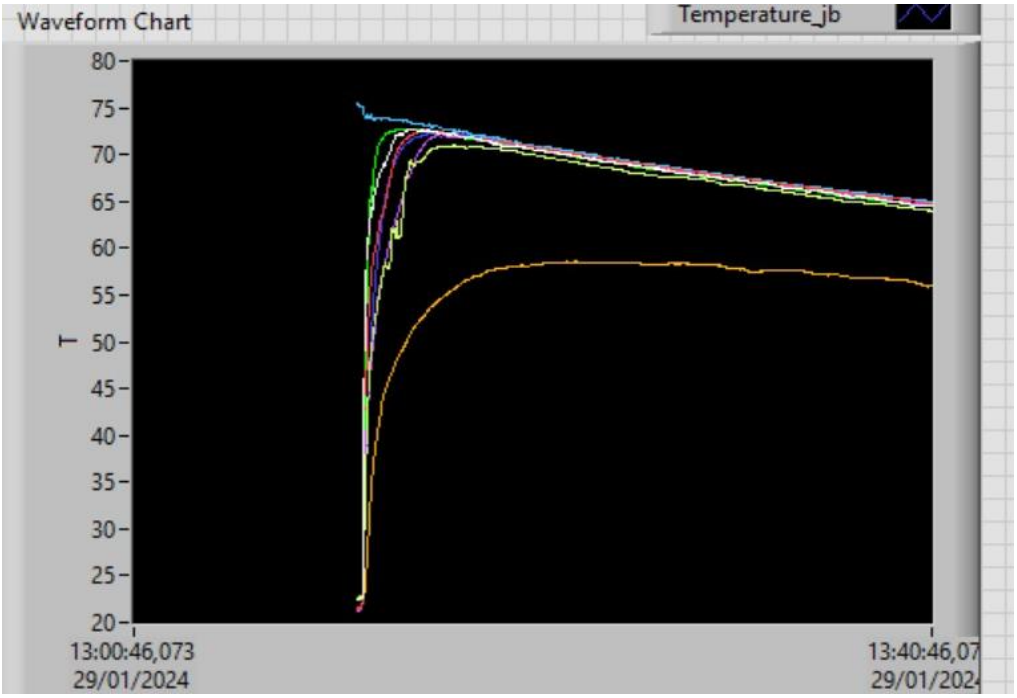

Figure 3.11 Temperature Evolution during Heating Process for Different Samples

3.3 Mathematical model

The lumped capacitance model is a simplification used in heat transfer analysis where a solid object's temperature is assumed to be uniform throughout its volume at any given time during a heating or cooling process. This simplification enables the use of ordinary differential equations rather than more complex partial differential equations. To assess the validity of applying the lumped capacitance model to the PCM's thermal behavior within the tubes, the Biot number (Bi) was calculated. The model is considered applicable when Bi < 0.1.

Biot number

The Biot number is a dimensionless parameter commonly used in heat transfer analysis to characterize the relative importance of surface convection compared to internal conduction within a solid. It was determined using Eq. (1), where k represents the thermal conductivity of the PCM.

$$Bi = \frac{h \cdot R}{2 \cdot K} \tag{1}$$

h: the convective heat transfer coefficient [$W/m^2 .k$]

R: the tube radius [m]

k: the thermal conductivity of the PCM [$W/m \cdot K$]

The convective heat transfer coefficient hhh was calculated using Eq. (2), considering natural convection around a vertical cylinder.

$$Nu_L = \frac{h.L}{K} \tag{2}$$

Nu_L: Nusselt number

L: the characteristic length of the system [m]

Nusselt number

The Nusselt number, "Nu," refers to a dimensionless value that represents the ratio of convective to conductive heat flow from a solid body to a fluid. For the present calculations, Nu was determined using Eq. (3). The correlation proposed by Churchill and Chu (1975) [102]

is a universal expression that has been widely accepted for determining values of heat transfer coefficient due to natural convection around an exterior vertical isothermal cylinder. This expression holds true for all values of Ra, no matter how low or how high.

$$Nu_L = \left\{ 0.825 + \frac{0.387 Ra_L^{\frac{1}{6}}}{\left[1 + \left(\frac{0.492}{Pr} \right)^{\frac{9}{16}} \right]^{\frac{8}{27}}} \right\}^2 \quad (3$$

Ra_L :Rayleigh number

Pr : Prandt number (physical propriety of the fluid)

Rayleigh number

The Rayleigh number Ra_L defined as the product of the Grashof number and the Prandtl number indicates the significance of buoyancy-driven natural convection in heat transfer. It can be calculated using Eq. (4).

$$Ra_L = \frac{g \cdot \beta \cdot \Delta T \cdot L^3}{\alpha \cdot \nu} \quad (4)$$

g : Gravitational force [m^2/s]

β : The coefficient of thermal expansion [k^{-1}]

ΔT : The temperature difference [$°C$]

L: the characteristic length of the system [m]

α : Thermal diffusivity [m^2/s]

ν: Dynamic viscosity [m^2/s]

To compute the Rayleigh number, which is needed in determining the value of the Nusselt number, a temperature difference ΔT was established as a difference between the PCM surface and air temperatures. In natural cooling with air ($T_\infty = 23°C$)), by approximation, the surface temperature of spheres was taken as an average between initial and final temperatures of PCM ($T_i \approx 63°C, T_f \approx 23°C$) so $T_s \approx \frac{T_i + T_f}{2} \approx 42.5°C$. Air properties like conduction and

viscosity were found using film temperature, taken as an average between surface and air temperatures $(T_{film} \approx \frac{T_s+T_\infty}{2} \approx 32.75°C)$.

With these values, the Rayleigh number was determined to be $Ra_L = 2.6\ 10^7$. Using the correlation for natural convection around a vertical cylinder as per Churchill and Chu, the corresponding value of the Nusselt number was determined to be $Nu = 41.1$, This value was used to find the convective heat flow coefficient, which came out to be $h = 4.4\ w/m^2.k$. o check that the use of the lumped analysis model is valid, a Biot number test was performed, which gave a value of 0.088. This value being below 0.1, it can be said that this model can be taken as valid.

3.4 T-history method. Examples of surface calculation

The regions below the cooling curve correspond to the integrated heat flow for both the PCM and the comparative sample of water. The corresponding area below the curve in the liquid-state nodes:

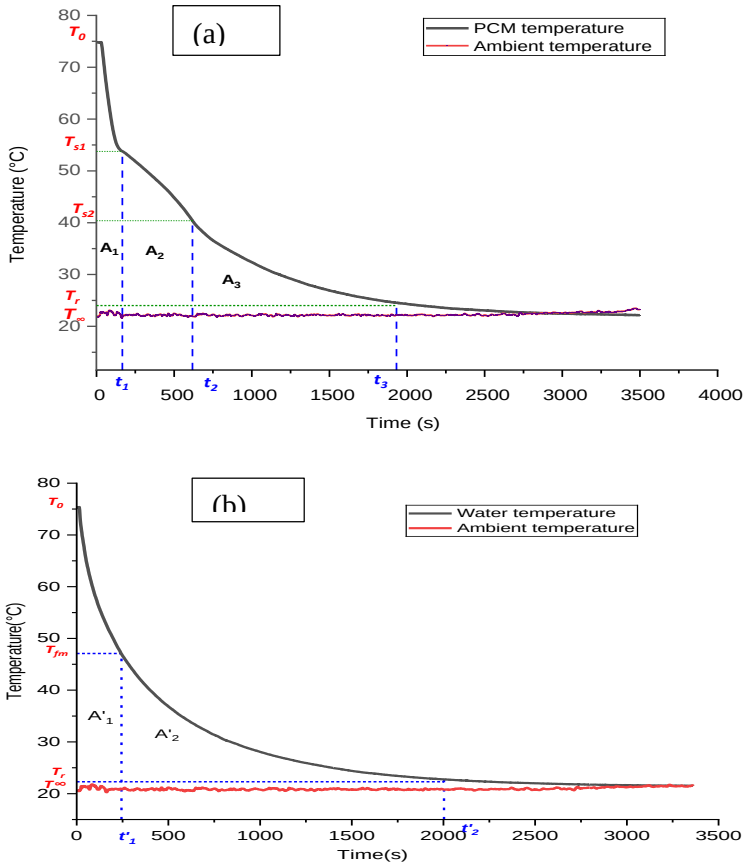

Figure 3.12 Representative T-history curves for (a) PCM and (b) water during cooling

A_1 ,A_2,A_3 for the PCM and A'_1 and A'_2 for the reference material (water)

The corresponding area below the curve in the liquid-state

$A_1 = \int_0^{t_1}(T - T_\infty)dt$

- The area under the curve during phase change

$A_2 = \int_{t_1}^{t_2}(T - T_\infty)dt$

- The area of the curve denoting the solid-state interval

$A_3 = \int_{t_2}^{t_3}(T - T_\infty)dt$

- The areas under the temperature-time cooling curve for the reference material (water)

$A'_1 = \int_0^{t'_1}(T - T_\infty)dt$

$A'_2 = \int_{t'_1}^{t'_2}(T - T_\infty)dt$

3.4.1 Measurement of Latent Heat and Specific Heat of PCMs

The PCM's thermophysical characteristics were determined based on formulas derived from the T-history method. [46], as outlined in Eqs. (5), (6), and (7).

$$Cp_l = \left(\frac{m_t \cdot Cp_t + m_w \cdot Cp_w}{m_p} \cdot \frac{A_1}{A'_1}\right) - \frac{m_t}{m_p} \cdot Cp_t \quad (5)$$

$$Cp_s = \left(\frac{m_t \cdot Cp_t + m_w \cdot Cp_w}{m_p} \cdot \frac{A_3}{A'_2}\right) - \frac{m_t}{m_p} \cdot Cp_t \quad (6)$$

$$H_m = \left(\frac{m_t \cdot Cp_t + m_w \cdot Cp_w}{m_p} \cdot \frac{A_2}{A'_1} \cdot (T_0 - T_{m1})\right) - \frac{m_t}{m_p} \cdot Cp_t \cdot (T_{m1} - T_{m2}) \quad (7)$$

Cps and *Cpl* *:* Average specific heats of solid-liquid PCM in the thawing/freezing temperature rang*e* [KJ/kg.K]

H_m : The heat of fusion of the paraffin [*J/kg*]

m_p : The masse of the PCM [*kg*]

m_t : The masse of the tube [*kg*]

m_w : The masse of the water [*kg*]

Cp_t , Cp_w : The specific heats of the tube and water, respectively [*KJ/kg.K*]

3.4.2 Measurement of PCM Thermal Conductivity

In the framework of the T-history method, heat transfer was represented using a cylindrical model and simplified to a one-dimensional analysis owing to the symmetry of the system. [46], as in Eq. (8).

$$\frac{1}{r}\frac{\partial}{\partial r}\left(r\frac{\partial T\left(r,t\right)}{\partial r}\right)=\frac{1}{\alpha_p}\frac{\partial T(r,t)}{\partial t} \qquad \left(\xi < r < R, t > 0\right) \tag{8}$$

Where $T(r, t)$ The temperature distribution of PCM with sample radius r and time t; ξ represents sample radius of the interface between PCM in solid and liquid form; h_w represents heat transfer coefficient for convection between tube surface and cooling water circulating in the tube; and αp represents sample thermal diffusivity of PCM

Using the perturbation approach, the thermal conductivity of the PCM in its solid state was determined as described in Eq. (11) [46]:

$$k_s=\frac{1+\dfrac{Cp\left(T_m-T_{\infty,w}\right)}{H_m}}{4\left(\dfrac{t_f\left(T_m-T_{\infty,w}\right)}{\rho_p R^2 H_m}-\dfrac{1}{h_w R}\right)} \tag{9}$$

Stefan number

The Stefan number (Ste), defined as the ratio between sensible and latent heat, was determined according to Eq. (10).

$$Ste=\frac{Cp(T_m-T_{\infty,w})}{H_m} \tag{10}$$

For simplification, the second term in the denominator was omitted, an approximation considered valid for most experimental scenarios. The simplified form of the equation is therefore:

$$k_s = \frac{1+Ste}{4\left(\frac{t_f\left(T_m - T_{\infty,w}\right)}{\rho_s R^2 H_m}\right)} \tag{11}$$

Following the same methodology, the liquid-state thermal conductivity of the PCM was calculated according to Eq. (12).

$$k_l = \frac{1+Ste}{4\left(\frac{t_m\left(T_{\infty,w} - T_m\right)}{\rho_l R^2 H_m}\right)} \tag{12}$$

t_m: The time of full melting of the solid PCM [s]

t_f: The time required for complete solidification of the molten PCM [s]

T_m: The melting temperature of PCM [°c]

$T_{\infty,w}$: The cool water bath temperature [°c]

ρ_s, ρ_l: The density of solid and liquid PCM [kg/m^3]

3.4.3 Uncertainty analysis

Uncertainty analysis was performed in order to estimate the error in measurement that can occur in experiments. The weighing of PCM samples was done using a 0.01g precise electronic balance, while data on temperature was measured using a type K thermocouple with a tolerance of 0.2°C. While acquiring data, a National Instruments cDAQ-9174 data acquisition system was used, which has a data resolution of 5 ppm. The uncertainties of measured parameters are shown in Table 3.2.

Table 3.2 Evaluation of Uncertainties in Experimental Measurements

Measuring parameter	Uncertainty
Experimental instrument	±1.25%
Specific heat	±1.25%
Heat of fusion	±1.77%
Thermal conductivity	±2.50%

Chapter 4 Results and discussion

4.1 Introduction

This chapter addresses the thermal analysis of the pure paraffin and paraffin-slack-wax mixtures using the T-history test. The test findings are examined for heating and cooling cycles of pure paraffin as well as for mixtures with 6%, 10%, 15%, and 20% slack-wax content. Such observations help in understanding how the addition of slack-wax affects the melting, enthalpy, and general thermal properties of modified PCMs.

4.2 Results and discussion:

4.2.1 Melting temperature

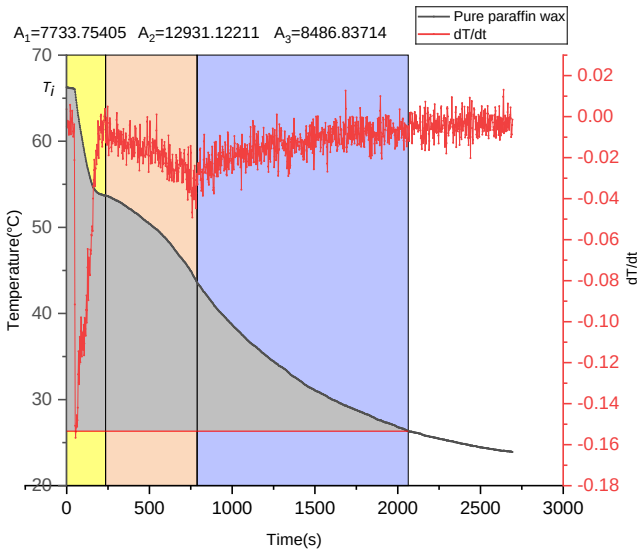

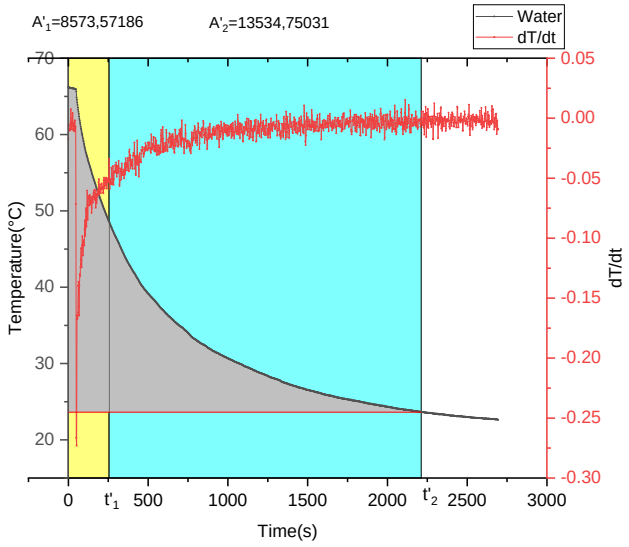

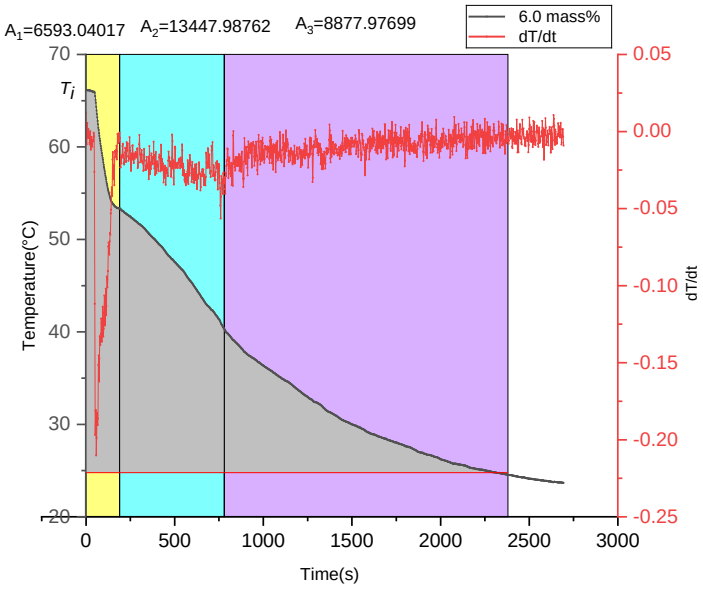

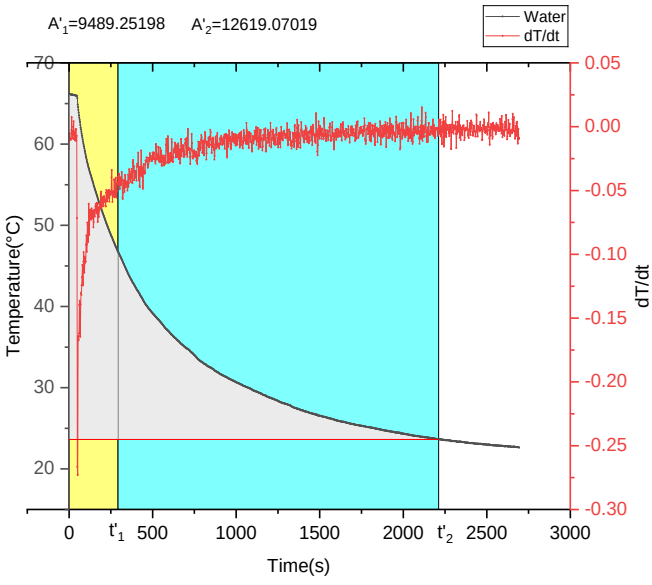

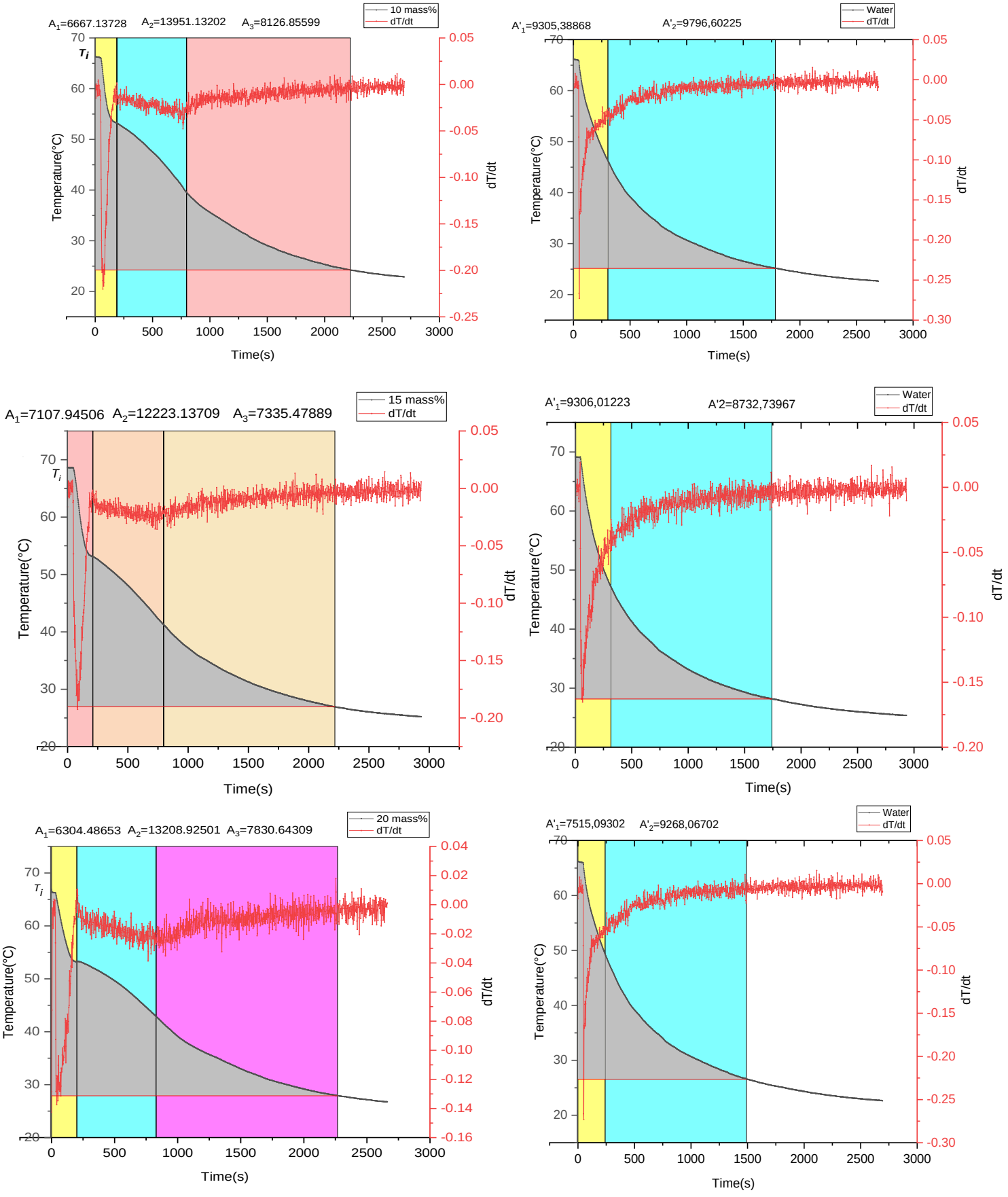

Figure 4.1 Temperature–time curves of the paraffin–slack wax PCM and the reference water sample.

Figure 4.1 below displays the cooling curves derived from performing the T-history tests. The plot with a red line represents the first derivative of temperature, i.e., dT/dt, which was utilized for determining the point of inflection that indicated the onset of the transition point. The cooling curve showed no signs of subcooling, as it distinctly marked the transition period and corresponding temperature range. Temperature decreased from 67°C to a value close to 25°C in a gradual manner, with the release of latent heat of fusion taking place in the period defined by t_2 and t_2, i.e., Ts_2. Lastly, t_3 marked where a thermodynamic state of equality prevailed between heat, matter, and energy, hence marking the end of solidification.

The above graph also shows how the water temperature in the test tube changes with time in the cooling period. The value of time t'_1 was obtained by extending the graph of the melting point of paraffin, T_{fm}, to the time axis, while that of t'_2 represents the point of stabilization. These characteristic times, t_1, t_2, t_3, t'_1, and t'_2, were used to set boundaries for all integration intervals.

Table 4.1 lists the data the scope of melting temperatures of the pure paraffin and slack-wax-improved samples. The addition of slack wax introduced a noticeable variation in the thermophysical properties of the mixtures. With every increase in slack wax proportion, it became apparent that there was a widening range of melting. While it would be ideal if the mixture melted in a sharp range for uses in which precise thermal switching was a priority, It should be noted that in situations in which a certain degree of thermal buffering were necessary, this wide range would, in point of fact, present a valuable characteristic that would ensure a continuous transition of heat release and absorption with fluctuations in temperature

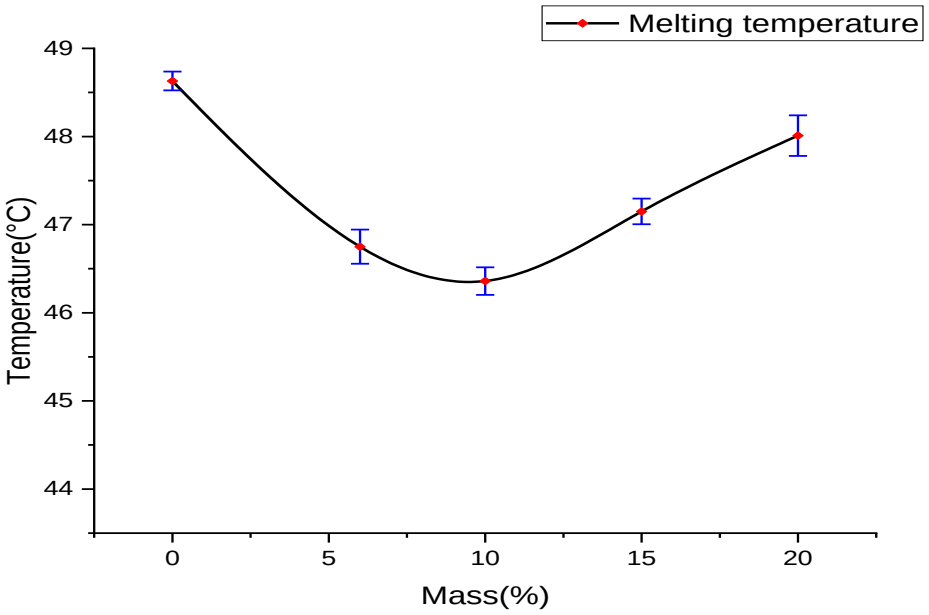

Figure 4.2 The mean melting point of various mass percentages of slack wax and pure paraffin.

Figure 4.2 above demonstrates that the variation in the melting point of paraffin-slack-wax mixtures with increasing proportion of slack wax is not a straight line. There appears to be a point of inflection, where a corresponding fall in melting point occurs until 10 wt.%, beyond which a minute increase in melting point follows. This variation can be explained on the basis of a conflict between two processes when a low concentration of slack wax is introduced, which has amorphous substances and oil that inhibits crystallinity, hence decreasing the lowest melting point. However, a higher extent of molecular interaction for long-chain compounds seems to increase partial crystallinity, hence a minute increase in the melting point above 10% slack wax.But it's important to note that this explanation of observations has not been as yet validated by direct microscopic analysis, even though similar observations were already reported in other studies. To cite an example, similar nonlinear patterns were also found in studies involving slack wax as a phase change medium by Dhivagar et al., and were related to their amorphous structure and inhomogeneous distribution of molecular chain lengths. Similar observations were also found by Geng et al., pointing towards the effects of variations in either hydrogen bond concentrations and molecular structures in ester-based PCM, resulting in noticeable differences in the range of variation of the transition period. Similar additive-induced changes in crystallinity were also found by [103] and [104].

Taken together, these findings reinforce the hypothesis that the non-linear melting behavior reported here results from the competition between crystalline disruption and molecular

reorganization processes that commonly occur in multi-component organic PCMs. To further substantiate this explanation, future studies will involve microscopic characterization (SEM/FTIR) in order to directly examine the crystalline morphology and phase distribution..

4.2.2 Specific heat

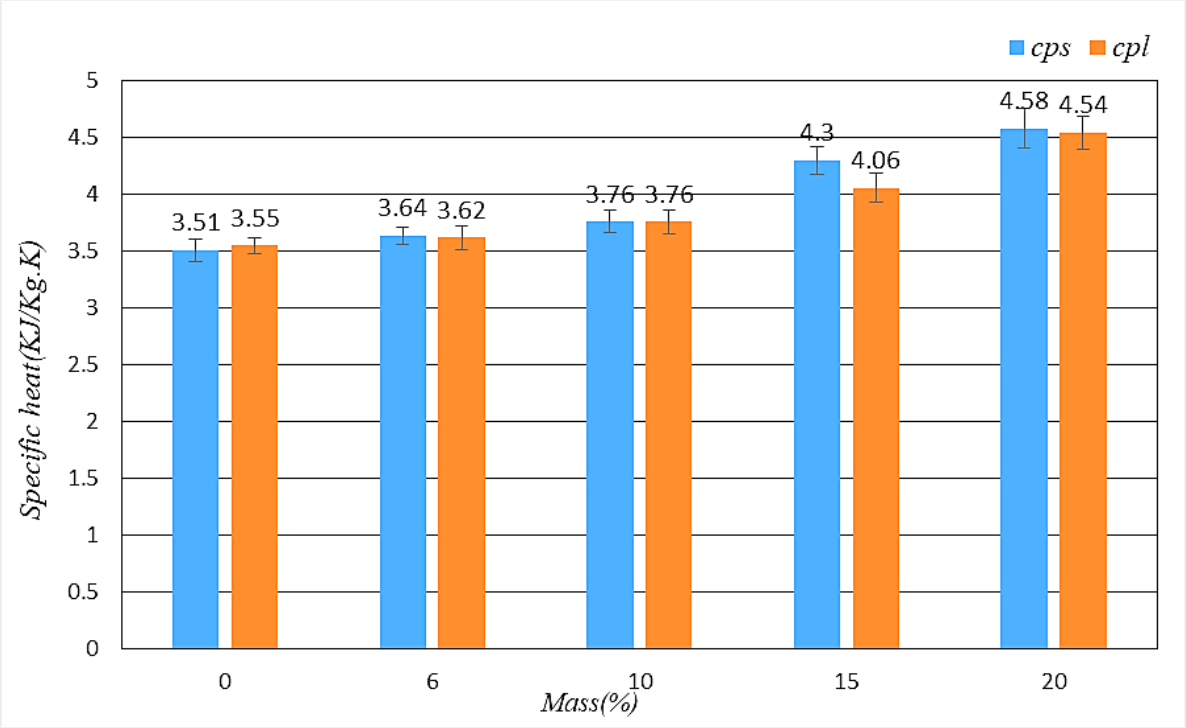

Figure 4.3 Variation of specific heat for different slack-wax mass percentages and pure paraffin.

Figure 4.3 demonstrates how the specific heat of paraffin varies with increasing slack-wax content. Incorporating 20 wt.% slack wax raised the specific heat from 3.51 to 4.58 kJ/kg·K, corresponding to an improvement of about 30%, and thereby enhanced the material's capacity for thermal energy storage. This improvement can be ascribed to the partial disruption of the crystalline lattice caused by the amorphous hydrocarbons in the slack-wax fraction, which promotes greater heat uptake and storage. In addition, changes in intermolecular interactions appear to slow heat release, contributing to a longer heat-retention period. The wider melting interval also supports a more homogeneous temperature distribution, limiting thermal gradients and reducing associated losses. Overall, these results indicate that adding slack wax significantly improves PCM performance, making the resulting composite more appropriate for thermal-management applications such temperature stabilization systems, passive heating, and solar energy storage.

4.2.3 Latent heat

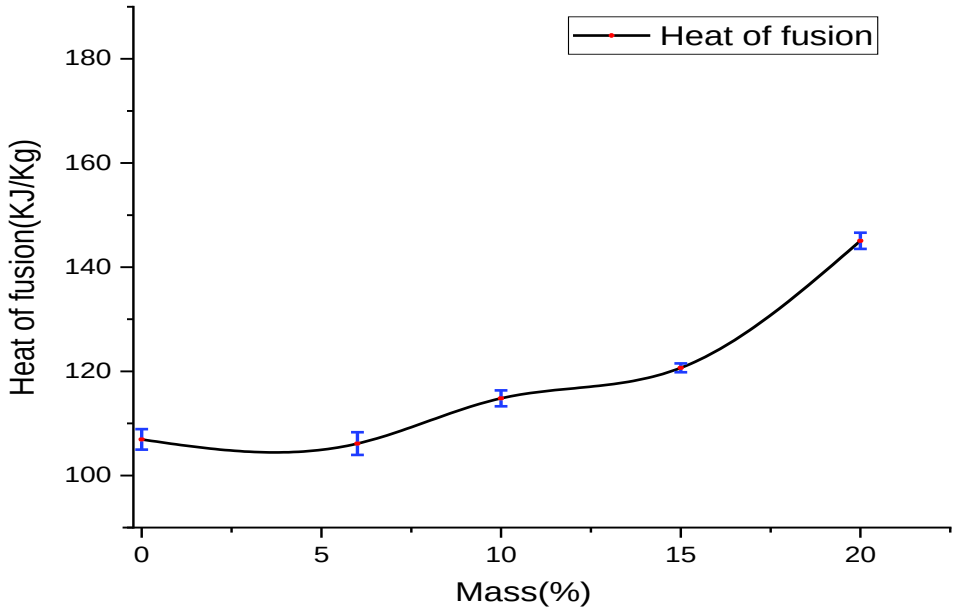

Figure 4.4 Variation of latent heat of fusion with slack-wax mass fraction relative to pure paraffin.

Figure 4.4 demonstrates how the percent values of slack wax affect the values of_the latent heat of fusion of the tested composite samples. Pure paraffin has a value of 106.93 kJ/kg for the latent heat of fusion, but with 20% slack wax, it becomes 145.06 kJ/kg, showing an increase of about 35%. This increase in the values of latent heat of fusion can be considered as a result of a certain hindrance to the perfect lattice structure of paraffin due to the presence of slack wax. This hindrance creates disordered crystalline structures that require a higher amount of energy for transition from the solid to the liquid state. Also, the presence of slack wax adds energy barriers in the matrix. Therefore, adding slack wax will enhance the performance of paraffin in terms of storing and releasing thermal energy.

Table 4.1 Summary of key thermophysical properties (melting temperature, specific heat, and latent heat of fusion) for paraffin wax modified with slack wax.

	Melting temperature (°c)	*Melting range (°c)*	*Cp_s (kJ/kg.K) ±sd*	*Cp_l (kJ/kg.K) ±sd*	*H_m (J/kg) ±sd*
Paraffin pure	43.63–53.63	10	3.51 ± 0.096	3.55 ±0.073	106.93 ±0.97
6%	40.33–53.16	12.83	3.62 ±0.075	3.65 ±0.1	106.1 ±1.17
10%	40.15–53.62	13.47	4.48 ±0.1	3.76 ±0.1	108.84 ±0.53
15%	41.24–53.07	11.83	4.55 ±0.12	4.06 ±0.11	130.71 ±0.84
20%	42.84–53.21	10.37	4.58 ±0.17	4.54 ±0.12	145.06 ±1.05

4.2.4 Thermal conductivity

The value of effective thermal conductivity of paraffin in a solid condition was determined using the total solidification time, measured between the start of the experiment and the completion of the solidification of PCM, as shown in Figure 4.5. Also, for the melted paraffin, total melting time of PCM, as shown in Figure 4.6, was measured for the estimation of its value of effective thermal conductivity.

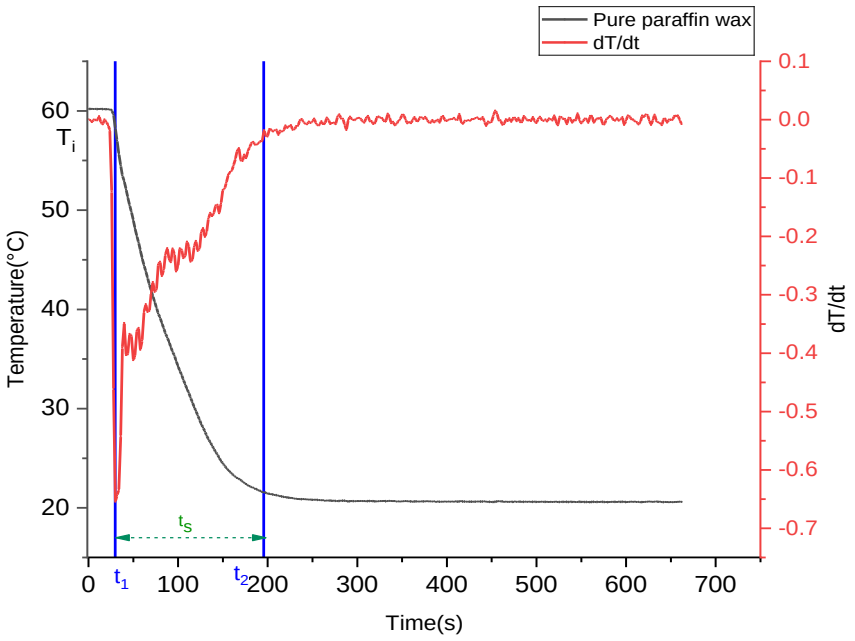
Pure paraffin wax
dT/dt
Temperature(°C)
dT/dt
Time(s)
T_i
t_1
t_2
t_s

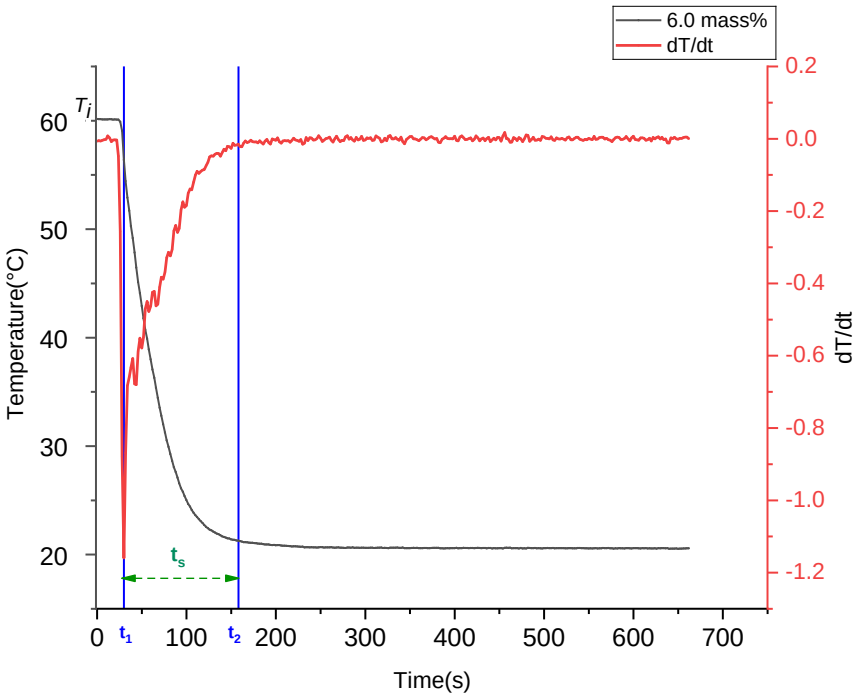
6.0 mass%
dT/dt
Temperature(°C)
dT/dt
Time(s)
T_i
t_1
t_2
t_s

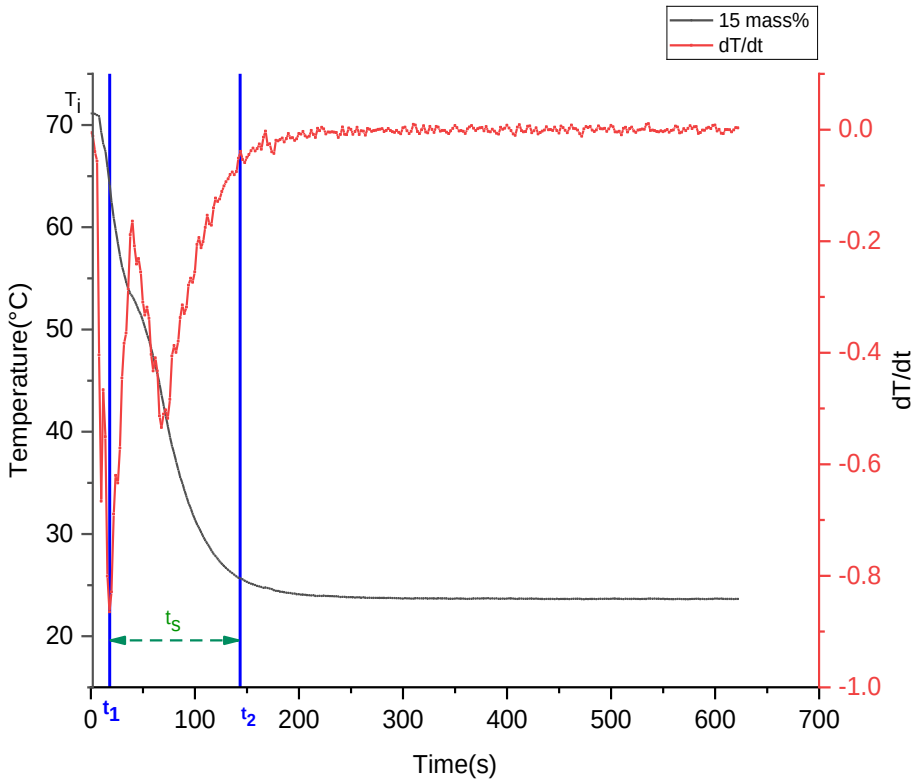
15 mass%
dT/dt
Ti
70
60
50
40
30
20
Temperature(°C)
0.0
-0.2
-0.4
-0.6
-0.8
-1.0
dT/dt
ts
0
t1
100
t2
200
300
400
500
600
700
Time(s)

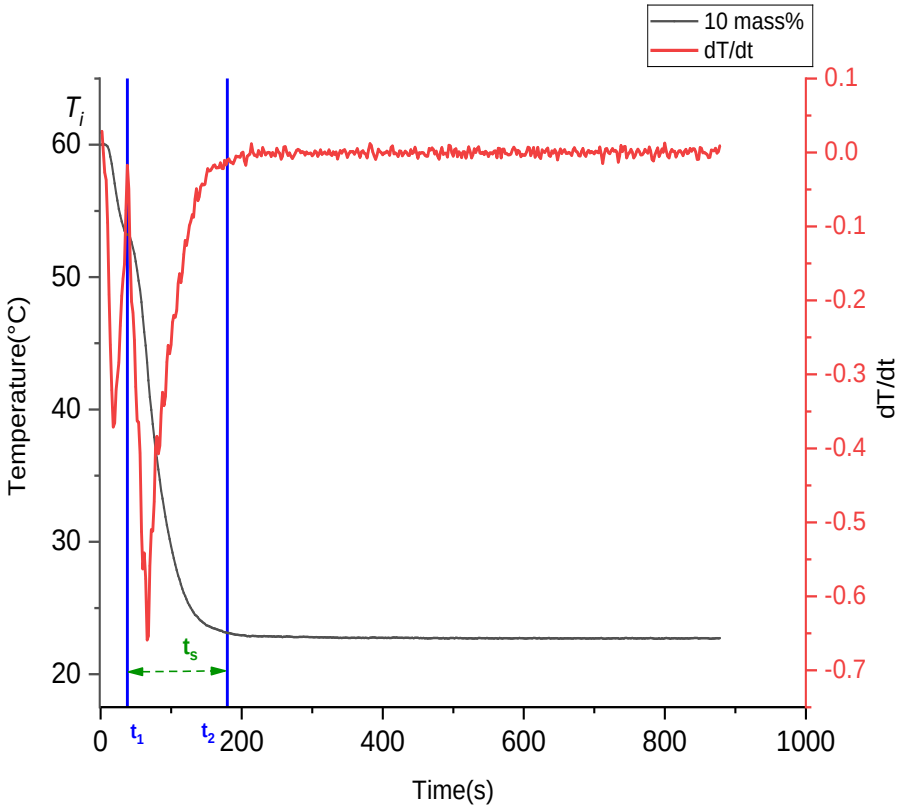
10 mass%
dT/dt
Ti
60
50
40
30
20
Temperature(°C)
0.1
0.0
-0.1
-0.2
-0.3
-0.4
-0.5
-0.6
-0.7
dT/dt
ts
0
t1
t2
200
400
600
800
1000
Time(s)

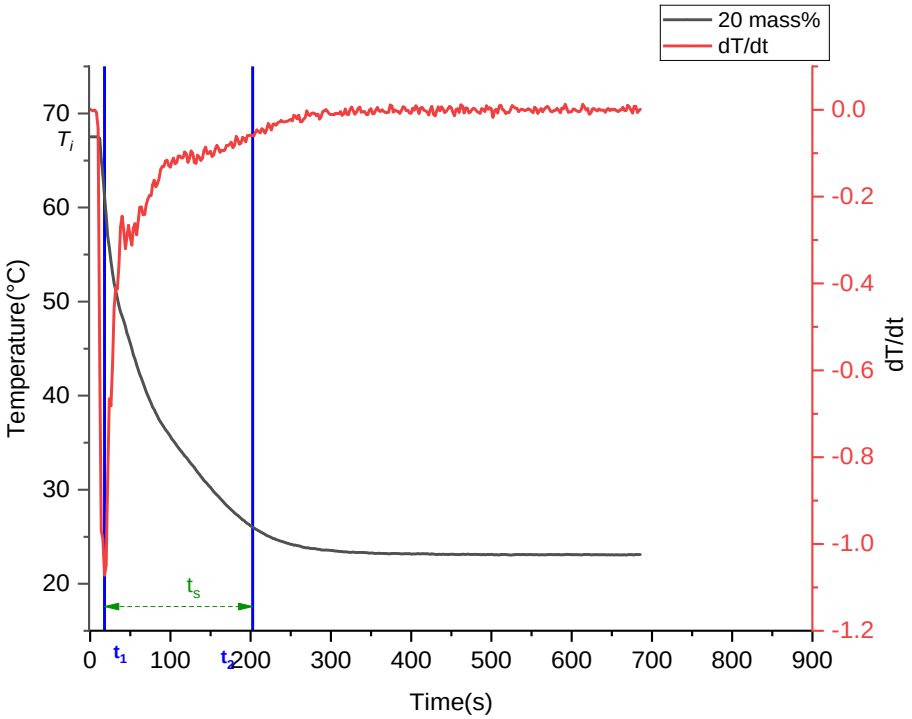

Figure 4.5 Temperature–time cooling curves of the samples

Figure 4.5 shows the cooling curves for the samples that were inserted into the water bath at 23 °C. Inflection points were obtained by analyzing the first derivative of the temperature curve, which provided the complete solidification time. For pure paraffin, this time corresponded to 165 s, while with the addition of slack wax at 6%, 10%, 15%, and 20%, the time reduced to 134 s, 132 s, 124 s, and 120 s, respectively.

These results demonstrate how adding slack wax changes the melting range and speeds up the solidification process under the same cooling circumstances. The quicker passage from liquid to solid can be attributed to molecular interactions induced by the slack wax. It broadened the melting interval by disturbing the crystalline structure, yet it simultaneously introduced additional nucleation sites that permit quicker crystallization once the PCM reaches its phase-change region. The end result is that solidification started sooner and proceeded more rapidly, even as the melting interval was broadened.

A reduced time of solidification is quite effective in applications that need the rapid release of heat, such as heat regulating systems during sudden temperature reductions. Combining high latent heat with faster energy discharge, slack-wax-modified paraffin improves both thermal energy storage and the material response. Overall, this reduction in solidification time shows that slack wax improves the energy storage capacity of paraffin, along with its thermal performance during the cooling phase.

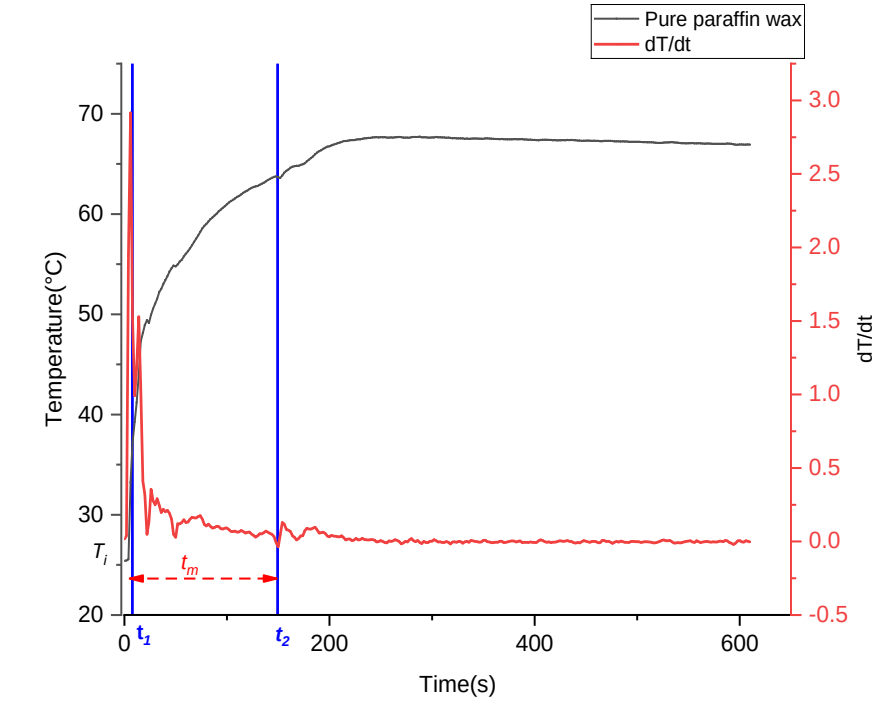
Pure paraffin wax
dT/dt
Temperature(°C)
dT/dt
Time(s)
T_i
t_m
t_1
t_2

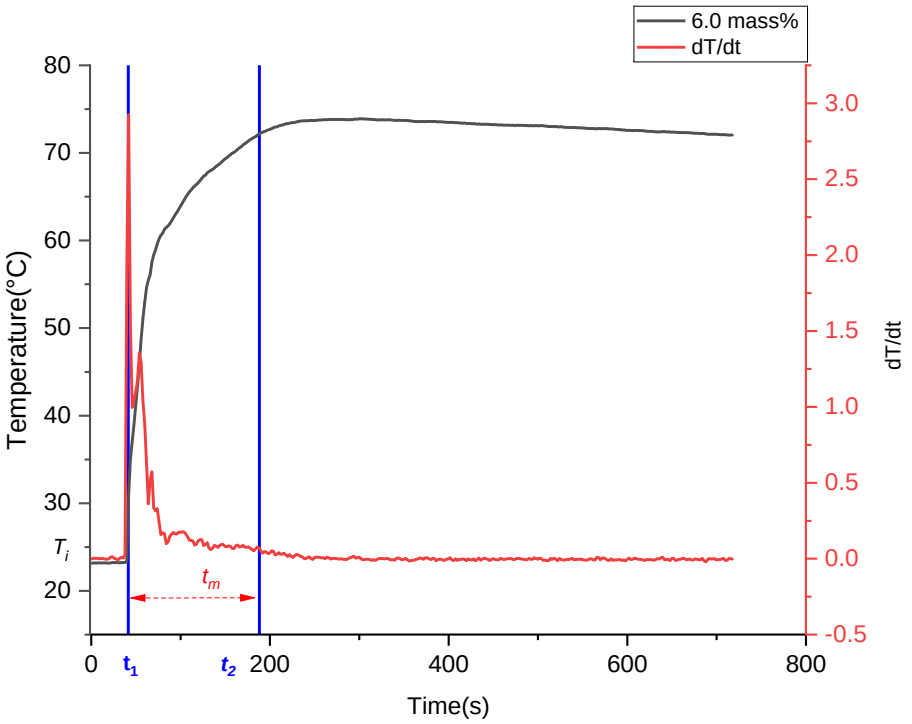
6.0 mass%
dT/dt
Temperature(°C)
dT/dt
Time(s)
T_i
t_m
t_1
t_2

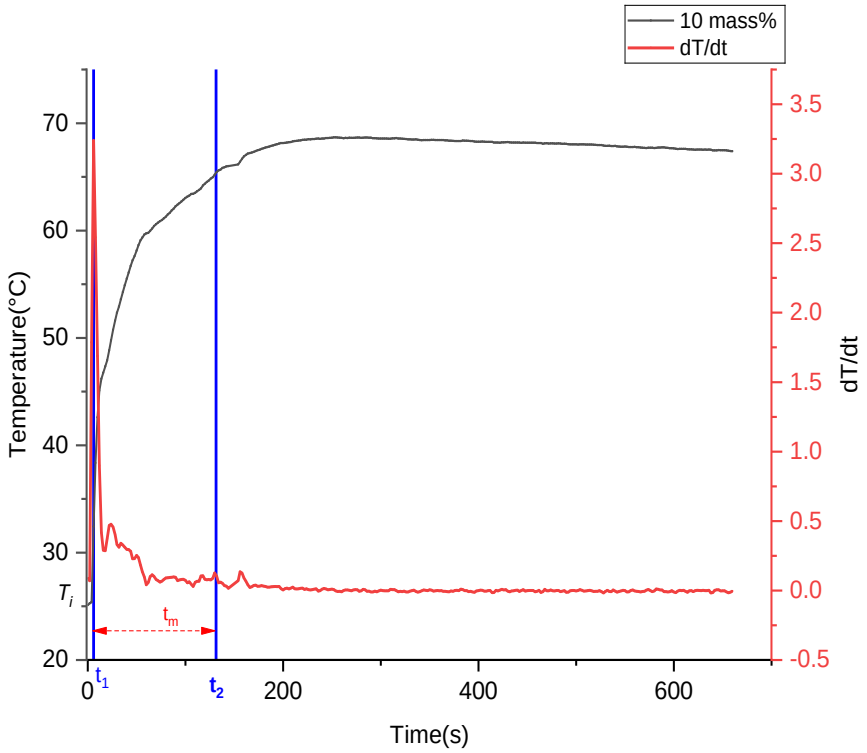
10 mass%
dT/dt
Temperature(°C)
dT/dt
Time(s)
T_i
t_m
t_1
t_2

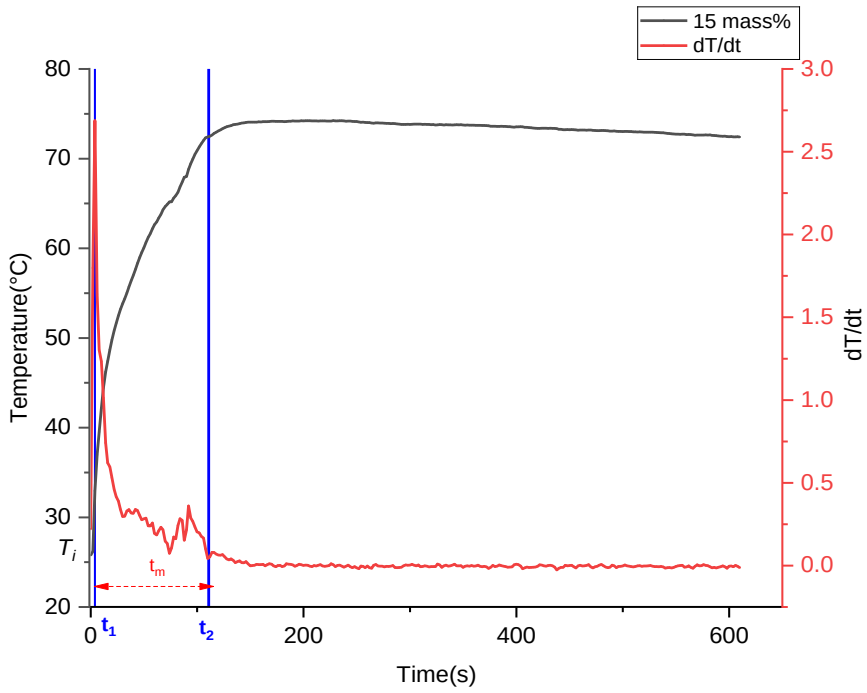
15 mass%
dT/dt
Temperature(°C)
dT/dt
Time(s)
T_i
t_m
t_1
t_2

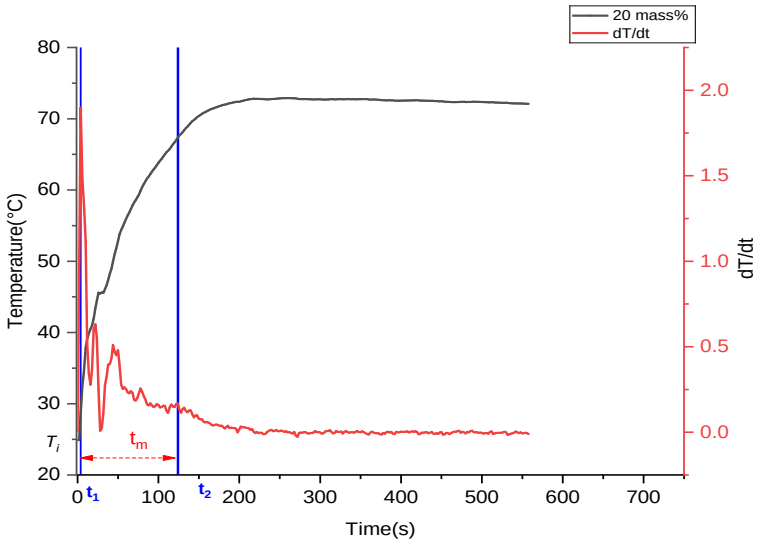

Figure 4.6 Temperature–time heating curves of the samples

Figure 4.6, on the other hand, illustrates the melt of paraffin-slack wax mixtures in a hot water bath set at 72°C, with increasing PCM temperatures from 25°C to 70°C. The first derivative of the heating curve was used to identify the melt duration (t_1–t_2), which relates to the solid-liquid transition. A melt duration of 125 seconds, 113 seconds, 111 seconds, 107 seconds, and 100 seconds was shown for pure paraffin, as well as for mixtures with 6%, 10%, 15%, and 20% slack wax, respectively.

These observations reveal that the addition of slack wax decreases the total duration of transition for the PCM from solid to liquid. This can be ascribed to the disruption of ordered crystallinity in paraffin due to slack wax, which possesses disordered crystal structures that melt easily. Therefore, an efficient fusion process takes place, which manifests a promotional role of slack wax in enhancing the thermeresponsiveness of this composite PCM.

In this particular case, it was found that by using slack wax, there was a structural transformation in the paraffin matrix, which aided in a gradual process of phase change. This result seems to support those of Geng et al.[44] , who prepared an ester-based PCM with a controllable phase transition interval through manipulation of the intermolecular hydrogen bond. Their findings proved that increasing the range of phase change temperatures can increase the versatility of PCM in various heating and cooling applications, especially in conditions requiring a constant release of heat. Also, Hachemi et al. [105] in their study on Phase Change Humidity Control Materials (PCHCMs) demonstrated that using different melting point values of 22°C and 28°C for individual PCMs enhanced the performance of these PCM-based

humidity-controlled materials in maintaining a comfortable range of air temperature and humidity in a building.

Effective thermal conductivity results of paraffin with the addition of slack wax using the T-history method are presented in Fig. 4.7 below. From this figure, a significant enhancement in effective thermal conductivity of paraffin was achieved by adding slack wax. Pure paraffin in solid form had a thermal conductivity value of about 0.18 W/m•K. Adding 20 wt.% slack wax caused an increase to 0.24 W/m•K, which is about 33% higher. This is primarily because slack wax contains high-molecular-weight hydrocarbons and semi-crystalline structures, which provide less phonon scattering at molecular interfaces and continuity in thermal conduction paths. Pure paraffin in the liquid phase showed thermal conductivity of 0.17 W/m•K, increased to 0.22 W/m•K at 20 wt.% slack wax. The increment of thermal conductivities can be comprehended through change in The molecular dynamics, as well as the contribution of long-chain hydrocarbons, which enhance energy transfer both by conduction and micro-convection in the molten state, are other factors.

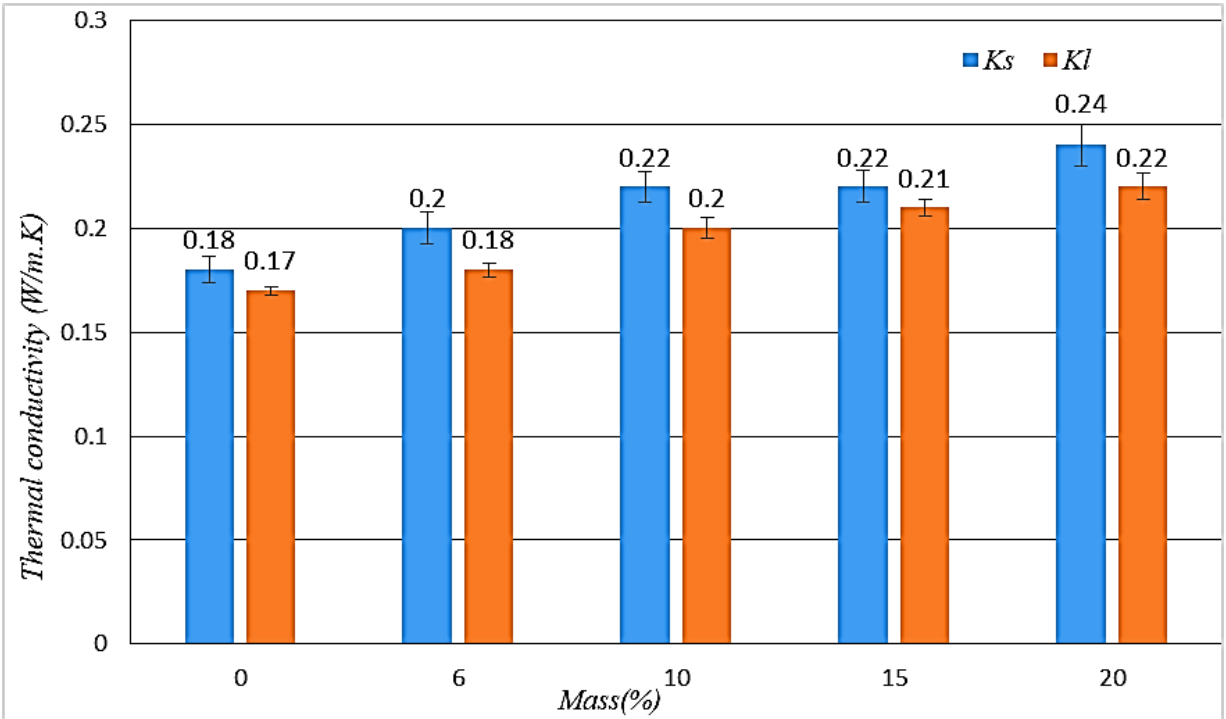

Figure 4.7 Measured thermal conductivity of the PCM samples

Finally, the reduced viscosity and better miscibility of the blend likely support a more homogeneous thermal energy distribution. These results confirm slack wax as an economically viable and performance-enhancing additive to paraffin-based PCMs that are especially required for faster thermal responses and higher heat storage efficiencies. The observed improvements in thermal conductivity for both the solid and liquid phases confirm the suitability of slack-wax-modified paraffin for thermal energy storage systems, building insulation, and temperature regulation technologies.The thermal properties of the modified paraffin, in summary, including those with slack wax addition, are systematically presented in Table 4.2 below.

Table 4.2 Effect of slack wax addition on the thermal conductivity of paraffin wax

	K_s *(W/m·K) ±sd*	K_l *(W/m·K) ±sd*
Paraffin pure	0.18 ±0.006	0.17 ±0.002
6%	0.20 ±0.007	0.18 ±0.003
10%	0.22 ±0.007	0.20 ±0.005
15%	0.22 ±0.007	0.21 ±0.004
20%	0.24 ±0.01	0.22 ±0.006

4.3 Comparative Analysis with Existing Studies

Table 4 compares the thermal properties of various composite PCMs with different additives, including this study. The paraffin-Algerian slack wax composite showed a marked improvement in their thermal properties; that is, there was a 35.65% increase in latent heat, a 30.48% increase in specific heat, and a 34% increase in thermal conductivity. These values are comparable, if not better, than those obtained from other studies. To be specific, the incorporation of exhaust carbon particles[106]showed a marked increase in latent heat of as much as 8% and a substantial increase in thermal conductivity of +155%, without affecting the specific heat, which was not measured. Likewise, adding wheat husk microparticles[107] showed a small amount of increase in this study, which was 4.57% for the latent heat and

66.66% for the thermal conductivity. Carbon quantum dots (CQDs) [108]showed the highest percentage increase in latent heat of 65.1%, without providing information on either of the other properties.

Table 4.3 Comparison of thermal properties of composite PCMs with various additives.

Added material	**Latent heat**	**Thermal conductivity**	**Specific heat capacity**
Algerian slack wax (present study)	+35.65 %	+33 %	+30.48 %
Exhaust carbon particles [106]	Up to 8 %	+155 %	Not mentioned
Wheat husk microparticles [107]	+4.57 %	+66.66 %	Not mentioned
Carbon quantum dots (CQDs) [108]	+65.1 %	Not mentioned	Not mentioned

Overall, it can be said that the paraffin and Algerian slack wax mixture showed a well-balanced improvement in various thermal properties. Unlike other additive materials, which usually enhance a certain property, this mixture enhanced not only the latent heat of fusion, but also the specific heat, as well as the thermal conduction property.

Although it has a superior thermophysical property profile, slack wax also has many other important advantages, including environmental and economic factors. Since it is a petroleum products refining by-product, using it as a PCM represents a form of effective valorization of this product, as it reduces landfilling, which in turn reduces emissions. On the economic side, it has been found that it costs 30-50% less than that of purified paraffin.

.

General Conclusion

General Conclusion

This thesis focused in the first section on the preparation and characterization of paraffin-based Phase Change Materials (PCMs) modified with Algerian slack wax with a view to ameliorating their thermal properties, as well as encouraging environmental sustainability with a focus on industrial by-product conversion.

The experiment proved that adding different mass fractions of slack wax, that is, 6%, 10%, 15%, and 20%, greatly improved the important properties of composites, that is, latent heat of fusion, specific heat capacity, and thermal conductivity.

A marked improvement of 35.65% in latent heat, 30.48% in specific heat, and 33% in thermal conductivity was obtained in the composite with 20 wt.% slack wax, which showed that there was a noticeable decrease in the charging and discharging times in conduction.

There are a number of important contributions that this project provides. Experiment-wise, it was able to examine large samples of data using the T-history test, which gave it a test in a real-world setting. Environment-wise, it has proven that slack wax is a low-cost, sustainable alternative to refined paraffin wax, reusing industrial waste reused in promoting circular economy concepts.

Therefore, this thesis verifies that Algerian slack wax has a promising application as an additive in paraffin-based PCMs, providing a dual benefit of performance improvement and effective use of a sustainable resource. The results obtained can form a basis for further development of low-cost, environmentally benign, and high-performance PCM materials for thermal energy storage.

References

References

[1] İ. Dinçer et M. A. Rosen, *Thermal Energy Storage: Systems and Applications*, 1re éd. Wiley, 2010. doi: 10.1002/9780470970751.

[2] K. S. Reddy, V. Mudgal, et T. K. Mallick, « Review of latent heat thermal energy storage for improved material stability and effective load management », *J. Energy Storage*, vol. 15, p. 205-227, févr. 2018, doi: 10.1016/j.est.2017.11.005.

[3] A. Sharma, V. V. Tyagi, C. R. Chen, et D. Buddhi, « Review on thermal energy storage with phase change materials and applications », *Renew. Sustain. Energy Rev.*, vol. 13, no 2, p. 318-345, févr. 2009, doi: 10.1016/j.rser.2007.10.005.

[4] P. Bose et V. A. Amirtham, « A review on thermal conductivity enhancement of paraffinwax as latent heat energy storage material », *Renew. Sustain. Energy Rev.*, vol. 65, p. 81-100, nov. 2016, doi: 10.1016/j.rser.2016.06.071.

[5] C. Amaral, R. Vicente, P. A. A. P. Marques, et A. Barros-Timmons, « Phase change materials and carbon nanostructures for thermal energy storage: A literature review », *Renew. Sustain. Energy Rev.*, vol. 79, p. 1212-1228, nov. 2017, doi: 10.1016/j.rser.2017.05.093.

[6] Z. Xie *et al.*, « Heat capacity study of fatty acids as phase change materials for thermal energy storage », *J. Chem. Thermodyn.*, vol. 197, p. 107338, oct. 2024, doi: 10.1016/j.jct.2024.107338.

[7] H. Nazir, M. Batool, M. Ali, et A. M. Kannan, « Fatty acids based eutectic phase change system for thermal energy storage applications », *Appl. Therm. Eng.*, vol. 142, p. 466-475, sept. 2018, doi: 10.1016/j.applthermaleng.2018.07.025.

[8] F. Berroug, E. K. Lakhal, M. El Omari, M. Faraji, et H. El Qarnia, « Thermal performance of a greenhouse with a phase change material north wall », *Energy Build.*, vol. 43, no 11, p. 3027-3035, nov. 2011, doi: 10.1016/j.enbuild.2011.07.020.

[9] A. Figueiredo, T. Silva, M. Gonçalves, et A. Samagaio, « Application of Novel Phase Change Material Constructive Solution for Thermal Regulation of Passive Solar Buildings », *Buildings*, vol. 14, no 2, p. 493, févr. 2024, doi: 10.3390/buildings14020493.

[10] K. Kaygusuz et A. Sari, « Thermal Energy Storage System Using a Technical Grade Paraffin Wax as Latent Heat Energy Storage Material », *Energy Sources*, vol. 27, no 16, p. 1535-1546, déc. 2005, doi: 10.1080/009083190914015.

[11] J. Wang, H. Xie, et Z. Xin, « Thermal properties of paraffin based composites containing multi-walled carbon nanotubes », *Thermochim. Acta*, vol. 488, nº 1-2, p. 39-42, mai 2009, doi: 10.1016/j.tca.2009.01.022.

[12] L. Xia, P. Zhang, et R. Z. Wang, « Preparation and thermal characterization of expanded graphite/paraffin composite phase change material », *Carbon*, vol. 48, nº 9, p. 2538-2548, août 2010, doi: 10.1016/j.carbon.2010.03.030.

[13] P. Chen, X. Gao, Y. Wang, T. Xu, Y. Fang, et Z. Zhang, « Metal foam embedded in SEBS/paraffin/HDPE form-stable PCMs for thermal energy storage », *Sol. Energy Mater. Sol. Cells*, vol. 149, p. 60-65, mai 2016, doi: 10.1016/j.solmat.2015.12.041.

[14] S. Wu, T. X. Li, T. Yan, Y. J. Dai, et R. Z. Wang, « High performance form-stable expanded graphite/stearic acid composite phase change material for modular thermal energy storage », *Int. J. Heat Mass Transf.*, vol. 102, p. 733-744, nov. 2016, doi: 10.1016/j.ijheatmasstransfer.2016.06.066.

[15] S. Lokesh, P. Murugan, A. Sathishkumar, V. Kumaresan, et R. Velraj, « Melting/solidification characteristics of paraffin based nanocomposite for thermal energy storage applications », *Therm. Sci.*, vol. 21, nº 6 Part A, p. 2517-2524, 2017, doi: 10.2298/TSCI150612170L.

[16] M. Amin, F. Afriyanti, et N. Putra, « Thermal properties of paraffin based nano-phase change material as thermal energy storage », *IOP Conf. Ser. Earth Environ. Sci.*, vol. 105, p. 012028, janv. 2018, doi: 10.1088/1755-1315/105/1/012028.

[17] N. Mekaddem, S. B. Ali, M. Fois, et A. Hannachi, « Paraffin/ Expanded Perlite/Plaster as Thermal Energy Storage Composite », *Energy Procedia*, vol. 157, p. 1118-1129, janv. 2019, doi: 10.1016/j.egypro.2018.11.279.

[18] L. Han, X. Jia, Z. Li, Z. Yang, G. Wang, et G. Ning, « Effective Encapsulation of Paraffin Wax in Carbon Nanotube Agglomerates for a New Shape-Stabilized Phase Change Material with Enhanced Thermal-Storage Capacity and Stability », *Ind. Eng. Chem. Res.*, vol. 57, nº 39, p. 13026-13035, oct. 2018, doi: 10.1021/acs.iecr.8b02159.

[19] B. Shang, J. Hu, R. Hu, J. Cheng, et X. Luo, « Modularized thermal storage unit of metal foam/paraffin composite », *Int. J. Heat Mass Transf.*, vol. 125, p. 596-603, oct. 2018, doi: 10.1016/j.ijheatmasstransfer.2018.04.117.

[20] M. Al-Jethelah, S. Ebadi, K. Venkateshwar, S. H. Tasnim, S. Mahmud, et A. Dutta, « Charging nanoparticle enhanced bio-based PCM in open cell metallic foams: An experimental investigation », *Appl. Therm. Eng.*, vol. 148, p. 1029-1042, févr. 2019, doi: 10.1016/j.applthermaleng.2018.11.121.

[21] P. Manoj Kumar, K. Mylsamy, et P. T. Saravanakumar, « Experimental investigations on thermal properties of nano-SiO_2 /paraffin phase change material (PCM) for solar thermal energy storage applications », *Energy Sources Part Recovery Util. Environ. Eff.*, vol. 42, n° 19, p. 2420-2433, oct. 2020, doi: 10.1080/15567036.2019.1607942.

[22] M. George, A. K. Pandey, N. Abd Rahim, V. V. Tyagi, S. Shahabuddin, et R. Saidur, « A novel polyaniline (PANI)/ paraffin wax nano composite phase change material: Superior transition heat storage capacity, thermal conductivity and thermal reliability », *Sol. Energy*, vol. 204, p. 448-458, juill. 2020, doi: 10.1016/j.solener.2020.04.087.

[23] G. Chen, Y. Su, D. Jiang, L. Pan, et S. Li, « An experimental and numerical investigation on a paraffin wax/graphene oxide/carbon nanotubes composite material for solar thermal storage applications », *Appl. Energy*, vol. 264, p. 114786, avr. 2020, doi: 10.1016/j.apenergy.2020.114786.

[24] P. Zhang, Y. Cui, K. Zhang, S. Wu, D. Chen, et Y. Gao, « Enhanced thermal storage capacity of paraffin/diatomite composite using oleophobic modification », *J. Clean. Prod.*, vol. 279, p. 123211, janv. 2021, doi: 10.1016/j.jclepro.2020.123211.

[25] M. Gogoi, B. Das, et P. K. Patowari, « Characterization and performance analysis of modified phase change material with paraffin wax and waste exhaust carbon particles for thermal energy storage », *J. Energy Storage*, vol. 108, p. 115068, févr. 2025, doi: 10.1016/j.est.2024.115068.

[26] D. G. Gunjo *et al.*, « Improvement in Thermal Storage Effectiveness of Paraffin with Addition of Aluminum Oxide Nanoparticles », *Materials*, vol. 15, n° 13, p. 4427, juin 2022, doi: 10.3390/ma15134427.

[27] Y. Grosu *et al.*, « Hierarchical macro-nanoporous metals for leakage-free high-thermal conductivity shape-stabilized phase change materials », *Appl. Energy*, vol. 269, p. 115088, juill. 2020, doi: 10.1016/j.apenergy.2020.115088.

[28] S. K. Suraparaju, A. Sampathkumar, et S. K. Natarajan, « Development of paraffin wax & used cooking oil based composite thermal energy storage for efficient potable water generation in a solar distillation unit », *J. Energy Storage*, vol. 69, p. 107856, oct. 2023, doi: 10.1016/j.est.2023.107856.

[29] A. P. Tetuko *et al.*, « Encapsulation of paraffin-magnetite, paraffin, and polyethylene glycol in concretes as thermal energy storage », *J. Energy Storage*, vol. 68, p. 107684, sept. 2023, doi: 10.1016/j.est.2023.107684.

[30] O. Younis, M. Mozaffari, A. Ahmed, et M. Ghalambaz, « Improvement of Latent Heat Thermal Energy Storage Rate for Domestic Solar Water Heater Systems Using

Anisotropic Layers of Metal Foam », *Buildings*, vol. 14, nº 8, p. 2322, juill. 2024, doi: 10.3390/buildings14082322.

[31] H. Samara, M. Hamdan, et O. Al-Oran, « Effect of Al2O3 nanoparticles addition on the thermal characteristics of paraffin wax », *Int. J. Thermofluids*, vol. 22, p. 100623, mai 2024, doi: 10.1016/j.ijft.2024.100623.

[32] Y. Zhao, G. Li, X. Zhang, et H. Wu, « Experimental research on the effect of graphite on heat transfer performance of a latent heat storage system », *Front. Energy Res.*, vol. 11, p. 1321088, déc. 2023, doi: 10.3389/fenrg.2023.1321088.

[33] J. Chen *et al.*, « Spatiotemporal Utilization of Latent Heat in Erythritol-based Phase Change Materials as Solar Thermal Fuels », *Angew. Chem. Int. Ed.*, vol. 63, nº 16, p. e202400759, avr. 2024, doi: 10.1002/anie.202400759.

[34] A. Yadav, M. Samykano, A. K. Pandey, K. Sharma, et V. V. Tyagi, « Experimental investigation on the thermophysical properties of Paraffin wax/wheat husk composite for thermal energy storage », *Mater. Lett.*, vol. 373, p. 137133, oct. 2024, doi: 10.1016/j.matlet.2024.137133.

[35] J. Emeema, G. Murali, B. V. Reddi, et V. L. Mangesh, « Investigations on paraffin wax/CQD composite phase change material - Improved latent heat and thermal stability », *J. Energy Storage*, vol. 85, p. 111056, avr. 2024, doi: 10.1016/j.est.2024.111056.

[36] A. Castell, C. Solé, M. Medrano, J. Roca, L. F. Cabeza, et D. García, « Natural convection heat transfer coefficients in phase change material (PCM) modules with external vertical fins », *Appl. Therm. Eng.*, vol. 28, nº 13, p. 1676-1686, sept. 2008, doi: 10.1016/j.applthermaleng.2007.11.004.

[37] J. Gasia, J. M. Maldonado, F. Galati, M. De Simone, et L. F. Cabeza, « Experimental evaluation of the use of fins and metal wool as heat transfer enhancement techniques in a latent heat thermal energy storage system », *Energy Convers. Manag.*, vol. 184, p. 530-538, mars 2019, doi: 10.1016/j.enconman.2019.01.085.

[38] Y.-T. Lee, Y.-R. Liao, L.-H. Chien, F.-B. Cheung, et A.-S. Yang, « Performance enhancement of latent heat thermal energy storage systems via dynamic melting process of PCM under different control strategies », *Appl. Therm. Eng.*, vol. 259, p. 124903, janv. 2025, doi: 10.1016/j.applthermaleng.2024.124903.

[39] J. Wang *et al.*, « Computational investigation of melting performance enhancement in PCM-based lobed triplex-tube heat exchangers with Y-shaped fins for solar thermal

energy storage », *Int. Commun. Heat Mass Transf.*, vol. 169, p. 109567, déc. 2025, doi: 10.1016/j.icheatmasstransfer.2025.109567.

[40] A. Pal, B. Assilbekov, et B. B. Saha, « Enhancement of PCM melting employing internal annular fins in triplex tube heat exchanger for thermal energy storage systems », *Int. J. Heat Mass Transf.*, vol. 253, p. 127601, déc. 2025, doi: 10.1016/j.ijheatmasstransfer.2025.127601.

[41] L. Crnjac, K. Siddiqui, et A. G. Straatman, « Heat transfer enhancement to promote melting and solidification in a PCM-based thermal storage module », *J. Energy Storage*, vol. 132, p. 117904, oct. 2025, doi: 10.1016/j.est.2025.117904.

[42] S. A. Marzouk, F. A. Almehmadi, A. Aljabr, M. A. Sharaf, T. Alam, et D. Dobrotă, « Study of effects of constructed fins on melting of PCM in helical coil heat exchanger », *Case Stud. Therm. Eng.*, vol. 68, p. 105896, avr. 2025, doi: 10.1016/j.csite.2025.105896.

[43] Z. Ahmed, A. B. M. Ali, O. J. AlKhatib, et I. Mahariq, « Melting behavior in a finned PCM solar thermal receiver/storage unit: A numerical study of heat load and orientation effects », *Energy Rep.*, vol. 14, p. 2927-2938, déc. 2025, doi: 10.1016/j.egyr.2025.09.037.

[44] B. Kamkari et D. Groulx, « Experimental investigation of melting behaviour of phase change material in finned rectangular enclosures under different inclination angles », *Exp. Therm. Fluid Sci.*, vol. 97, p. 94-108, oct. 2018, doi: 10.1016/j.expthermflusci.2018.04.007.

[45] A. Ochman, W.-Q. Chen, P. Błasiak, M. Pomorski, et S. Pietrowicz, « The Use of Capsuled Paraffin Wax in Low-Temperature Thermal Energy Storage Applications: An Experimental and Numerical Investigation », *Energies*, vol. 14, nº 3, p. 538, janv. 2021, doi: 10.3390/en14030538.

[46] Z. Yinping, J. Yi, et J. Yi, « A simple method, the -history method, of determining the heat of fusion, specific heat and thermal conductivity of phase-change materials », *Meas. Sci. Technol.*, vol. 10, nº 3, p. 201-205, mars 1999, doi: 10.1088/0957-0233/10/3/015.

[47] A. Lázaro, E. Günther, H. Mehling, S. Hiebler, J. M. Marín, et B. Zalba, « Verification of a T-history installation to measure enthalpy versus temperature curves of phase change materials », *Meas. Sci. Technol.*, vol. 17, nº 8, p. 2168-2174, août 2006, doi: 10.1088/0957-0233/17/8/016.

[48] J. N. W. Chiu et V. Martin, « Submerged finned heat exchanger latent heat storage design and its experimental verification », *Appl. Energy*, vol. 93, p. 507-516, mai 2012, doi: 10.1016/j.apenergy.2011.12.019.

[49] M. Rady, « Granular phase change materials for thermal energy storage: Experiments and numerical simulations », *Appl. Therm. Eng.*, vol. 29, n° 14-15, p. 3149-3159, oct. 2009, doi: 10.1016/j.applthermaleng.2009.04.018.

[50] L. T. I et V. R, « Thermophysical characterization and comparison of PCMs using DSC and T-History experimental setup », *Mater. Res. Express*, vol. 6, n° 12, p. 125527, déc. 2019, doi: 10.1088/2053-1591/ab5aae.

[51] I. M. Sutjahja, A. O. Silalahi, D. Kurnia, et S. Wonorahardjo, « The role of particle dopant to the thermal conductivities of PCM coconut oil by means of the T-history method », *J. Phys. Conf. Ser.*, vol. 1204, p. 012056, avr. 2019, doi: 10.1088/1742-6596/1204/1/012056.

[52] N. Radhakrishnan, S. Thomas, et C. B. Sobhan, « Characterization of thermophysical properties of nano-enhanced organic phase change materials using T-history method », *J. Therm. Anal. Calorim.*, vol. 140, n° 5, p. 2471-2484, juin 2020, doi: 10.1007/s10973-019-08976-1.

[53] Y. Jiang, M. Liu, et Y. Sun, « Review on the development of high temperature phase change material composites for solar thermal energy storage », *Sol. Energy Mater. Sol. Cells*, vol. 203, p. 110164, déc. 2019, doi: 10.1016/j.solmat.2019.110164.

[54] G. Alva, Y. Lin, et G. Fang, « An overview of thermal energy storage systems », *Energy*, vol. 144, p. 341-378, févr. 2018, doi: 10.1016/j.energy.2017.12.037.

[55] I. Sarbu et C. Sebarchievici, « A Comprehensive Review of Thermal Energy Storage », *Sustainability*, vol. 10, n° 1, p. 191, janv. 2018, doi: 10.3390/su10010191.

[56] A. Kumar et S. K. Shukla, « A Review on Thermal Energy Storage Unit for Solar Thermal Power Plant Application », *Energy Procedia*, vol. 74, p. 462-469, août 2015, doi: 10.1016/j.egypro.2015.07.728.

[57] C. N. Elias et V. N. Stathopoulos, « A comprehensive review of recent advances in materials aspects of phase change materials in thermal energy storage », *Energy Procedia*, vol. 161, p. 385-394, mars 2019, doi: 10.1016/j.egypro.2019.02.101.

[58] U. Herrmann et D. W. Kearney, « Survey of Thermal Energy Storage for Parabolic Trough Power Plants », *J. Sol. Energy Eng.*, vol. 124, n° 2, p. 145-152, mai 2002, doi: 10.1115/1.1467601.

[59] J. Sunku Prasad, P. Muthukumar, F. Desai, D. N. Basu, et M. M. Rahman, « A critical review of high-temperature reversible thermochemical energy storage systems », *Appl. Energy*, vol. 254, p. 113733, nov. 2019, doi: 10.1016/j.apenergy.2019.113733.

[60] A. H. Abedin, « A Critical Review of Thermochemical Energy Storage Systems », *Open Renew. Energy J.*, vol. 4, nº 1, p. 42-46, août 2011, doi: 10.2174/1876387101004010042.

[61] R. N *et al.*, « Performance evaluation and machine learning-based prediction of PCM-integrated solar chimney drying for black dates », *Results Eng.*, vol. 28, p. 108218, déc. 2025, doi: 10.1016/j.rineng.2025.108218.

[62] A. Vedrtnam, K. Kalauni, et N. Soares, « Hybrid optimization of phase change material-based thermal storage for HVAC efficiency in commercial buildings », *Appl. Therm. Eng.*, vol. 279, p. 128143, nov. 2025, doi: 10.1016/j.applthermaleng.2025.128143.

[63] J. Skovajsa, P. Drabek, et S. Sehnalek, « Solution of the modular PCM-based cooling ceiling and ventilation system », *Appl. Therm. Eng.*, vol. 257, p. 124169, déc. 2024, doi: 10.1016/j.applthermaleng.2024.124169.

[64] S. Wieser, L. Naveau, W. Kraft, R. A. Beristain, et A. Anson, « Modeling and simulation of thermal management in battery electric rail vehicles for the sizing of thermal storage systems », *Energy Convers. Manag.*, vol. 346, p. 120489, déc. 2025, doi: 10.1016/j.enconman.2025.120489.

[65] S. Zeinali et E. Neshat, « Numerical investigation on thermal management system of lithium-ion battery pack of electric vehicles based on hybrid cooling of porous media, phase change materials, and liquid cooling », *Case Stud. Therm. Eng.*, vol. 74, p. 106732, oct. 2025, doi: 10.1016/j.csite.2025.106732.

[66] N. Y. Çam, M. A. Ezan, I. Ghiat, et Y. Biçer, « Modeling of a solar-aided heating and cooling system with thermal energy storage for a sustainable agricultural greenhouse », *Appl. Therm. Eng.*, vol. 280, p. 128714, déc. 2025, doi: 10.1016/j.applthermaleng.2025.128714.

[67] S. S. Magendran *et al.*, « Synthesis of organic phase change materials (PCM) for energy storage applications: A review », *Nano-Struct. Nano-Objects*, vol. 20, p. 100399, oct. 2019, doi: 10.1016/j.nanoso.2019.100399.

[68] A. Abhat, « Low temperature latent heat thermal energy storage: Heat storage materials », *Sol. Energy*, vol. 30, nº 4, p. 313-332, 1983, doi: 10.1016/0038-092X(83)90186-X.

[69] A. Fallahi, G. Guldentops, M. Tao, S. Granados-Focil, et S. Van Dessel, « Review on solid-solid phase change materials for thermal energy storage: Molecular structure and thermal properties », *Appl. Therm. Eng.*, vol. 127, p. 1427-1441, déc. 2017, doi: 10.1016/j.applthermaleng.2017.08.161.

[70] Maria De Los Angeles Ortega Del Rosario, « Customizable latent heat thermal energy storage and transfer system for air-cooling in buildings : design and thermal analysis ». [En ligne]. Disponible sur: https://tel.archives-ouvertes.fr/tel-01945962

[71] D. Li, Y. Wu, B. Wang, C. Liu, et M. Arıcı, « Optical and thermal performance of glazing units containing PCM in buildings: A review », *Constr. Build. Mater.*, vol. 233, p. 117327, févr. 2020, doi: 10.1016/j.conbuildmat.2019.117327.

[72] « George A. Hand book of thermal design. In: Guyer C, editor. Phase change thermal storage materials. McGraw Hill Book Co.; 1989 [chapter 1 ».

[73] « Mehling et al. [1], source: ZAE Bayern). Mehling, H.; Cabeza, L.F. Heat and Cold Storage with PCM; Springer: Berlin/Heidelberg, Germany, 2008; ISBN 978-3-540-68556-2. [Google Scholar] ». [En ligne]. Disponible sur: http://www.springer.com/chemistry/industrial+chemistry+and+chemical+engineering/book/978-3-540-68556-2

[74] V. V. Tyagi et D. Buddhi, « PCM thermal storage in buildings: A state of art », *Renew. Sustain. Energy Rev.*, vol. 11, n° 6, p. 1146-1166, août 2007, doi: 10.1016/j.rser.2005.10.002.

[75] M. A. Kibria, M. R. Anisur, M. H. Mahfuz, R. Saidur, et I. H. S. C. Metselaar, « A review on thermophysical properties of nanoparticle dispersed phase change materials », *Energy Convers. Manag.*, vol. 95, p. 69-89, mai 2015, doi: 10.1016/j.enconman.2015.02.028.

[76] M. Jowzi et J. Jamaati, « Experimental and numerical investigation of the effect of adding metal fibers on enhancing the thermal conductivity of PCM: a novel method for predicting effective thermal conductivity of fibrous materials », *Appl. Therm. Eng.*, vol. 279, p. 127824, nov. 2025, doi: 10.1016/j.applthermaleng.2025.127824.

[77] S. Wu, T. Yan, Z. Kuai, et W. Pan, « Thermal conductivity enhancement on phase change materials for thermal energy storage: A review », *Energy Storage Mater.*, vol. 25, p. 251-295, mars 2020, doi: 10.1016/j.ensm.2019.10.010.

[78] W. Zhou, K. Li, J. Zhu, R. Li, X. Cheng, et F. Liu, « Preparation and thermal cycling of expanded graphite/adipic acid composite phase change materials », *J. Therm. Anal. Calorim.*, vol. 129, n° 3, p. 1639-1645, sept. 2017, doi: 10.1007/s10973-017-6385-2.

[79] A. Al-Masri, K. Khanafer, et A. Sedaghat, « Passive thermal management of PV solar panels using carbon fiber-enhanced phase change materials: A numerical and optimization study », *Int. Commun. Heat Mass Transf.*, vol. 167, p. 109278, sept. 2025, doi: 10.1016/j.icheatmasstransfer.2025.109278.

[80] J. Song *et al.*, « Thermophysical properties of high-density graphite foams and their paraffin composites », *New Carbon Mater.*, vol. 27, nº 1, p. 27-34, févr. 2012, doi: 10.1016/S1872-5805(12)60002-X.

[81] X. Yang, W. Wang, C. Yang, L. Jin, et T. J. Lu, « Solidification of fluid saturated in open-cell metallic foams with graded morphologies », *Int. J. Heat Mass Transf.*, vol. 98, p. 60-69, juill. 2016, doi: 10.1016/j.ijheatmasstransfer.2016.03.023.

[82] B. V. S. Dinesh et A. Bhattacharya, « Effect of foam geometry on heat absorption characteristics of PCM-metal foam composite thermal energy storage systems », *Int. J. Heat Mass Transf.*, vol. 134, p. 866-883, mai 2019, doi: 10.1016/j.ijheatmasstransfer.2019.01.095.

[83] S. Liu, H. Wang, Q. Ying, et L. Guo, « Numerical study on the combined application of multiple phase change materials and gradient metal foam in thermal energy storage device », *Appl. Therm. Eng.*, vol. 257, p. 124267, déc. 2024, doi: 10.1016/j.applthermaleng.2024.124267.

[84] P. D. Dhabarde, R. P. Soni, et J. G. Suryawanshi, « Passive-cooling of Li-ion batteries using PCM-metal foam in honeycomb enclosure », *Appl. Therm. Eng.*, vol. 281, p. 128543, déc. 2025, doi: 10.1016/j.applthermaleng.2025.128543.

[85] S. A. Shehzad, B. Alshuraiaan, M. S. Kamel, M. Izadi, et T. Ambreen, « Influence of fin orientation on the natural convection of aqueous-based nano-encapsulated PCMs in a heat exchanger equipped with wing-like fins », *Chem. Eng. Process. - Process Intensif.*, vol. 160, p. 108287, mars 2021, doi: 10.1016/j.cep.2020.108287.

[86] Z. Khan et Z. A. Khan, « Role of extended fins and graphene nano-platelets in coupled thermal enhancement of latent heat storage system », *Energy Convers. Manag.*, vol. 224, p. 113349, nov. 2020, doi: 10.1016/j.enconman.2020.113349.

[87] L. Lyu, H. Gu, S. Li, W. Yu, Y. Ren, et X. Liu, « Performance enhancement of PCM-based heat sinks with plate heat-pipe fins and metal foam networks », *Case Stud. Therm. Eng.*, vol. 75, p. 107046, nov. 2025, doi: 10.1016/j.csite.2025.107046.

[88] C. Xia, G. Chen, X. Bao, J. Shi, H. Cui, et X. Chen, « Thermal performance of heat storage-enhanced PCM energy pipe pile with heat conduction fin », *Appl. Therm. Eng.*, vol. 272, p. 126407, août 2025, doi: 10.1016/j.applthermaleng.2025.126407.

[89] P. Zare, N. Perera, J. Lahr, et R. Hasan, « A novel thermal management system for cylindrical lithium-ion batteries using internal-external fin-enhanced phase change material », *Appl. Therm. Eng.*, vol. 238, p. 121985, févr. 2024, doi: 10.1016/j.applthermaleng.2023.121985.

[90] M. Telkes, « Nucleation of Supersaturated Inorganic Salt Solutions », *Ind. Eng. Chem.*, vol. 44, n° 6, p. 1308-1310, juin 1952, doi: 10.1021/ie50510a036.

[91] V. Ayyagari, A. Shooshtari, et M. Ohadi, « Glauber's Salt Composites for HVAC Applications: A Study on the Use of the T-History Method with a Modified Data Evaluation Methodology », *Materials*, vol. 18, n° 13, p. 2998, juin 2025, doi: 10.3390/ma18132998.

[92] X. Xu, Z. Dong, S. Memon, X. Bao, et H. Cui, « Preparation and Supercooling Modification of Salt Hydrate Phase Change Materials Based on CaCl2·2H2O/CaCl2 », *Materials*, vol. 10, n° 7, p. 691, juin 2017, doi: 10.3390/ma10070691.

[93] V. J. Reddy, J. S. Yadav, et S. Chattopadhyay, « Phase change material loaded form-stable composites for low temperature thermal buffering application », *Mater. Chem. Phys.*, vol. 247, p. 122859, juin 2020, doi: 10.1016/j.matchemphys.2020.122859.

[94] Y. Li, S. Zhou, M. Di, W. Tan, et Q. Zhu, « Effect of Microstructure on Thermal Properties of EG/MA Shaped Composite Phase Change Materials », *Int. J. Thermophys.*, vol. 44, n° 2, p. 19, févr. 2023, doi: 10.1007/s10765-022-03130-w.

[95] K. Liu, H. Zhao, Z. Yuan, F. Zhao, D. Chen, et C. Shi, « Preparation and characterization of steel slag-based low, medium, and high-temperature composite phase change energy storage materials », *J. Energy Storage*, vol. 57, p. 106309, janv. 2023, doi: 10.1016/j.est.2022.106309.

[96] Y. Lv, W. Situ, X. Yang, G. Zhang, et Z. Wang, « A novel nanosilica-enhanced phase change material with anti-leakage and anti-volume-changes properties for battery thermal management », *Energy Convers. Manag.*, vol. 163, p. 250-259, mai 2018, doi: 10.1016/j.enconman.2018.02.061.

[97] S.-P. Wang *et al.*, « Enhanced leakage-proof performance of flexible phase change materials through the transformation of physicochemical crosslinked networks », *Polymer*, vol. 326, p. 128357, mai 2025, doi: 10.1016/j.polymer.2025.128357.

[98] Y. A. Bhutto, A. K. Pandey, A. Islam, R. K. Rajamony, et R. Saidur, « Lauric acid based form-stable phase change material for effective electronic thermal management and energy storage application », *Mater. Today Sustain.*, vol. 28, p. 100931, déc. 2024, doi: 10.1016/j.mtsust.2024.100931.

[99] J. Yu et J. Feng, « Form-stable phase change materials with enhanced thermal conductivity via segregated BN network within SEBS-supported paraffin wax for electronics thermal management », *Compos. Part Appl. Sci. Manuf.*, vol. 199, p. 109187, déc. 2025, doi: 10.1016/j.compositesa.2025.109187.

[100] H. Sun *et al.*, « Regulation of carbonized cellulose nanofiber pore structure by artificially cultured diatom frustules for leakage-proof phase change composites », *Chem. Eng. J.*, vol. 504, p. 158482, janv. 2025, doi: 10.1016/j.cej.2024.158482.

[101] H. Wei *et al.*, « Fabrication and building energy-saving performance evaluation of polyethylene glycol/polymethyl methacrylate/expanded graphite thermal enhanced shape-stable phase change material », *Appl. Therm. Eng.*, vol. 257, p. 124410, déc. 2024, doi: 10.1016/j.applthermaleng.2024.124410.

[102] S. W. Churchill et H. H. S. Chu, « Correlating equations for laminar and turbulent free convection from a vertical plate », *Int. J. Heat Mass Transf.*, vol. 18, nº 11, p. 1323-1329, nov. 1975, doi: 10.1016/0017-9310(75)90243-4.

[103] J. Wang, Y. Hao, B. Zhu, T. Han, Z. Li, et J. Zhang, « Crystalline Behavior of Paraffin Wax », *J. Phys. Chem. B*, vol. 126, nº 4, p. 985-995, févr. 2022, doi: 10.1021/acs.jpcb.1c10000.

[104] M. Elkatory, « Chemical mitigation technology for wax deposition in submarine oil pipeline systems », *Egypt. J. Chem.*, vol. 0, nº 0, p. 0-0, juill. 2021, doi: 10.21608/ejchem.2021.72586.3604.

[105] H. Hachemi, C. Seladji, Y. Fraine, et B. F. Houti, « Experimental and numerical evaluation of the hygrothermal performance of three different building finishing layers including phase change materials », *J. Build. Pathol. Rehabil.*, vol. 8, nº 2, p. 103, déc. 2023, doi: 10.1007/s41024-023-00349-4.

[106] D. Gowthami, R. K. Sharma, A. K. Ansu, A. Sarı, V. V. Tyagi, et P. Rathore, « Evaluation of carbonized cotton stalk for development of novel form stable composite phase change materials for solar thermal energy storage », *Process Saf. Environ. Prot.*, vol. 188, p. 1037-1048, août 2024, doi: 10.1016/j.psep.2024.06.030.

[107] O. M. Hamdoon, Z. M. Almakhyoul, O. R. Alomar, et S. Q. Khalil, « Improvement of the Performance of Solar Underfloor Heating System Integrated With Phase Change Material », *Energy Storage*, vol. 7, nº 5, p. e70227, août 2025, doi: 10.1002/est2.70227.

[108] Z. Cao *et al.*, « Phase change materials for efficient thermal energy storage and its potential applications in sustainable facility agriculture: A critical review », *Renew. Sustain. Energy Rev.*, vol. 225, p. 116169, janv. 2026, doi: 10.1016/j.rser.2025.116169.